

**DIAGNOSING SPATIAL VARIATION PATTERNS IN
MANUFACTURING PROCESSES**

A Dissertation

by

HO YOUNG LEE

Submitted to the Office of Graduate Studies of
Texas A&M University
in partial fulfillment of the requirements for the degree of

DOCTOR OF PHILOSOPHY

May 2003

Major Subject: Industrial Engineering

**DIAGNOSING SPATIAL VARIATION PATTERNS IN
MANUFACTURING PROCESSES**

A Dissertation

by

HO YOUNG LEE

Submitted to Texas A&M University
in partial fulfillment of the requirements
for the degree of

DOCTOR OF PHILOSOPHY

Approved as to style and content by:

Daniel Apley
(Chair of Committee)

Way Kuo
(Member)

Yu Ding
(Member)

Michael T. Longnecker
(Member)

Brett A. Peters
(Head of Department)

May 2003

Major Subject: Industrial Engineering

ABSTRACT

Diagnosing Spatial Variation Patterns In Manufacturing Processes

(May 2003)

Ho Young Lee, B.S., Seoul National University

M.S., Texas A&M University

Chair of Advisory Committee: Dr. Daniel Apley

This dissertation discusses a method that will aid in diagnosing the root causes of product and process variability in complex manufacturing processes when large quantities of multivariate in-process measurement data are available. As in any data mining application, this dissertation has as its objective the extraction of useful information from the data. A linear structured model, similar to the standard factor analysis model, is used to generically represent the variation patterns that result from the root causes. Blind source separation methods are investigated to identify spatial variation patterns in manufacturing data. Further, the existing blind source separation methods are extended, enhanced and improved to be a more effective, accurate and widely applicable method for manufacturing variation diagnosis. An overall strategy is offered to guide the use of the presented methods in conjunction with alternative methods.

ACKNOWLEDGMENTS

First of all I would like to thank God through Whom all blessings flow.

I would like to express my very sincere gratitude to Dr. Daniel Apley, the chairman of my advisory committee, for his guidance, support, and advice during my research work. This work could not have been completed without his generosity and patience as well as his profound knowledge. I would also like to express my appreciation to Dr. Way Kuo, Dr. Yu Ding, and Dr. Michael Longnecker for serving on my committee and to Dr. Paul Baumann as the graduate council representative (GCR). I would like to thank all the past and current students in our data analysis laboratory who provided advice and encouragement. I would like to show my deepest appreciation to my parents, Mr. & Mrs. Yoon-Sang Lee (Kyung-Hee Oh), for their endless love and support and also to my brother, Ki-Young Lee, for his encouragement. Also, special thanks to my Aggie parents John and Kathy Deishers, and Becky Nelson who always pray for me and love me.

My special thanks go to my best friends, Mr. Seongmin Yim and Mr. Jihwan Choi, for their friendship and helpful advice.

TABLE OF CONTENTS

	Page
ABSTRACT	iii
ACKNOWLEDGMENTS	iv
TABLE OF CONTENTS	v
LIST OF FIGURES	vii
LIST OF TABLES.....	x
 CHAPTER	
I INTRODUCTION	1
I.1 Representing and illustrating spatial variation patterns	3
I.2 Prior work on classifying pre-modeled variation patterns	7
I.3 Prior work on blindly identifying un-modeled variation patterns.....	9
I.4 Outline of the dissertation	13
 II MANUFACTURING VARIATION DIAGNOSIS USING BLIND SOURCE SEPARATION APPROACH.....	 17
II.1 Blind source separation problem	17
II.2 Blind source separation methods	20
II.2.1 Second-order methods	22
II.2.2 Fourth-order methods.....	24
II.3 An illustrative example	27
II.4 Discussions of the assumptions	35
II.4.1 Comparing the assumptions.....	35
II.4.2 Verifying the assumptions	40
II.5 Effect of violating assumptions	44
II.6 Accomodating other noise covariance structure.....	57
II.7 Chapter summary	59

CHAPTER	Page
III	COMBINING SECOND-ORDER AND FOURTH-ORDER CRITERIA 61
	III.1 Combining second-order and fourth-order statistics with optimal weighting 62
	III.2 Uniqueness condition for the combined method 68
	III.3 Performance analysis 71
	III.4 Chapter summary 80
IV	BLIND SOURCE SEPARATION WITH PARTIAL PRIOR KNOWLEDGE 81
	IV.1 Pre-modeling spatial variation patterns from engineering knowledge 89
	IV.2 Limitation of classifying pre-modeled variation patterns 90
	IV.3 Blind separation approach with partial prior knowledge 94
	IV.3.1 Estimating the un-modeled variation patterns 95
	IV.3.2 Classifying the pre-modeled variation patterns 102
	IV.4 Performance comparison 106
	IV.5 Chapter summary 115
V	OVERALL STRATEGY 116
	V.1 Block separability of the blind separation methods 116
	V.2 Overall strategy for identifying spatial variation patterns 119
	V.3 Illustration of applying the overall strategy 123
	V.4 Chapter summary 129
VI	CONCLUSION AND FUTURE WORKS 131
	REFERENCES 135
	APPENDIX A 139
	VITA 141

LIST OF FIGURES

FIGURE	Page
1 Illustration of linear spatial variation patterns in autobody assembly: a rotation of the quarter panel subassembly around locating-hole 5	5
2 Illustration of linear spatial variation patterns in autobody assembly: a translation of the D-pillar in the z -direction	6
3 Illustration of the blind separation problem for speaker localization	19
4 Geometry of the crankshaft in the example of Section II.3	28
5 Estimates of the first pattern vector \mathbf{c}_1 (top panel) and source signal $v_{1,t}$ (bottom panel)	30
6 Estimates of the second pattern vector \mathbf{c}_2 (top panel) and source signal $v_{2,t}$ (bottom panel)	31
7 Estimates of the third pattern vector \mathbf{c}_3 (top panel) and source signal $v_{3,t}$ (bottom panel)	32
8 Histograms for the three source signal from the crankshaft example	41
9 Sample autocorrelation functions for the three source signal from the crankshaft example	42
10 Illustration of the two variation patterns in the example: (a) \mathbf{c}_1 , which represents a beam translation and (b) \mathbf{c}_2 , which represents a beam rotation	45
11 Estimates of the pattern vectors and source signals in the simulation example; (a) the estimate of \mathbf{c}_1 and (b) the estimate of $v_{1,t}$	49
12 Estimates of the pattern vectors and source signals in the simulation example; (a) the estimate of \mathbf{c}_2 and (b) the estimate of $v_{2,t}$	50

FIGURE	Page
13 Histograms of the estimated source signals in the simulation example; (a) histogram of estimates of v_1 and (b) histogram of estimates of v_2	51
14 Sample autocorrelation functions of the estimated source signals in the simulation example; (a) sample autocorrelation function of estimates of v_1 and (b) sample autocorrelation function of estimates of v_2	52
15 The Bernoulli, uniform, triangular, and Gaussian distributions (with mean zero and unit variance) used for the second source. The Bernoulli distribution is discrete, whereas the others are continuous distributions	55
16 Autocorrelation function $\rho_{1,\tau} = \phi^\tau$ of the first-order AR source v_1 , for various ϕ	56
17 Illustration of the third variation pattern \mathbf{c}_3 in the example: \mathbf{c}_3 representing a beam bending	72
18 Illustration of first-order AR source signals with different levels of autocorrelation: (a) high autocorrelation ($\phi = 0.9$); (b) moderate autocorrelation ($\phi = 0.6$); (c) no autocorrelation ($\phi = 0$)	74
19 Illustration of autocorrelated Bernoulli sources with different levels of autocorrelation (different values of q)	75
20 Illustration of the bottom of an autobody in the y-z plane: (a) bottom of the autobody, (b) a rounded hole, and (c) a translation of the entire autobody	85
21 Illustration of the pre-modeled measurement variation pattern in autobody assembly (a translation of the entire autobody).....	87
22 Illustration of \mathbf{c}_1 in autobody assembly(a translation of the right bodyside).	94
23 Illustration of the three variation patterns used in Section IV.4: (a) \mathbf{b}_1 , representing a beam rotation, (b) \mathbf{c}_1 , representing a beam translation, and (c) \mathbf{c}_2 , representing a beam bending	106

FIGURE	Page
24 Histograms (left panels) and sample autocorrelation functions (right panels) for three source signals, using the blind separation method with partial prior knowledge.....	111
25 Estimates of the three pattern vectors \mathbf{b}_1 , \mathbf{c}_1 and \mathbf{c}_2 (left panels) and source signal $u_{1,t}$, $v_{1,t}$ and $v_{2,t}$ (right panels), using the blind separation method with partial prior knowledge.....	112
26 Histograms (left panels) and sample autocorrelation functions (right panels) for three source signals, using the combined method	113
27 Estimates of the three pattern vectors \mathbf{b}_1 , \mathbf{c}_1 and \mathbf{c}_2 (left panels) and source signals $u_{1,t}$, $v_{1,t}$ and $v_{2,t}$ (right panels), using the combined method	114
28 Flowchart of the overall strategy	121
29 Illustration of the four variation patterns used in Chapter V: (a) \mathbf{b}_1 , represents a large measurement error at the left-most point, (b) \mathbf{c}_1 , (c) \mathbf{c}_2 and (d) \mathbf{c}_3	123
30 Illustration of estimates of the un-modeled variation patterns used in Section V.3: (a) the estimates of \mathbf{c}_1 , (b) the estimates of \mathbf{c}_2 and (c) the estimates of \mathbf{c}_3	125
31 Illustration of histograms of the estimated source signals.....	127
32 Illustration of sample autocorrelation functions of v_2 and v_3	128
33 Estimates of \mathbf{c}_2 and \mathbf{c}_3 using the A&S method: (a) estimates of \mathbf{c}_2 , and (b) estimates of \mathbf{c}_3	129

LIST OF TABLES

TABLE		Page
1	Performance of the second-order and fourth-order methods as their assumptions come closer to being violated	53
2	Summary of the Monte Carlo simulation results comparing the performance of the three methods	77
3	Advantages and disadvantages of the method of blindly identifying un-modeled variation patterns and the method of classifying pre-modeled variation patterns	83
4	Summary of the Monte Carlo simulation results comparing the performance of the two methods	108

CHAPTER I

INTRODUCTION

A common characteristic of many modern complex manufacturing processes is the availability of large amounts of multivariate in-process measurement and inspection data for quality control purposes. One example is automobile body assembly, in which laser-optical measurement stations are built into the assembly line at various stages, typically immediately after major subassemblies are completed (Apley and Shi, 2001). In each measurement station, well over 100 key dimensional characteristics distributed over the subassembly may be measured. Moreover, 100% of the autobodies produced are measured. Another prime example is printed circuit board (PCB) assembly. In PCB assembly, laser-optical measurement is also commonly used to obtain detailed dimensional characteristics of the wet solder paste, after it is deposited onto the board during the screen printing stage. After the electronic components are placed in position on the board and the solder is cured in the reflow oven, additional dimensional characteristics of each cured solder joint are obtained via X-ray laminography (Glass and Thomsen, 1993). In state-of-the-art PCB assembly operations, the solder paste is measured in-process for 100% of the boards produced, and the cured solder joints are measured for nearly 100% of the boards.

This dissertation follows style of *Technometrics*.

The measurement data may contain a wealth of buried diagnostic information concerning the numerous variation sources that contribute to overall levels of process variability. Each variation source will typically result in a distinct variation pattern in the data. The patterns will have "spatial" characteristics that indicate how a variation source causes different measured variables or features to interact, as well as "temporal" characteristics that indicate how a variation source evolves over time. As in any data mining application, a primary objective is to extract concise, relevant information from the raw data in a form that can be clearly presented to a human operator. For the purpose of understanding and reducing process variation, relevant information refers to the precise nature of the variation pattern caused by each source. The presumption throughout this dissertation is that process operators and engineers, when provided a clearer understanding of the nature of each variation pattern, will be better equipped to identify and eliminate the underlying root causes of process variation.

In the rest of the introduction, the model for representing spatial variation patterns is discussed using the autobody assembly process as an illustrative example. Also in this chapter, background information on the limitations of prior related work is presented. The end of the introduction provides an overview of the remaining chapters of this dissertation and discusses the potential contributions and practical significance of this work.

I.1 Representing and illustrating spatial variation patterns

Let $\mathbf{x} = [x_1, x_2, \dots, x_n]'$ be an $n \times 1$ random vector that represents a set of n measured characteristics from the product or process. Let \mathbf{x}_i , $i = 1, 2, \dots, N$, be a sample of N observations of \mathbf{x} . In autobody assembly, for example, \mathbf{x} would represent the vector of all measured dimensional characteristics across a given autobody, and N would be the number of autobodies in the sample. It is assumed that \mathbf{x} obeys the model

$$\mathbf{x} = \mathbf{C}\mathbf{v} + \mathbf{w}, \quad (1)$$

where $\mathbf{C} = [\mathbf{c}_1, \mathbf{c}_2, \dots, \mathbf{c}_p]$ is an $n \times p$ constant matrix with linearly independent columns. The vector $\mathbf{v} = [v_1, v_2, \dots, v_p]'$ is a $p \times 1$ zero-mean random vector with independent components, each scaled (without loss of generality) to have unit variance. The vector $\mathbf{w} = [w_1, w_2, \dots, w_n]'$ is an $n \times 1$ zero-mean random vector that is independent of \mathbf{v} .

The interpretation of the model is that there are p independent *variation sources* $\{v_i: i = 1, 2, \dots, p\}$ that affect the measurement vector \mathbf{x} . Each source has a linear effect on \mathbf{x} that is represented by the corresponding column of \mathbf{C} . Together, $\mathbf{c}_i v_i$ describes the effect of the i^{th} source on \mathbf{x} . The variation *pattern vector* \mathbf{c}_i indicates the spatial nature of the variation caused by the i^{th} source. Since the elements of \mathbf{v} are

scaled to have unit variance, \mathbf{c}_i also indicates the magnitude or severity of the i^{th} source. The random vector \mathbf{w} represents the aggregated effects of measurement noise and any inherent variation that is not attributed to the sources. Unless otherwise noted, it is assumed throughout that the covariance matrix of \mathbf{w} is $\Sigma_{\mathbf{w}} = \sigma^2 \mathbf{I}$, a scalar multiple of the identity matrix. Section II.6 discusses how to apply the methods of this dissertation in situations where this assumption would not be reasonable. All random variables are assumed to be zero mean. If not, the mean of \mathbf{x} should be estimated and subtracted from the data.

The objective of this dissertation is to estimate the pattern vectors $\{\mathbf{c}_i: i = 1, 2, \dots, p\}$ based on a sample of data and then to use the estimates to gain insight into the root cause of the variation patterns. To illustrate this, consider the following example from autobody assembly. Figure 1 shows a rear quarter panel subassembly of an autobody. The measurement vector \mathbf{x} for the quarter panel subassembly consists of $n = 10$ y/z-plane coordinates of five separate features that are numbered 1 through 5 in Figure 1. The measurements are taken after the quarter panel subassembly is joined to the bodyside, which is not shown in the Figure. Apley and Shi (1998) and Apley and Shi (2001) should be referred to for a more detailed description of the assembly process.

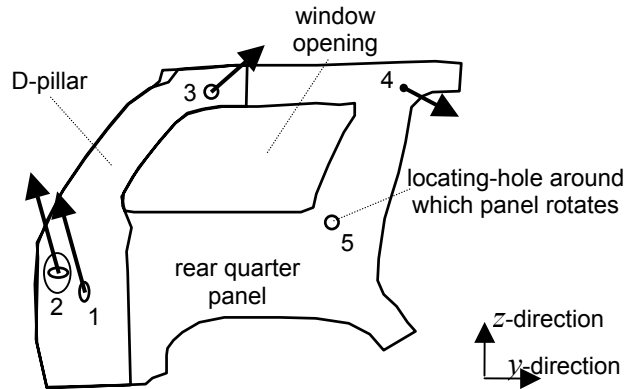


Figure 1 Illustration of linear spatial variation patterns in autobody assembly: a rotation of the quarter panel subassembly around locating-hole 5.

In a sample of $N = 200$ measured autobodies, there were two major variation patterns present, and estimates of \mathbf{c}_1 and \mathbf{c}_2 were obtained using the methods to be described in this dissertation. The estimates of \mathbf{c}_1 and \mathbf{c}_2 are illustrated on a figure of the autobody in Figure 1 and Figure 2, respectively. The elements of each variation pattern vector have been plotted as arrows at the locations of the features to which they correspond. The y/z coordinates of each feature have been combined into a single arrow. The estimate of \mathbf{c}_1 shown in Figure 1 appears to be a rotation of the entire subassembly about Feature 5. The source signal v_1 would be a random variable that is proportional to the angle of rotation (clockwise on some autobodies; counter-clockwise on others) of each quarter panel subassembly. The estimate of \mathbf{c}_2 shown in Figure 2 appears to be a z -direction (up/down) translation of the D-pillar with respect

to the rest of the quarter panel subassembly. The source signal v_2 would be a random variable that is proportional to the amount of translation (up on some autobodies; down on others) of each D-pillar.

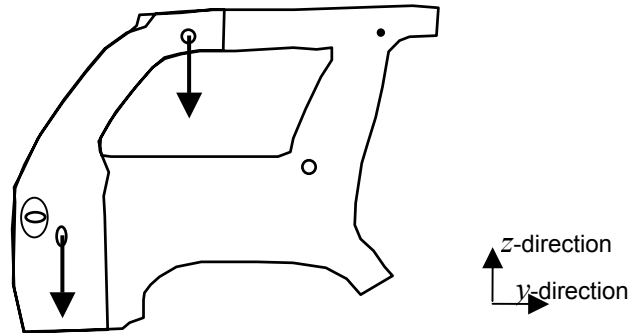


Figure 2 Illustration of linear spatial variation patterns in autobody assembly: a translation of the D-pillar in the z -direction.

Graphical displays of the estimated variation pattern vectors, such as in Figure 1 and Figure 2, generally facilitate identification of the root causes of variability. The root cause of the first variation pattern was found to be a loose locating element that failed to properly constrain the quarter panel subassembly when it was placed into a fixture and welded to the bodyside. The geometry of the fixture and the position of the loose locating element were such that the quarter panel subassembly was free to rotate by small amounts about Feature 5 (a hole that mates with a pin rigidly attached to the fixture). The root cause of the second variation pattern was found to be an elongated hole in the D-pillar that was due to improper stamping. The hole mated with a pin

whose purpose was to constrain the D-pillar when it was welded to the quarter panel. The elongated hole allowed the D-pillar to translate by small amounts in the z-direction, relative to the rest of the quarter panel.

I.2 Prior work on classifying pre-modeled variation patterns

One approach to identifying and diagnosing the root causes of variation sources involves off-line analysis based on adequate understanding of the manufacturing processes. For example, consider again the autobody assembly process. In a set of case studies, 72 percent of the major root causes of variation were fixture failures, which usually happens when tooling elements for locating parts fail (Ceglarek, Shi and Zhou, 1993). When adequate knowledge about the process is provided, it may be possible to model corresponding potential variation patterns. For example, consider the quarter panel subassembly process in Section I.1. As discussed before, a loose locating element is one of the root causes of the potential variation, and this might cause a rotation of the quarter panel subassembly about Feature 5. If the geometry of the fixture is available from the CAD system (the CAD system involves knowledge about the layout of the tooling element and the measurement position of the fixture), the effect of the loose locating element can be analytically modeled off-line. Likewise, other *potential* variation pattern vectors may also be amenable to modeling through extensive off-line analysis. Apley and Shi (1998) described how to analytically model potential variation sources from off-line analysis based on engineering knowledge of the process. Alternatively, Barton and Gonzalez-Barreto

(1996) suggested modeling potential pattern vectors from past experience with a process or through off-line experiments based on Design of Experiments.

If all of the potential variation patterns are pre-modeled off-line, the on-line task reduces to classifying which of the pre-modeled patterns are actually present in the on-line measurement data. Ceglarek and Shi (1996) proposed to use principal component analysis (PCA) to accomplish this. From the on-line measurement data, the principal component (linear combination of the measurement variable x that produces the largest variance) can be estimated. By comparing the estimated principal component and the set of pre-modeled variation patterns, the single variation source resulting in process variation can be identified.

The method proposed by Ceglarek and Shi (1996) classifies variation patterns effectively when only a single variation source is present. When there are multiple variation sources present, however, the method is unable to classify the different variation patterns. Apley and Shi (1998) proposed a method that is able to classify multiple variation patterns. The first part of this method involves estimating the severity of each of the potential variation sources using a least-squares approach. Based on the estimated severity of the sources, multiple variation sources can be detected and classified using a form of F-test. An extension of this method will be discussed in detail in Section IV.2.

All of the methods for classifying pre-modeled variation patterns rely on the assumption that every potential variation source has been pre-modeled off-line. If a variation source that has not been pre-modeled is present in the on-line data, then the

methods described in this section produce erroneous classification results (see Section IV.2). Therefore, the methods discussed in this section can be applied only in situations where it is possible to pre-model all of the potential variation sources. Pre-modeling every potential variation source is not possible in some manufacturing processes, however. Although the number p of actual sources present at any given time may be reasonable, the number of potential variation sources may be too large to model. In addition, the physics of the process may be so complex that off-line modeling becomes impossible. The necessity for off-line pre-modeling therefore limits the applicability of the methods in this section.

I.3 Prior work on blindly identifying un-modeled variation patterns

An approach to overcoming the limitation described above involves identifying the pattern vector blindly from the on-line measurement data, without pre-modeling the potential patterns. This section discusses prior works related to this objective. Note that the requirement of off-line modeling is the main distinction between the methods in Section I.2 and this section.

Since the model (1) is similar to what is assumed in standard linear orthogonal factor analysis and principal components analysis (Jackson, 1980; Jackson, 1981; Johnson and Wichern, 1998), one may consider using those methods to estimate manufacturing variation patterns from on-line measurement data. Factor analysis was originally developed for psychometrics and the social sciences. Its main purpose is to extract unobservable common factors from a covariance matrix of many variables. For

example, the test scores of students in statistics, mathematics, English and foreign language courses may have two unobservable common factors regarding math intelligence and language intelligence.

Let Σ_x denote the covariance matrix of \mathbf{x} . From the model structure and assumptions, the covariance of \mathbf{x} is

$$\Sigma_x = E[(\mathbf{C}\mathbf{v} + \mathbf{w})(\mathbf{C}\mathbf{v} + \mathbf{w})'] = \mathbf{C}\mathbf{C}' + \sigma^2\mathbf{I}. \quad (2)$$

Most factor analysis methods are based on PCA, which involves analyzing the eigenvectors and eigenvalues of Σ_x . Let $\{\lambda_i: i = 1, 2, \dots, n\}$ denote the eigenvalues of Σ_x arranged in descending order, and let $\{\mathbf{z}_i: i = 1, 2, \dots, n\}$ denote the corresponding eigenvectors, which are taken to be an orthonormal set. Define $\mathbf{Z}_p = [\mathbf{z}_1, \mathbf{z}_2, \dots, \mathbf{z}_p]$ and $\Lambda_p = \text{diag}\{\lambda_1, \lambda_2, \dots, \lambda_p\}$, which are constructed from the p largest eigenvalues and their associated eigenvectors. A PCA decomposition of Σ_x also yields

$$\Sigma_x = \sum_{i=1}^n \lambda_i \mathbf{z}_i \mathbf{z}_i' = \sum_{i=1}^p (\lambda_i - \sigma^2) \mathbf{z}_i \mathbf{z}_i' + \sigma^2 \sum_{i=1}^n \mathbf{z}_i \mathbf{z}_i' = \mathbf{Z}_p [\Lambda_p - \sigma^2 \mathbf{I}] \mathbf{Z}_p' + \sigma^2 \mathbf{I}, \quad (3)$$

where $\mathbf{Z}_p = [\mathbf{z}_1, \mathbf{z}_2, \dots, \mathbf{z}_p]$, and $\Lambda_p = \text{diag}\{\lambda_1, \lambda_2, \dots, \lambda_p\}$. In order for the covariance structures in (2) and (3) to be consistent, \mathbf{C} must be of the form $\mathbf{Z}_p [\Lambda_p - \sigma^2 \mathbf{I}]^{1/2} \mathbf{Q}$ for some $p \times p$ orthogonal matrix \mathbf{Q} .

The methods in this dissertation are presented in the context that the true covariance matrix Σ_x and certain other distribution parameters are available. To implement the methods, all parameters are replaced by their estimates, which are obtained from the sample of data. The number of "dominant" eigenvalues in the sample covariance matrix serves as an estimate of p , and the average of the remaining $n-p$ eigenvalues serves as an estimate of σ^2 . Estimates of \mathbf{Z}_p , and Λ_p are constructed from the eigenvectors and eigenvalues of the sample covariance matrix. Apley and Shi (2001) discuss this in more detail, and they include statistical tests for determining how many eigenvalues are dominant.

Since p , σ^2 , \mathbf{Z}_p , and Λ_p are all available from PCA, the problem reduces to finding an appropriate $p \times p$ orthogonal (rotation) matrix \mathbf{U} and then using $\mathbf{Z}_p[\Lambda_p - \sigma^2 \mathbf{I}]^{1/2} \mathbf{U}$ as an estimate of \mathbf{C} . This is referred to as factor rotation (Jackson, 1981; Johnson and Wichern, 1998). Let \mathbf{Q} denote the value of \mathbf{U} that yields the true \mathbf{C} . In other words, $\mathbf{C} = \mathbf{Z}_p[\Lambda_p - \sigma^2 \mathbf{I}]^{1/2} \mathbf{Q}$. An underlying premise of this dissertation is that there is some "true" \mathbf{C} whose structure is dictated entirely by the physics of the process (refer to Apley and Shi, 2001, for a more detailed discussion). Each column of the true \mathbf{C} represents a distinct variation pattern with a distinct physical root cause. In the autobody assembly example in the introduction, the root cause of the first pattern was a loose tooling element that caused a rotation of the entire quarter panel subassembly about Feature 5. The first column \mathbf{c}_1 (illustrated in Figure 1) represents that rotation. The root cause of the second pattern was an elongated hole that caused a

translation of the D-pillar, and the second column \mathbf{c}_2 (illustrated in Figure 2) represents that translation.

Standard factor rotation techniques are not intended to produce a \mathbf{U} that is necessarily close to \mathbf{Q} . Rather, they produce a \mathbf{U} that optimizes a somewhat artificial interpretability criterion such as the varimax criterion (Johnson and Wichern, 1998). Consequently, they do not necessarily produce an estimate of \mathbf{C} that is close to the true \mathbf{C} . In terms of understanding the root causes of variability, however, the most effective interpretation of an estimate of \mathbf{C} will surely result when it equals the true \mathbf{C} . The methods discussed in the remainder of this dissertation are intended to accomplish this.

The method proposed in Apley and Shi (2001) (hereafter referred to as A&S) can be viewed as a form of factor rotation that, rather than using some pre-defined interpretability criterion, attempts to rotate the estimate of \mathbf{C} so that it is as close as possible to the true \mathbf{C} . This will presumably result in the clearest interpretability, in the sense of leading to the clearest understanding of the true nature of the variation sources and their root causes. To accomplish this, the method of A&S assumes certain structural constraints on the true \mathbf{C} . Although their assumptions are less restrictive than the implicit assumptions involved in the varimax method (see Section II.4), they limit the applicability of the method to some extent. In addition, the method of A&S involves a level of user subjectivity that may prohibit its use by process operators and engineers who have limited statistical training. This motivates us to turn to blind source separation methods to solve the manufacturing variation diagnosis problem.

I.4. Outline of the dissertation

A class of signal processing methods, usually referred to as blind source separation methods (Cardoso, 1998; Haykin, 2000), appears to provide a more black-box approach to identifying un-modeled manufacturing variation patterns. Blind separation methods were originally developed for processing sensor array (e.g., radar, sonar, wireless communication) signals. Even though these blind separation methods were developed for a very different setting, signal processing problems employ a model whose structure is nearly identical to (1) (see Section II.1); therefore, it is natural to speculate that the blind separation approach can be applied to the manufacturing variation diagnosis problem. However, because signal processing problems differ in many respects from manufacturing variation diagnosis problems, a number of application issues must be considered.

In Chapter II, two blind separation methods – second-order methods and fourth-order methods – are extensively investigated for the manufacturing variation diagnosis problem. Second-order and fourth-order methods require their own set of additional assumptions to estimate \mathbf{Q} uniquely, which will be discussed in Section II.2. A portion of the work involves investigating the assumptions required in blind source separation algorithms to determine whether they are satisfied in typical manufacturing processes. These assumptions are compared with the required assumptions of the varimax factor rotation method and the method of A&S in Section II.4.1. Furthermore, it is difficult to know a priori whether the required assumptions of

each method will be satisfied or not. Accordingly, methods for verifying whether the assumptions are satisfied are discussed in Section II.4.2.

The performances of fourth-order and second-order methods have been already analyzed in signal processing applications. As mentioned before, however, there are some differences between signal processing applications and manufacturing variation diagnosis. For example, noise is usually negligible in signal processing applications, but not in manufacturing variation diagnosis. Consequently, the performances of second-order and fourth-order methods are studied specifically in the context of manufacturing variation diagnosis in Section II.5. In addition to the issues related to additional assumptions, Section II.6 discusses how to apply the blind separation methods in situations where the assumed noise structure of model (1) would not be reasonable in the manufacturing process.

The fourth-order and second-order methods can produce unique estimates of the variation patterns when the required assumptions are satisfied. If their uniqueness conditions are violated, however, they cannot estimate the variation patterns uniquely. To overcome this limitation, Chapter III develops a new method for estimating the variation patterns by optimally combining the second-order and fourth-order statistics. Conceptually, the fourth-order information is more heavily weighted than the second-order information when the fourth-order assumptions are satisfied and the second-order assumptions are violated. In the opposite case, the second-order information is more heavily weighted than the fourth-order information. Numerically, the optimal weights are derived to minimize some measure of estimation accuracy. The theoretical

uniqueness conditions of the new method are derived in Section III.2. The uniqueness conditions of the new method are less restrictive than the uniqueness conditions of either the second-order or the fourth-order method. Thus, the new method is more of a black-box type method for identifying manufacturing variation patterns.

As mentioned above, the existing methods for classifying pre-modeled variation patterns require that all of the potential variation patterns be pre-modeled. Due to the complexity of the process and the wide variety of potential variation sources, it is often impossible to pre-model all of them. But even when it is difficult or impossible to model *all* of the variation patterns off-line, a small subset can often be pre-modeled. However, the current methods for blind identifying un-modeled variation patterns (including the methods to be discussed in Chapters II and III) cannot utilize this partial information. Chapter IV presents a new method of identifying un-modeled variation patterns by utilizing information on some pre-modeled variation patterns. The new method blindly identifies un-modeled variation patterns from on-line measurement data, while simultaneously classifying some pre-modeled variation patterns by using some test statistics. The new method also has wider applicability than other existing methods of classifying pre-modeled variation patterns, since not all of the patterns need to be pre-modeled for its application (see Section IV.2). By utilizing partial a priori knowledge, the new method can estimate un-modeled variation patterns more accurately than the methods of purely blindly identifying un-modeled variation patterns (see Section IV.4).

The blind separation methods (including the methods to be discussed in Chapters II, III and IV) require additional assumptions regarding source distributions while the method of A&S requires certain structural conditions on the true \mathbf{C} . These methods can be used together to identify many un-modeled variation patterns. Chapter V presents an overall strategy for combining the methods. Moreover, the chapter specifies in detail how to verify whether or not the estimates of the un-modeled variation patterns that result from the blind separation methods are reasonable.

CHAPTER II

MANUFACTURING VARIATION DIAGNOSIS USING BLIND SOURCE SEPARATION APPROACH

The existing methods (PCA, factor rotation and A&S method) for identifying un-modeled manufacturing variation patterns have certain limitations, as discussed in Section I.3. The blind source separation methods seem to provide effective tools, which may overcome the limitations of existing methods. This chapter analyzes the blind separation methods in manufacturing situations, and also discusses several issues related to applying blind source separation methods for manufacturing variation diagnosis. The advantages of the blind separation methods over the existing methods will be discussed as well as the capabilities and limitations of the blind separation methods.

II.1 Blind source separation problem

Blind source separation is a term used to describe a number of related signal processing problems in which there is an array of spatially distributed sensors, each of which picks up signals from a number of distinct, signal-emitting sources (Cardoso, 1998; Haykin, 2000). Applications include radar and sonar signal processing, biomedical (e.g., EEG, EKG, fetal heartbeat) and geophysical signal monitoring, wireless communications, and speaker localization. For example, the situation with the classic blind separation example of speaker localization, sometimes referred to as the

cocktail-party problem, is illustrated. Suppose there are a number of people (the sources) speaking simultaneously in a room, and that there are also a number of microphones (the sensors) spatially distributed throughout the room. Let p and n denote the number of speakers and microphones, respectively, as shown in Figure 3. Let $x_{i,t}$ denote the signal recorded by the i^{th} microphone at time t , and let $v_{j,t}$ denote the speech signal emitted by the j^{th} speaker at time t . Each microphone signal will generally be a mixture of source signals received from all of the speakers (typically assumed to be a weighted linear combination) plus additive noise. Ignoring any time delays, the model can be written as

$$x_{i,t} = c_{i,1}v_{1,t} + c_{i,2}v_{2,t} + \dots + c_{i,p}v_{p,t} + w_{i,t}, \quad i = 1, 2, \dots, n, \quad (4)$$

where each $c_{i,j}$ is a weighting coefficient that depends on the distance between the i^{th} microphone and the j^{th} speaker. The quantity $w_{i,t}$ is the noise affecting microphone i at time t . Combining (4) for $i = 1, 2, \dots, n$, the form of the speaker localization model is identical to (1). Many other sensor-array signal processing problems yield a sensor/source model with this same linear structure. In radar signal processing, for example, the sources are p spatially distributed objects to be detected, and the sensors are an array of n spatially selective radar antennae. It is generally assumed that the p source signals are random and independent. The noise is sometimes assumed negligible in sensor-array signal processing, whereas in most manufacturing applications it would be non-negligible.

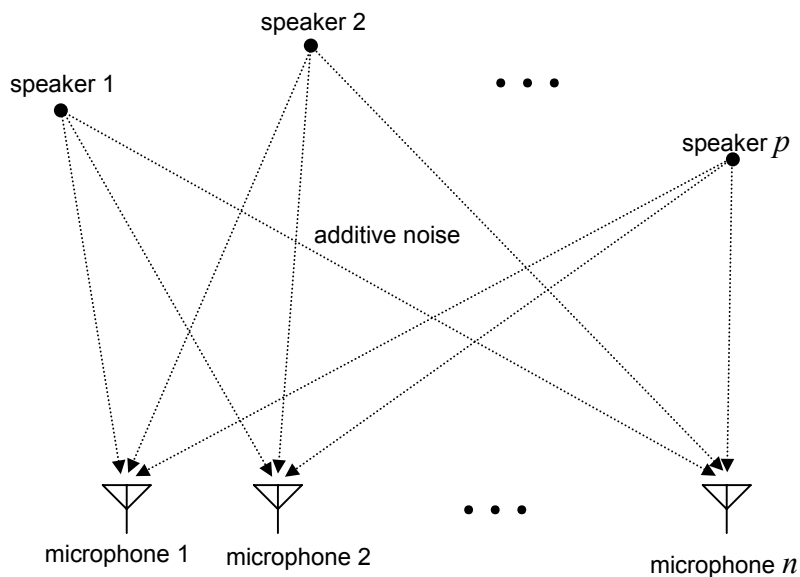


Figure 3 Illustration of the blind separation problem for speaker localization.

The term "blind" in blind separation refers to the situation where information on the sources must be determined solely from the data sample $(\mathbf{x}_t, t = 1, 2, \dots, N)$, with no prior knowledge of the relationship between the source and sensor signals other than the assumed structure of (1). To accomplish this, it is necessary to first estimate \mathbf{C} "blindly" from the data. If the objective in the speaker localization problem were purely to identify and track the location of each speaker, then estimation of \mathbf{C} would be the primary objective. Because the weighting coefficients contained in \mathbf{C} depend on the distances between the speakers and the microphones, triangulation

principles could be used to determine the location of each speaker. In radar, sonar, and other applications, the location of the sources can also be determined based on the weighting coefficients in \mathbf{C} (Monzingo and Miller, 1980). If, on the other hand, the objective in the speaker localization problem were to distinguish between the speech signals of each speaker, estimation of \mathbf{C} would only be an intermediate step. Once an estimate of \mathbf{C} is obtained, straightforward linear regression could be used to estimate each of the p individual speech signals over the data sample. This is similar to the objective in typical wireless communications applications, where the original source signals bear some transmitted information.

In manufacturing variation diagnosis, it may be useful to estimate both \mathbf{C} and the source signals. The columns of \mathbf{C} provide information on the spatial nature of the variation patterns, and the estimated source signals provide information on the temporal nature of the variation over the data sample. Although the primary focus of this dissertation is on estimating \mathbf{C} , the simulation example in Section II.3 illustrates how the source signals may be estimated and utilized.

II.2 Blind source separation methods

Since the classic blind source separation model is identical to (1), many of the blind separation methods apply directly to manufacturing variation diagnosis. This section discusses two main classes of blind separation algorithms – second-order methods and fourth-order methods. Each class involves a different set of additional assumptions regarding the characteristics of the source distributions, discussed in

Sections II.2.1 and II.2.2. Within each class, there are many variants. Rather than provide a comprehensive survey of the different variants, it is focused on a single method from each class that illustrates the main principles and that is relatively straightforward to implement. Comprehensive discussions can be found in Cardoso (1998), Hyvarinen and Oja (2000), and Hyvarinen (1999).

Most blind separation methods, including those discussed in this dissertation, use a form of PCA as the first step. As discussed in Section II.1, PCA reduces a problem to find an orthogonal matrix \mathbf{Q} that yields true \mathbf{C} . To estimate \mathbf{Q} uniquely, second-order method and fourth-order method use a different set of additional assumptions regarding the characteristics of the source distributions, to be discussed in Section II.4. This section provides backgrounds how the second-order and fourth-order methods can estimate \mathbf{Q} uniquely under certain constraints on source distributions.

Both the second-order and fourth-order methods work with a transformed version of the data with spatially white (uncorrelated) components. The whitened data vector is defined as $\mathbf{y} = \mathbf{W}\mathbf{x}$, where $\mathbf{W} = [\Lambda_p - \sigma^2 \mathbf{I}]^{-1/2} \mathbf{Z}_p'$ is the $p \times n$ "whitening matrix". Premultiplying (1) by \mathbf{W} and using the relationship $\mathbf{C} = \mathbf{Z}_p [\Lambda_p - \sigma^2 \mathbf{I}]^{1/2} \mathbf{Q}$, the transformed data vector becomes

$$\mathbf{y} = \mathbf{W}\mathbf{x} = \mathbf{W}[\mathbf{C}\mathbf{v} + \mathbf{w}] = \mathbf{Q}\mathbf{v} + \mathbf{W}\mathbf{w}. \quad (5)$$

Rather than working directly with the measurements \mathbf{x} , blind separation methods usually work with a transformed version with spatially whitened

(uncorrelated) components. The p -length whitened vector of measurements is defined as $\mathbf{y} = \mathbf{W}^{-1}\mathbf{x}$, where $\mathbf{W} = \mathbf{Z}_p[\Lambda_p - \sigma^2\mathbf{I}]^{1/2}$, and $\mathbf{W}^{-1} = [\Lambda_p - \sigma^2\mathbf{I}]^{-1/2}\mathbf{Z}_p'$ is a left inverse of \mathbf{W} ($\mathbf{W}^{-1}\mathbf{W} = \mathbf{I}$). From the relationship $\mathbf{C} = \mathbf{Z}_p[\Lambda_p - \sigma^2\mathbf{I}]^{1/2}\mathbf{Q} = \mathbf{W}\mathbf{Q}$, it follows that

$$\mathbf{y} = \mathbf{W}^{-1}\mathbf{x} = \mathbf{W}^{-1}[\mathbf{C}\mathbf{v} + \mathbf{w}] = \mathbf{Q}\mathbf{v} + \mathbf{W}^{-1}\mathbf{w}. \quad (6)$$

Since \mathbf{y} has diagonal covariance matrix $\mathbf{I} + \sigma^2[\Lambda_p - \sigma^2\mathbf{I}]^{-1}$, \mathbf{W}^{-1} is often referred to as the whitening matrix.

II.2.1 Second-order methods

Second-order methods utilize only second-order statistics (covariance and autocovariance) of the data. These methods impose the additional assumption that, of the p sources that are present, no pair has the exact same autocorrelation function. A necessary condition for this assumption to hold is that at least $p-1$ of the p sources are temporally autocorrelated. The noise is assumed to be temporally uncorrelated.

Let \mathbf{v}_t denote the source vector at time t . Define $\Sigma_{\mathbf{v}, \tau} = E[\mathbf{v}_t\mathbf{v}_{t+\tau}']$ to be the autocovariance matrix of \mathbf{v} at lag $\tau \geq 0$. By the assumption of source independence, $\Sigma_{\mathbf{v}, \tau}$ is a diagonal matrix with diagonal elements $\rho_{1, \tau}, \rho_{2, \tau}, \dots, \rho_{p, \tau}$ where $\rho_{i, \tau}$ is the autocorrelation function of v_i (the autocorrelation and autocovariance functions of the sources are equivalent, since they are scaled to have unit variance). From (6), the autocovariance matrix of \mathbf{y} at lag $\tau \geq 1$ is $\Sigma_{\mathbf{y}, \tau} = E[(\mathbf{Q}\mathbf{v}_t + \mathbf{W}^{-1}\mathbf{w}_t)(\mathbf{Q}\mathbf{v}_{t+\tau} + \mathbf{W}^{-1}\mathbf{w}_{t+\tau})'] = \mathbf{Q}\Sigma_{\mathbf{v}, \tau}\mathbf{Q}'$. Because \mathbf{Q} is an orthogonal matrix,

$$\mathbf{Q}'\Sigma_{y, \tau}\mathbf{Q} = \Sigma_{v, \tau} = \begin{bmatrix} \rho_{1, \tau} & & & \\ & \rho_{2, \tau} & & \\ & & \ddots & \\ & & & \rho_{p, \tau} \end{bmatrix} \quad (7)$$

is diagonal for all $\tau \geq 1$. Equation (7) forms the basis for second-order blind separation methods. Its significance is that the $p \times p$ orthogonal matrix \mathbf{Q} that yield true \mathbf{C} is the matrix that jointly diagonalizes the entire set $\Sigma_{y, \tau}$, $\tau \geq 1$. This joint diagonalizer is unique if the assumption holds that no pair of sources have the exact same autocorrelation function (see Theorem 3 of Belouchrani, Abed-Meraim, Cardoso, and Moulines, 1997).

When working with *sample* data, no single \mathbf{Q} will jointly diagonalize the sample $\Sigma_{y, \tau}$'s for all $\tau \geq 1$. Tong, Soon, Huang, and Liu (1990) proposed choosing \mathbf{Q} to be the orthogonal matrix that diagonalizes $\Sigma_{y, \tau}$ for a single specified τ . Belouchrani, et al. (1997) improved the approach by choosing \mathbf{Q} to be the orthogonal matrix that jointly, approximately diagonalizes $\Sigma_{y, \tau}$ for a set of τ 's (e.g., $\tau = 1, 2, \dots, 10$). Specifically, \mathbf{Q} is chosen to minimize the sum of the squares of the off-diagonal elements of the set of matrices $\mathbf{Q}'\Sigma_{y, \tau}\mathbf{Q}$ for the specified set of τ 's. Fortunately, there is a computationally efficient numerical method for accomplishing this. Belouchrani, et al. (1997) is referred for details of the algorithm, which is a generalization the Jacobi technique (Golub and Loan, 1989) for exactly diagonalizing a single matrix.

The reason the second-order method requires that the autocorrelation functions differ is somewhat apparent from the relationship $\Sigma_{y, \tau} = \mathbf{Q}\Sigma_{v, \tau}\mathbf{Q}'$. Consider the extreme case where all p sources have the exact same autocorrelation function $\rho_{i, \tau} = \rho_{\tau}$, $i = 1, 2, \dots, p$. Then for each τ , $\Sigma_{y, \tau} = \mathbf{Q}\Sigma_{v, \tau}\mathbf{Q}' = \rho_{\tau}\mathbf{Q}\mathbf{Q}' = \rho_{\tau}\mathbf{I}$, a scalar multiple of the identity matrix. *Any* orthogonal matrix will therefore diagonalize the entire set, and \mathbf{Q} cannot be uniquely identified.

II.2.2 Fourth-order methods

As the name suggests, fourth-order methods utilize fourth-order statistics to uniquely estimate \mathbf{Q} under their own specific set of additional assumptions. Whereas second-order methods impose assumptions on the source and noise autocorrelation, fourth-order methods impose the assumptions that **i**) no more than one of the p sources follows a Gaussian distribution, and **ii**) the noise is either negligible or follows a Gaussian distribution. Fourth-order methods can be derived as approximate maximum likelihood estimation (MLE) methods (Cardoso, 1998). In addition to the above assumptions, exact MLE methods typically assume that additional characteristics of the source distributions are known (e.g., that the sources follow uniform distributions). In this sense, the fourth-order methods involve a more relaxed set of assumptions and less *a priori* knowledge than exact MLE methods. There also exists a computationally efficient algorithm for their implementation (Cardoso and Souloumiac, 1993).

For an arbitrary zero-mean random vector $\mathbf{u} = [u_1, u_2, \dots, u_p]'$, the fourth-order cumulant of its i^{th} , j^{th} , k^{th} , and l^{th} elements, $1 \leq i, j, k, l \leq p$, is defined as

$$C_{i,j,k,l}(\mathbf{u}) = E[u_i u_j u_k u_l] - E[u_i u_j]E[u_k u_l] - E[u_i u_k]E[u_j u_l] - E[u_i u_l]E[u_j u_k]. \quad (8)$$

Note that $C_{i,i,i,i}(\mathbf{u})$ is the kurtosis of u_i . Three important cumulant properties are (Rosenblatt, 1985; Stuart and Ord, 1987): **i**) If \mathbf{u} is Gaussian, all of its fourth-order cumulants are zero; **ii**) If \mathbf{u} and \mathbf{z} are independent and of equal dimension, $C_{i,j,k,l}(\mathbf{u} + \mathbf{z}) = C_{i,j,k,l}(\mathbf{u}) + C_{i,j,k,l}(\mathbf{z})$; and **iii**) If the elements of \mathbf{u} are independent, all cross-cumulants of \mathbf{u} are zero. A cross-cumulant is defined as $C_{i,j,k,l}(\mathbf{u})$ with $i, j, k, l \neq i, i, i, i$.

Let \mathbf{U} be an arbitrary $p \times p$ orthogonal matrix, and consider the transformation $\mathbf{U}'\mathbf{y}$ of the whitened data. Since \mathbf{w} is assumed Gaussian and independent of \mathbf{v} , properties **i**) and **ii**) and Equation (6) imply that $C_{i,j,k,l}(\mathbf{U}'\mathbf{y}) = C_{i,j,k,l}(\mathbf{U}'\mathbf{Q}\mathbf{v})$. When \mathbf{U} is the desired orthogonal matrix \mathbf{Q} , $\mathbf{U}'\mathbf{Q}\mathbf{v} = \mathbf{v}$ has independent components, and all cross-cumulants of $\mathbf{U}'\mathbf{y}$ are zero by property **iii**). This fact forms the basis for fourth-order methods. The objective is to find the orthogonal matrix \mathbf{U} that minimizes the cross-cumulants of $\mathbf{U}'\mathbf{y}$, and \mathbf{Q} is then taken to be the minimizer. This can be viewed as finding the orthogonal transformation of (the already spatially uncorrelated) \mathbf{y} whose components are as independent as possible, where the cross-cumulants provide the measure of independence. This bears a close relationship to PCA, in which the data are transformed to have uncorrelated, but not necessarily independent, components.

Because of this, Comon (1994) has referred to blind separation methods of this type as independent components analysis.

Comon (1994) has suggested taking \mathbf{Q} to be the minimizer (over all $p \times p$ orthogonal matrices \mathbf{U}) of the sum of the squares of the entire set of cross-cumulants of $\mathbf{U}'\mathbf{y}$. Cardoso and Souloumiac (1993) proposed taking \mathbf{Q} to be the minimizer of a similar criterion

$$\sum_{\substack{1 \leq i, j, k, l \leq p \\ l \neq k}} C_{i, j, k, l}^2(\mathbf{U}'\mathbf{y}), \quad (9)$$

which involves only a subset of the cross-cumulants. For both of these criteria, $\mathbf{U} = \mathbf{Q}$ is the unique minimizer if there is at most one Gaussian source (Cardoso and Souloumiac, 1993). The advantage of (9), which is referred to as the joint approximate diagonalization of eigenmatrices (JADE) criterion, is that there exists a computationally efficient method for finding its minimizer. Cardoso and Souloumiac (1993) have shown that an equivalent expression for (9) is

$$\sum_{\substack{1 \leq i, j, k, l \leq p \\ l \neq k}} C_{i, j, k, l}^2(\mathbf{U}'\mathbf{y}) = \sum_{\substack{1 \leq i, j, k, l \leq p \\ l \neq k}} [\mathbf{U}'\mathbf{M}(i, j)\mathbf{U}]_{k, l}^2 \quad (10)$$

where $[\bullet]_{k, l}$ denote the k^{th} -row, l^{th} -column element of a matrix, and each $p \times p$ cumulant matrix $\mathbf{M}(i, j)$ ($1 \leq i, j \leq p$) is defined such that $[\mathbf{M}(i, j)]_{k, l} = C_{i, j, k, l}(\mathbf{y})$.

From (10), the JADE criterion is equivalent to finding the orthogonal matrix \mathbf{U} that minimizes the sum of the squares of the off-diagonal elements of the set of

transformed cumulant matrices $\{\mathbf{U}^T \mathbf{M}(i,j) \mathbf{U} : 1 \leq i, j \leq p\}$. This gives rise to the "joint diagonalization" term in the JADE acronym. The "approximate" term in the acronym stems from the fact that with sample data, no orthogonal transformation will result in all sample cross-cumulants exactly equal to zero. The sample cumulant matrices can only be approximately diagonalized in the sense that (10) is minimized. The sample cumulants are defined in the obvious way by replacing the expectations of the quantities in (8) with their sample averages.

Since the second-order and fourth-order methods involve similar joint approximate diagonalizations, the same computationally efficient generalization of the Jacobi technique can be used for both cases. Cardoso and Souloumiac (1993) is referred for details on the JADE algorithm, which is often used as a benchmark for evaluating other algorithms (Reed and Yao, 1998; Wax and Sheinvald, 1997).

II.3 An illustrative example

Consider the automotive crankshaft manufacturing process, which consists of a number of steps, including forging, rough cutting, finish cutting, drilling, grinding, and polishing. Figure 4 shows the geometry of a crankshaft produced in a manufacturing line in which there was an extensive amount of in-process measurement and inspection. Near the end of the line, for example, stylus traces around the circumference at a number of locations on the main bearings and pin bearings are taken automatically (for 100% of the crankshafts produced). The difference between the target diameter and the maximum, minimum, and average

diameter at each location is then logged (this example considers only the maximum diameter measurements). The bullet "•" symbols in Figure 4 indicate the locations at which the diameter measurements are taken. The diameters are measured at three locations along each of the five main bearings (Mains 1 through 5) and at five locations along each of the four pin bearings (Pins 1 through 4). The measurement vector \mathbf{x} for each crankshaft therefore consists of $n = 35$ diameter measurements.

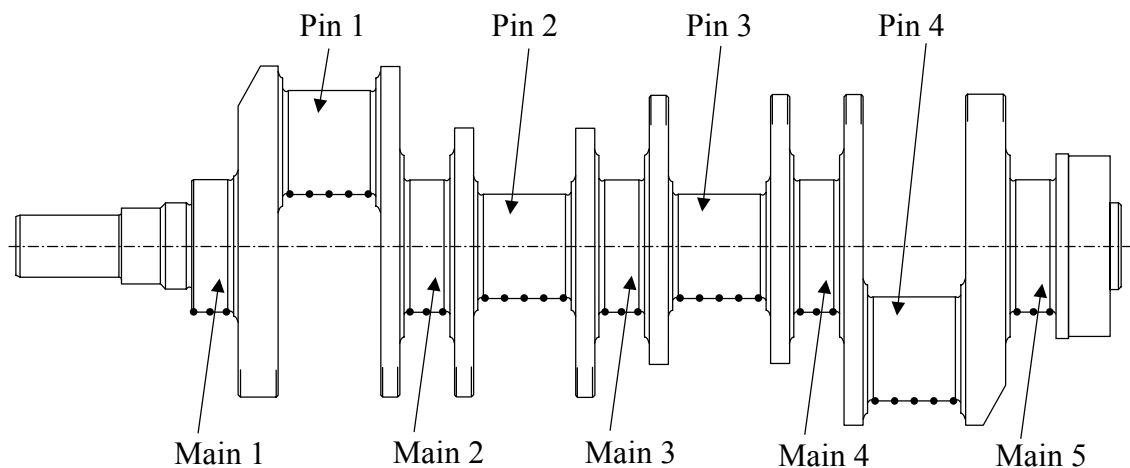


Figure 4 Geometry of the crankshaft in the example of Section II.3.

Based on a sample of $N = 247$ crankshafts, it was estimated (using the methods discussed in Apley and Shi, 2001) that $p = 3$ major variation sources were present. Estimates of the three variation pattern vectors and the corresponding source signals

using the fourth-order method are shown in Figures 5 through 7. The rotated version $\mathbf{Q}'\mathbf{y}_t$ of the whitened data was used as an estimate of \mathbf{v}_t . Each element of a pattern vector is represented as an arrow at the location of the corresponding diameter measurement. The length of the arrow is proportional to the magnitude of the element (the same scaling was used in all three figures). The sign of each element is represented by the direction of the arrow (pointing out of the crankshaft for a positive element and into the crankshaft for a negative element). Many elements of each pattern vector were negligibly small, in which case their arrows were omitted. Note that we could reverse the direction of all arrows without changing the meaning of the patterns. In other words, the i^{th} pattern represents *variation* in \mathbf{x} in both the positive \mathbf{c}_i and the negative \mathbf{c}_i directions. Whether the i^{th} pattern causes a diameter to increase or to decrease on a particular crankshaft (say crankshaft t) depends on whether $v_{i,t}$ is positive or negative. An arrow pointing out of the crankshaft, coupled with a positive source signal, represents an increase in diameter.

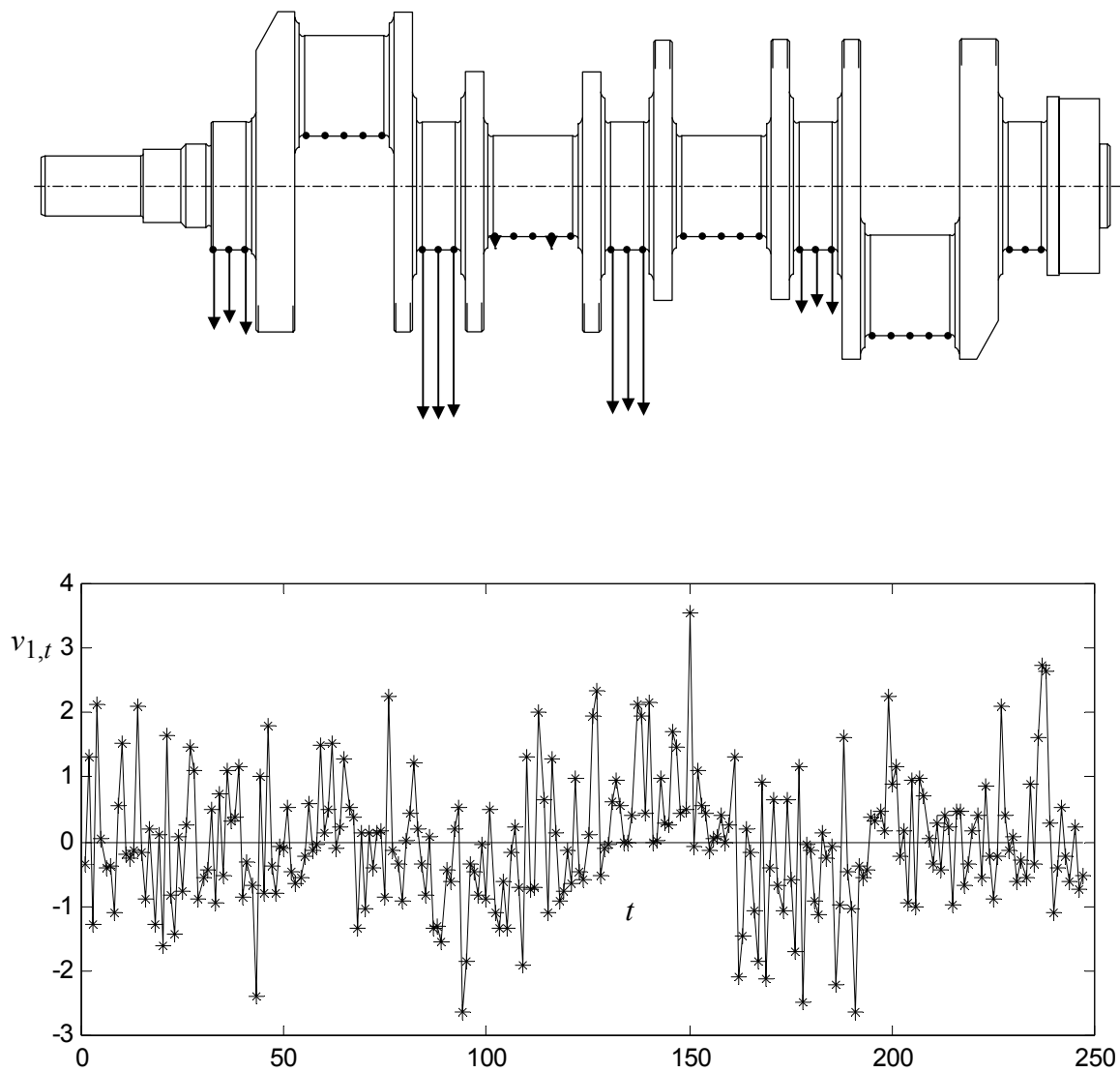


Figure 5 Estimates of the first pattern vector \mathbf{c}_1 (top panel) and source signal $v_{1,t}$ (bottom panel).

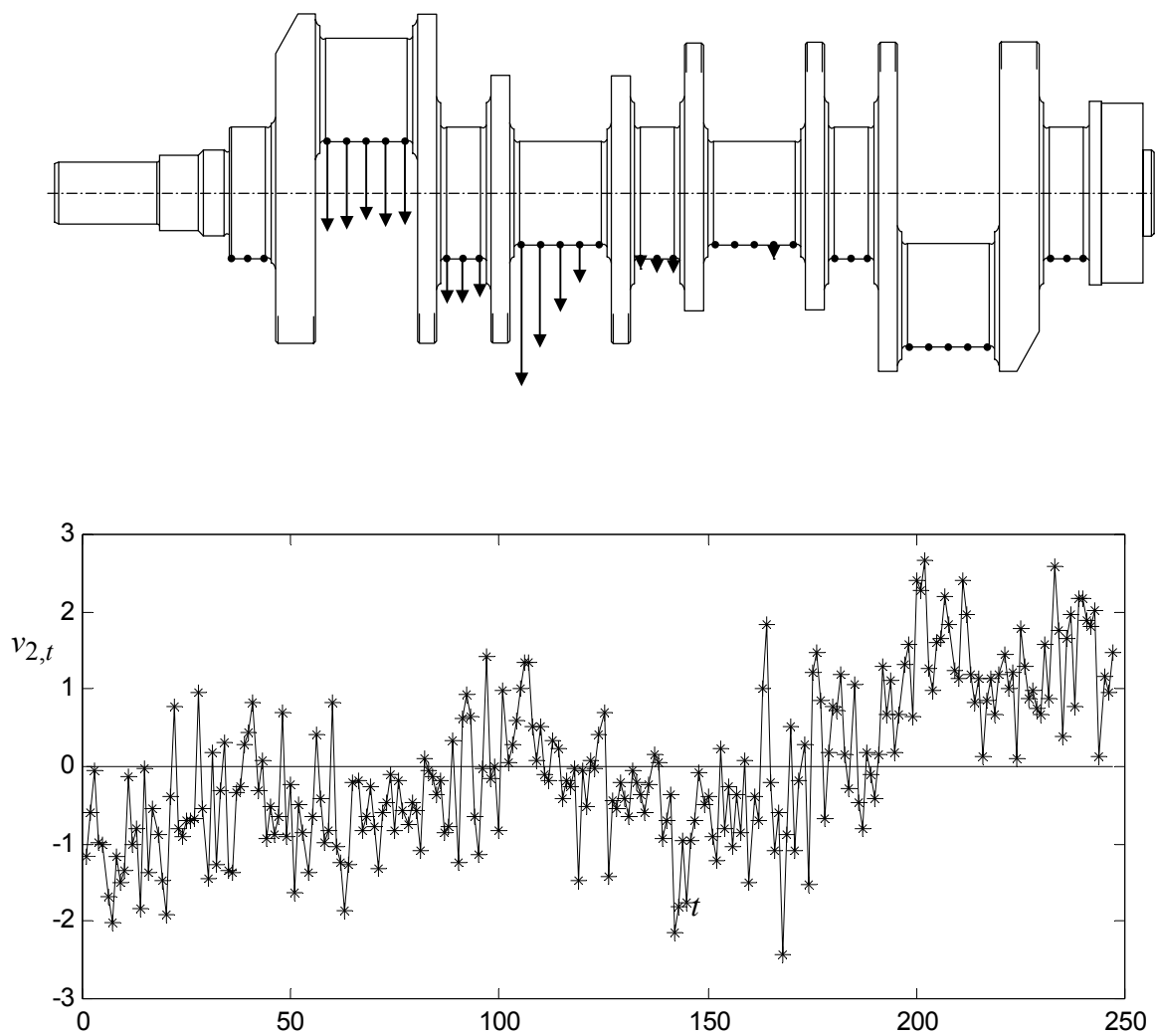


Figure 6 Estimates of the second pattern vector \mathbf{c}_2 (top panel) and source signal $v_{2,t}$ (bottom panel).

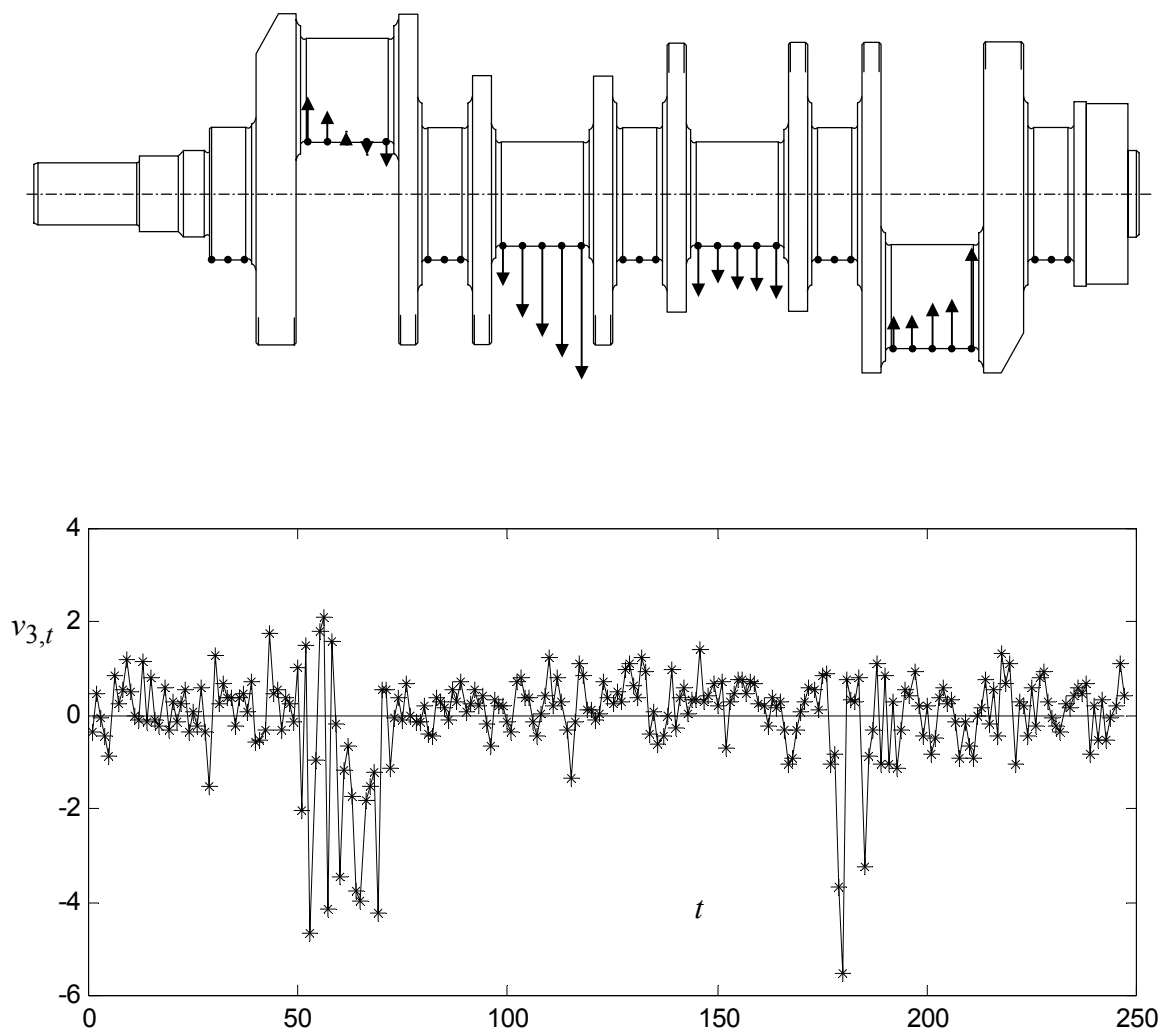


Figure 7 Estimates of the third pattern vector \mathbf{c}_3 (top panel) and source signal $v_{3,t}$ (bottom panel).

The three variation patterns were ordered in terms of decreasing severity, which is somewhat apparent by comparing the lengths of the arrows in Figures 5 through 7. We can quantify the severity of each source by noting that the *total variance* of \mathbf{x} is

$$\sum_{i=1}^n E[x_i^2] = E[\mathbf{x}'\mathbf{x}] = \sum_{i=1}^p E[(\mathbf{c}_i v_i)(\mathbf{c}_i v_i)] + E[\mathbf{w}'\mathbf{w}] = \sum_{i=1}^p \mathbf{c}_i' \mathbf{c}_i + n\sigma^2.$$

The contribution of the i^{th} source to the total variance is therefore $\mathbf{c}_i' \mathbf{c}_i$. The total variance for this example was 113, and the contributions of the three sources were $\mathbf{c}_1' \mathbf{c}_1 = 44.5$ (39.3%), $\mathbf{c}_2' \mathbf{c}_2 = 17.2$ (15.2%), and $\mathbf{c}_3' \mathbf{c}_3 = 16.0$ (14.2%). Together, the three sources account for 68.7% of the total variance of \mathbf{x} .

The illustrations in Figures 5 through 7 might be used by process operators and engineers to aid in diagnosing the major root causes of variation in the bearing diameters. The first variation source, illustrated in Figure 5, has a pronounced effect on all but one of the main bearings and no effect on the pin bearings. Since the arrows on Mains 1 through 4 all point in the same direction, this source causes all of the diameters on these bearings to either increase together or decrease together from crankshaft to crankshaft. The relative lengths of the arrows indicate that the diameters located near the middle of the crankshaft (Mains 2 and 3) vary by a much larger amount (roughly 2.5 times larger) than the diameters located nearer to the ends of the crankshaft (Mains 1 and 4). The diameters on Main 5, which is nearest to the end of the crankshaft, do not vary at all. One possible explanation is that the large cutting

forces generated during rough cut machining cause the middle of the crankshaft to flex more than the ends, which are held securely in chucks. We note that the first variation source alone accounted for 83.5% of the total variance of the Main 2 and Main 3 diameters.

The second variation source, illustrated in Figure 6, primarily affects Pins 1 and 2. Main 2, which is located between Pins 1 and 2, is slightly affected. The arrows in Figure 6 indicate that the second source causes the diameters on Pin 1 to increase/decrease uniformly along its length, while simultaneously causing a taper along Pin 2. The estimated source signal also provides insight into the temporal nature of the variation pattern that may aid in identifying its root cause. The plot of $v_{2,t}$ in Figure 6 shows that the second source tends to wander both above and below the zero value for extended periods of time, with a substantial shift occurring around the time of crankshaft 200. The third variation source, illustrated in Figure 7, affects only the Pins. If we visually smooth the arrows for this pattern, it appears that when the diameters near the middle of the crankshaft (Pins 2 and 3) increase, the diameters near the ends of the crankshaft (Pins 1 and 4) tend to decrease, and vice-versa. The plot of $v_{3,t}$ in Figure 7 also reveals an interesting temporal pattern. A large portion of the variation in the third source is due to only a few spikes in the data, occurring at around the times of crankshafts number 60 and 180. By inspection of the plot of $v_{3,t}$, it appears that the third source may come from a mixture of two different distributions during these temporary periods of large variability. The suspected root cause relates to the use of parallel machines to perform the same operation at certain locations in the

production line. The mixture distribution observed in $v_{3,t}$ most likely resulted from an intermittent problem experienced by only one of the parallel machines.

II.4 Discussion of the assumptions

Virtually all methods that attempt to uniquely estimate \mathbf{C} impose either explicit or implicit assumptions regarding either the structure of \mathbf{C} or the source distributions. This includes the method of A&S, blind source separation, and the varimax factor rotation method. Which method may produce a better estimate of \mathbf{C} depends largely on which assumptions are better satisfied. The purpose of this section is to compare the various assumptions and provide guidelines for how one may verify whether they are satisfied.

II.4.1 Comparing the assumptions

The varimax optimization criterion is intended to produce an estimate of \mathbf{C} whose elements are either large in magnitude or small in magnitude, with as few moderate sized elements as possible (Johnson and Wichern, 1998). For any valid estimate of \mathbf{C} , the sum of the squares of the elements of any one of its rows is a fixed quantity (equal to the variance of the corresponding element of \mathbf{x} , minus σ^2). Consequently, the varimax method seeks an estimate of \mathbf{C} whose structure is as close as possible to what is referred to as the ideal varimax structure:

$$\mathbf{C} = \begin{bmatrix} \mathbf{c}_{1,1} & & & \\ & \mathbf{c}_{2,2} & & \\ & & \ddots & \\ & & & \mathbf{c}_{p,p} \end{bmatrix}, \quad (11)$$

where $\mathbf{c}_{i,i}$ is an $n_i \times 1$ vector with $\sum_{i=1}^p n_i = n$. This assumes an appropriate re-ordering of the elements of \mathbf{x} . Hence, the ideal varimax structure is that the p variation sources affect p *disjoint* subsets of the elements of \mathbf{x} . If the true \mathbf{C} does not have this implicitly assumed structure, the varimax estimate would most likely be inaccurate.

The method of A&S assumes that \mathbf{C} has the ragged lower triangular structure

$$\mathbf{C} = \begin{bmatrix} \mathbf{c}_{1,1} & & & & \\ \mathbf{c}_{2,1} & \mathbf{c}_{2,2} & & & \\ \mathbf{c}_{3,1} & \mathbf{c}_{3,2} & \mathbf{c}_{3,3} & & \\ \vdots & \vdots & \vdots & \ddots & \\ \mathbf{c}_{p,1} & \mathbf{c}_{p,2} & \mathbf{c}_{p,3} & \cdots & \mathbf{c}_{p,p} \end{bmatrix}, \quad (12)$$

where $\mathbf{c}_{i,j}$ is an $n_j \times 1$ vector with $\sum_{i=1}^p n_i = n$. An additional assumption that each n_i is strictly greater than one is required in order that the subsets discussed below can be identified. The interpretation of (12) is that there exists a subset of n_1 measurements $\{x_1, x_2, \dots, x_{n_1}\}$ that are affected by only a single variation source, which will be called as the first source. The effects of the first source on the first measurement subset is represented by $\mathbf{c}_{1,1}$. There must also exist a second subset of n_2 measurements $\{x_{n_1+1}, x_{n_1+2}, \dots, x_{n_1+n_2}\}$ that are affected by only one of the *remaining* $p-1$ variation sources, which will be called as the second source. The

second subset of measurements may also be affected by the first source ($c_{2,1} \neq \mathbf{0}$), however, which is a major distinction between the ideal varimax structure and the assumed structure of A&S. There must also exist a third subset of measurements affected by only one of the remaining $p-2$ sources (although these measurements may also be affected by the first two sources), and so on.

Comparing (11) and (12), it is clear that the ideal varimax structure is a rather restrictive special case of the structure assumed in A&S. Hence, their method could be expected to produce a reasonable estimate of \mathbf{C} in many situations where the varimax method would not. Consider the crankshaft example discussed in Section II.3, and assume the true \mathbf{C} coincides with the estimates shown in Figures 5 through 7. Since the second source and the third source both have strong effect on the diameter measurements for Pins 1 and 2, \mathbf{C} does not possess the ideal varimax structure. In contrast, \mathbf{C} does possess the structure of (12). Pins 3 and 4 are affected by only a single source (the source illustrated in Figure 7). The first measurement subset $\{x_1, x_2, \dots, x_{n_1}\}$ would consist of the 10 diameter measurements taken on Pins 3 and 4. Although Pins 1 and 2 are also affected by this source, they are affected by only one (the source illustrated in Figure 6) of the *remaining* two sources. The second measurement subset $\{x_{n_1+1}, x_{n_1+2}, \dots, x_{n_1+n_2}\}$ would therefore consist of the 10 diameter measurements taken on Pins 1 and 2. The situation is similar for the two variation patterns depicted in Figures 1 and 2. Since Features 2 and 4 are affected by

only one of the two variation sources, \mathbf{C} possesses the structure of (12), but it does not possess the ideal varimax structure.

Even when \mathbf{C} possesses the structure (12) required in the A&S method, there is often ambiguity in selecting the measurement subset affected by a single source, for reasons that are discussed in Section II.4.2. When this measurement subset is selected incorrectly, or when \mathbf{C} does not possess the required structure, the method of A&S would not be expected to produce accurate estimates. Blind separation methods may still apply in these situations, since they make no assumptions regarding the structure of \mathbf{C} . This broader applicability with respect to the structure of \mathbf{C} comes at the expense of narrower applicability with respect to the source distributions. Recall that the fourth-order method requires that no more than one of the p sources follows a Gaussian distribution, and the second-order method requires that no pair of sources shares the same autocorrelation function. The latter is equivalent to requiring that for each pair (i, j) with $1 \leq i \neq j \leq p$, there exists a $\tau = \tau(i, j)$ such that $\rho_{i, \tau} \neq \rho_{j, \tau}$. In other words, the second-order assumptions are satisfied as long as the autocorrelation functions for each pair of sources differ for at least one time lag (providing the autocovariance matrix at this time lag is included in the set to be jointly diagonalized).

In Chapter III, a method is developed for optimally combining the second-order and fourth-order joint diagonalization criteria in order to relax the blind separation assumptions required for uniquely identifying \mathbf{C} . Section III.2 shows that the condition for uniquely identifying \mathbf{C} using the combined criteria is that no pair of *Gaussian* sources share the same autocorrelation function. This is weaker than the

assumption in the second-order method that no pair of sources, Gaussian or not, share the same autocorrelation function. It is also weaker than the assumption in the fourth-order method that no more than one source is Gaussian, since two or more Gaussian sources are allowed if their autocorrelation functions differ. Hence, the combined method would have broader applicability than either the second-order method or the fourth-order method, individually.

It should be noted that the blind separation conditions are theoretical conditions that result in the unique identification of \mathbf{C} in the hypothetical situation where one has available the theoretical covariances and cumulants (or, equivalently, infinitely large samples). With finite sample sizes, the performance of the methods depends on the *extent* to which their assumptions are satisfied, as will be illustrated in Section II.5.

II.4.2 Verifying the assumptions

Regardless of which method is used, an attempt to verify that its assumptions are satisfied is recommended. In this respect, the blind separation methods have an advantage over the method of A&S. First note that the original sources satisfy the required assumptions of the methods if, and only if, the estimated sources do. The rotated version $\mathbf{Q}'\mathbf{y}_t$ of the whitened data can be used as an estimate of \mathbf{v}_t . For the fourth-order method, histograms of the estimated sources are useful for determining whether there are more than one Gaussian source. For the second-order method, a plot of the sample autocorrelation functions of the estimated sources is useful for determining whether a pair of sources share the same autocorrelation function. Figures 8 and 9 show histograms and sample autocorrelation functions for the three source signals from the crankshaft example (the estimated signals are shown in Figures 5 through 7). The distributions of the second and third sources appear to be non-Gaussian, which satisfies the assumptions of the fourth-order method. In contrast, the autocorrelation functions for the first and third sources appear quite similar, which would violate the assumptions of the second-order method.

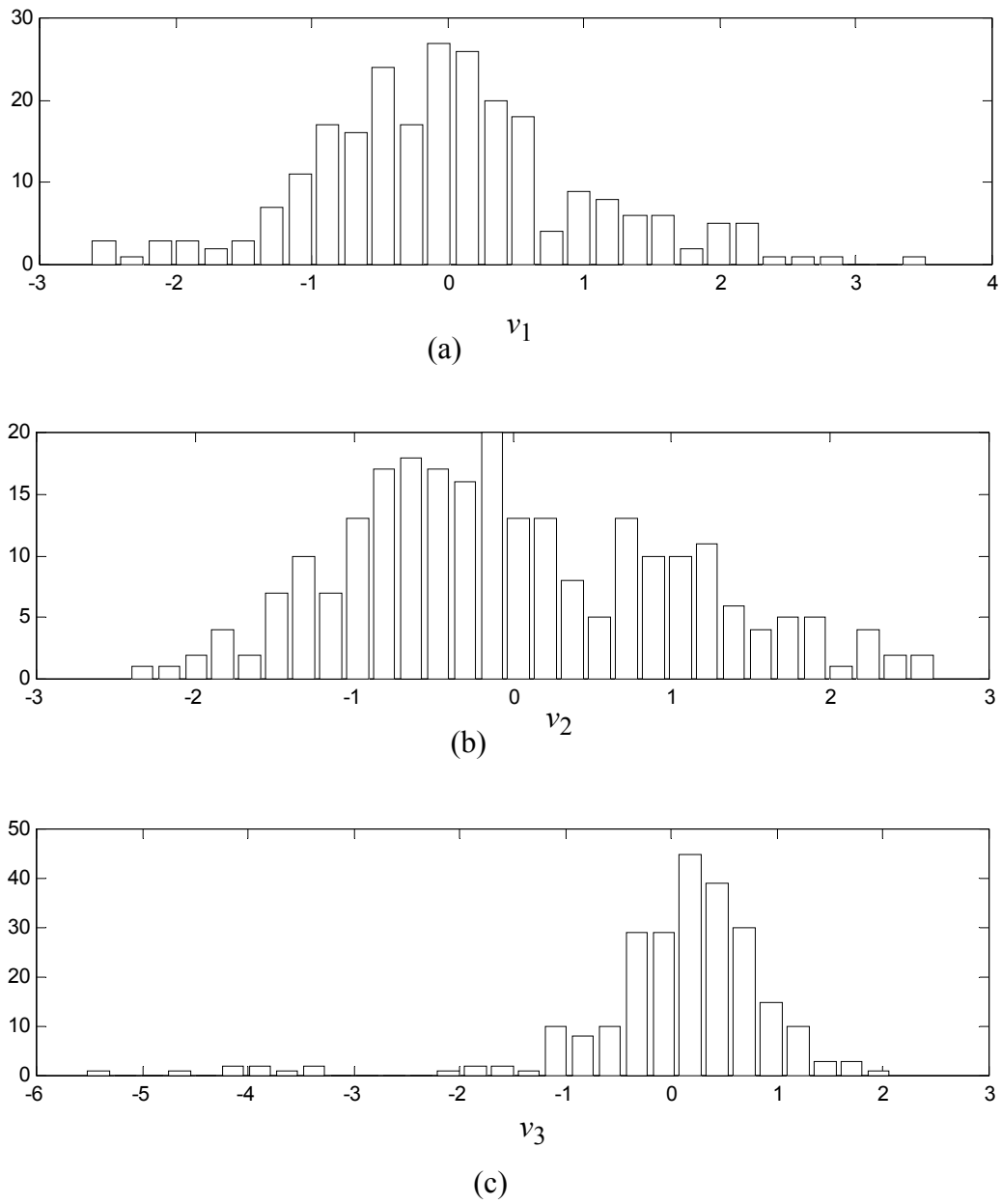


Figure 8 Histograms for the three source signal from the crankshaft example.

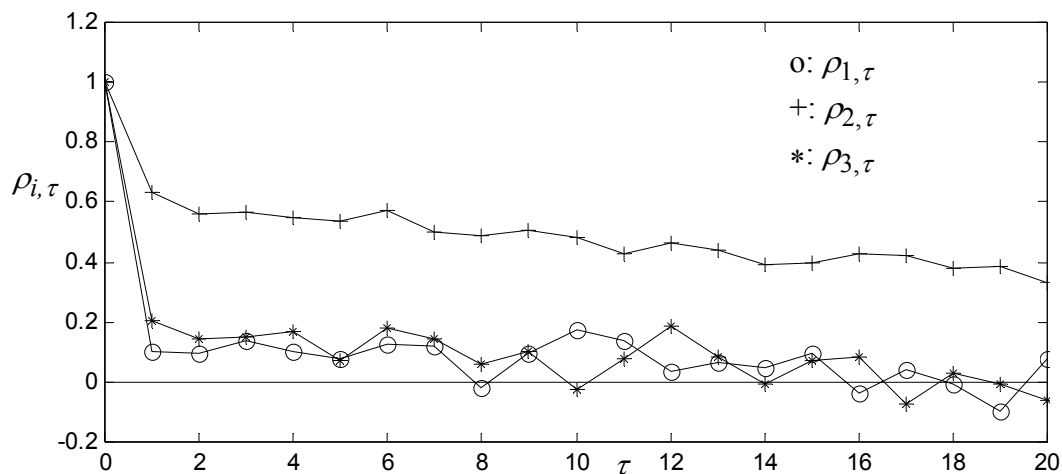


Figure 9 Sample autocorrelation functions for the three source signal from the crankshaft example.

When using the method of A&S, it is more difficult to verify whether the structural requirement (12) for \mathbf{C} is satisfied. This relates to how one identifies the measurement subset that is affected by only one source. The strategy described in A&S is as follows. The latent covariance matrix is defined as the portion of $\Sigma_{\mathbf{x}}$ that is due to the sources. From (2) and (3), the latent covariance matrix is $\mathbf{C}\mathbf{C}' = \mathbf{Z}_p[\Lambda_p - \sigma^2\mathbf{I}]\mathbf{Z}_p'$, which can be determined from the PCA step. The latent correlation matrix is defined in the usual way from the latent covariance matrix. Apley and Shi (2001) have shown that if a subset of measurements are affected by a single variation source, their

(theoretical) latent correlation coefficients are all ± 1 . The procedure for finding the subsets is to inspect the (sample) latent correlation matrix for a subset of measurements with latent correlation coefficients that are all close to one in magnitude.

While a subset of measurements affected by a single source will have latent correlation coefficients that are all ± 1 , the converse is not always true. Consider the situation where $n = 4$, $p = 2$, $\mathbf{c}_1 = [1 \ 1 \ 1 \ 1]'$, and $\mathbf{c}_2 = [1 \ 1 \ -1 \ -1]'$. The latent correlation matrix in this case is

$$\begin{bmatrix} 1 & 1 & 0 & 0 \\ 1 & 1 & 0 & 0 \\ 0 & 0 & 1 & 1 \\ 0 & 0 & 1 & 1 \end{bmatrix}.$$

Since two measurement subsets $\{x_1, x_2\}$ and $\{x_3, x_4\}$ have unit magnitude latent correlation coefficients, one might incorrectly conclude that each of these subsets is affected by only a single source. The reason these subsets have a high latent correlation value is that the effects on $\{x_1, x_2\}$ of the first and second source are $[1 \ 1]'$ and $[1 \ 1]'$, respectively, which are identical. Likewise, the effects on $\{x_3, x_4\}$ of the first and second source are $[1 \ 1]'$ and $[-1 \ -1]'$, respectively, which only differ by a constant scale factor. If the method of A&S were applied using either of these two subsets, the estimates of \mathbf{c}_1 and \mathbf{c}_2 would be $[\sqrt{2} \ \sqrt{2} \ 0 \ 0]'$ and $[0 \ 0 \ \sqrt{2} \ \sqrt{2}]'$, which differ substantially from the true pattern vectors. Note that these also coincide with the varimax estimates. In situations like this, it is difficult to verify whether high

latent correlation is the result of \mathbf{C} truly possessing the structure of (12), or the result of two or more sources having exactly the same effect (up to a constant scale factor) on a measurement subset.

Because of this, there is a higher level of subjectivity involved in the A&S method than in the blind separation methods. The primary subjectivity in blind separation lies in deciding whether the fourth-order or second-order method should be used, which relates to verifying whether the fourth-order or second-order assumptions are better satisfied. It is relatively straightforward to do this using histograms and autocorrelation plots, as described earlier. This subjectivity may be further reduced if the fourth-order and second-order criteria are combined as in Chapter III.

II.5 Effect of violating assumptions

The purpose of this section is to provide insight into how the performance of the blind separation methods is affected when their assumptions are violated or are close to being violated. A simulation example is used, in which a beam represents the part being manufactured, and $n = 20$ measurements are distributed uniformly across the beam. There are two variation sources, with \mathbf{c}_1 and \mathbf{c}_2 as illustrated in Figures 10(a) and 10(b), respectively. For purpose of simplicity, the number of sources is assumed to be known for simplicity, although in practice this must also be estimated. Apley and Shi (2001) discuss in detail a number of methods for estimating p .

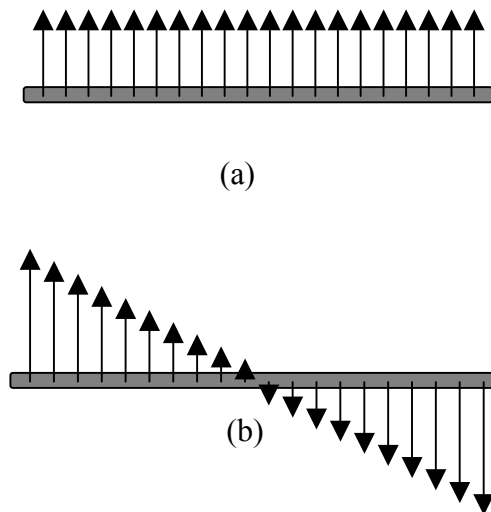


Figure 10 Illustration of the two variation patterns in the example: (a) \mathbf{c}_1 , which represents a beam translation and (b) \mathbf{c}_2 , which represents a beam rotation.

The beam can be considered a subcomponent of a larger assembly, in which case the variation patterns may represent assembly variation. The first pattern represents a rigid vertical translation of the beam, and the second pattern a rigid rotation around the beam centroid. Alternatively, the beam can be considered a separate part, in which case the variation patterns may represent fabrication (e.g., extrusion) variation. In this case, the first pattern represents variation in the thickness of the beam that occurs uniformly across its length. The second pattern represents thickness variation that, when larger on one end of the beam, is smaller on the other end.

Both pattern vectors are scaled so that the total variance due to each source ($\mathbf{c}_i' \mathbf{c}_i$) is equal to the total variance due to the noise ($n\sigma^2$). In other words, the signal-to-noise ratio $\mathbf{c}_i' \mathbf{c}_i (n\sigma^2)^{-1}$ is unity for each source. The noise variance σ^2 is also unity. The first source follows a first-order autoregressive (AR) model $v_{1,t} = \phi v_{1,t-1} + a_t$, where $\phi = 0.9$, and the a_t 's are zero-mean, independent, Gaussian random variables with variance $\sigma_a^2 = 1 - \phi^2$. First-order AR processes are widely encountered in industrial environments (Box, et al., 1994). The variance and autocorrelation function of a first-order AR process are $\sigma_a^2 (1 - \phi^2)^{-1}$ and $\rho_\tau = \phi^\tau$ ($\tau = 0, 1, 2, \dots$), respectively. The marginal distribution of the first source is therefore Gaussian with zero mean and unit variance, and its autocorrelation function is $\rho_{1,\tau} = 0.9^\tau$. The second source $v_{2,t}$ follows a (scaled and shifted) Bernoulli distribution, where the two values ± 1 each occur with equal probability 0.5. Variation sources of this nature are also commonly observed in manufacturing, the root cause of which may be two parallel machines performing the same operation or the use of components or raw materials from two different suppliers. The second source is temporally uncorrelated. Since only one source is Gaussian, and the autocorrelation functions for the two sources differ, the assumptions of both the second-order method and the fourth-order method are satisfied.

By inspection of Figure 10, $\mathbf{C} = [\mathbf{c}_1 \ \mathbf{c}_2]$ possesses neither the ideal varimax structure (11) nor the structure (12) required in the A&S method. The structure of \mathbf{C} is

close to (12), however, since the second source has very little effect on the two measurements that lie closest to the beam centroid. Ordering the measurements from left to right, these two measurements are referred to as x_{10} and x_{11} . The elements of \mathbf{c}_1 and \mathbf{c}_2 associated with $\{x_{10}, x_{11}\}$ are $[1 \ 1]'$ and $[0.087 \ -0.087]'$, respectively. It can be shown that the latent correlation coefficient for x_{10} and x_{11} is 0.985, which is relatively large. When $\{x_{10}, x_{11}\}$ is selected as the measurement subset affected by only a single source, the performance of the A&S method is quite similar to the blind separation performance discussed below. One must use caution when applying the A&S method in this example, however. The elements of \mathbf{c}_1 and \mathbf{c}_2 associated with the two left-most measurements $\{x_1, x_2\}$ are $[1 \ 1]'$ and $[1.65 \ 1.47]'$, respectively. It follows that the latent correlation coefficient for x_1 and x_2 is 0.9986, which is even larger than the latent correlation for x_{10} and x_{11} . When $\{x_1, x_2\}$ is selected as the measurement subset affected by only a single source, the A&S estimates (using the theoretical covariance matrix) of the two pattern vectors are the orthogonal linear combinations $0.55\mathbf{c}_1+0.84\mathbf{c}_2$ and $0.84\mathbf{c}_1-0.55\mathbf{c}_2$ of the true pattern vectors.

A Monte Carlo simulation with 10,000 replicates is used to compare the second-order and fourth-order blind separation methods. A sample size of $N = 200$ is assumed, and the autocovariance matrices for lags $\tau = 1, 2, \dots, 6$ are used in the second order-method. Figure 11 and Figure 12 show the estimated pattern vectors and source signals for a typical replicate. The estimated pattern vectors are reasonably close to the true pattern vectors shown in Figure 10 and would most likely be correctly interpreted as a translation and a rotation of the beam. The estimated source signals shown in Figure 11(b) and Figure 12(b) are noisy versions of the true source signals. From the histograms of the estimated signals shown in Figure 13, the second source is clearly non-Gaussian, which indicates that the fourth-order assumptions are met. Figure 14 shows that the two sources have substantially different sample autocorrelation functions, which indicates that the second-order assumptions are also met.

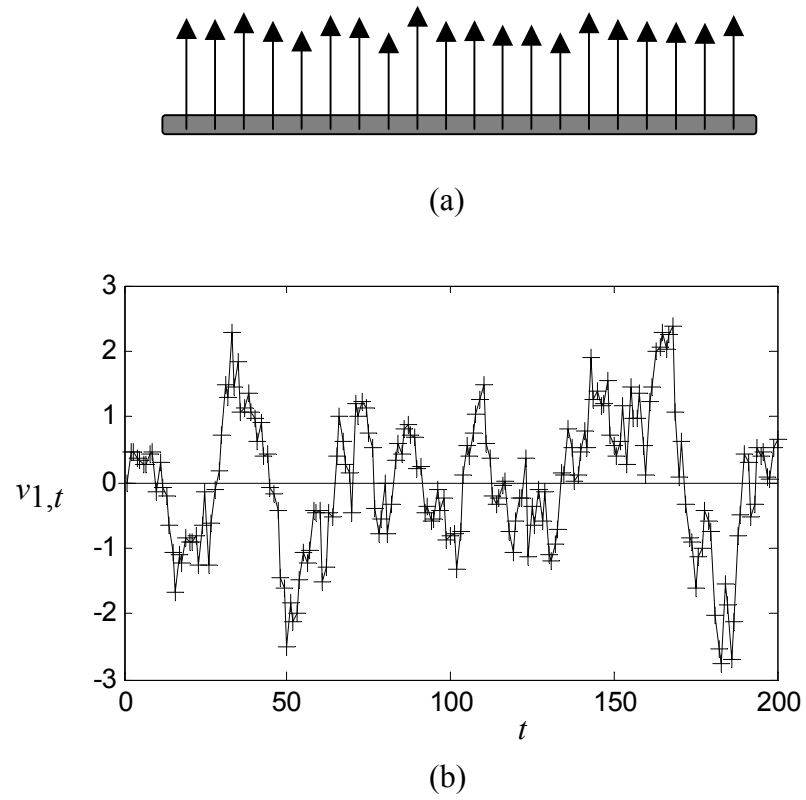


Figure 11 Estimates of the pattern vectors and source signals in the simulation example; (a) the estimate of \mathbf{c}_1 and (b) the estimate of $v_{1,t}$

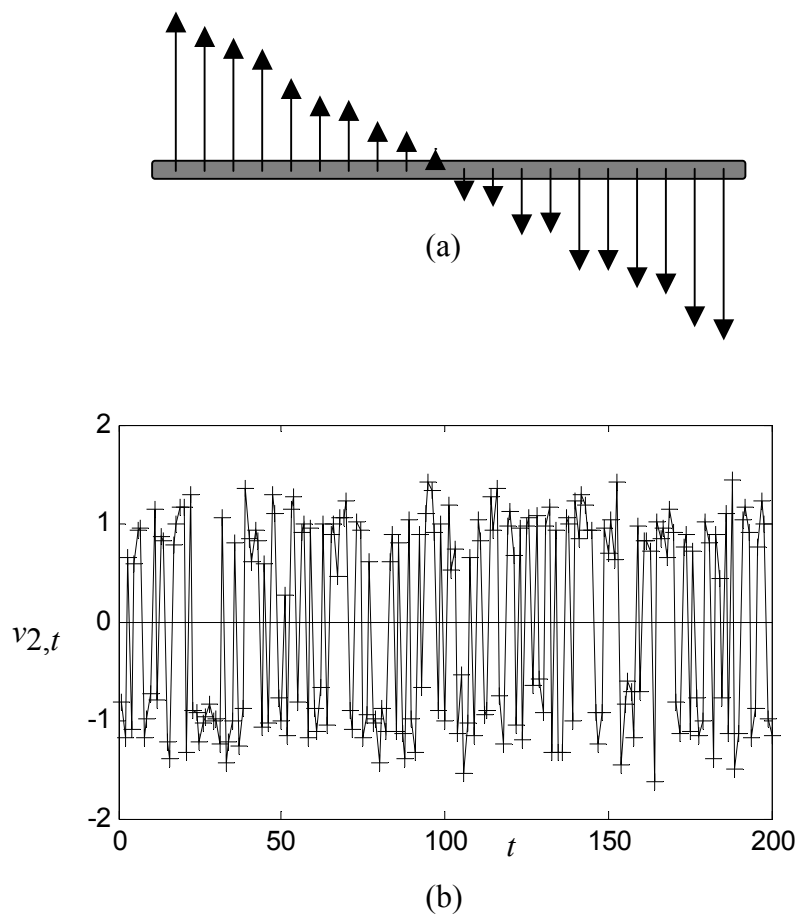
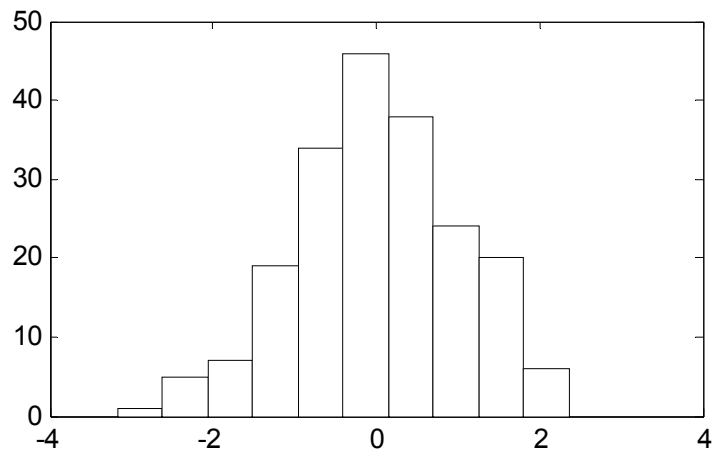
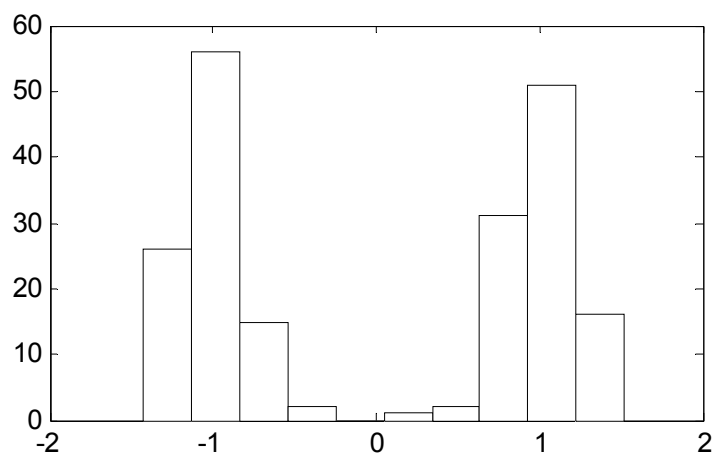


Figure 12 Estimates of the pattern vectors and source signals in the simulation example; (a) the estimate of \mathbf{c}_2 and (b) the estimate of $v_{2,t}$



(a)



(b)

Figure 13 Histograms of the estimated source signals in the simulation example; (a) histogram of estimates of v_1 and (b) histogram of estimates of v_2

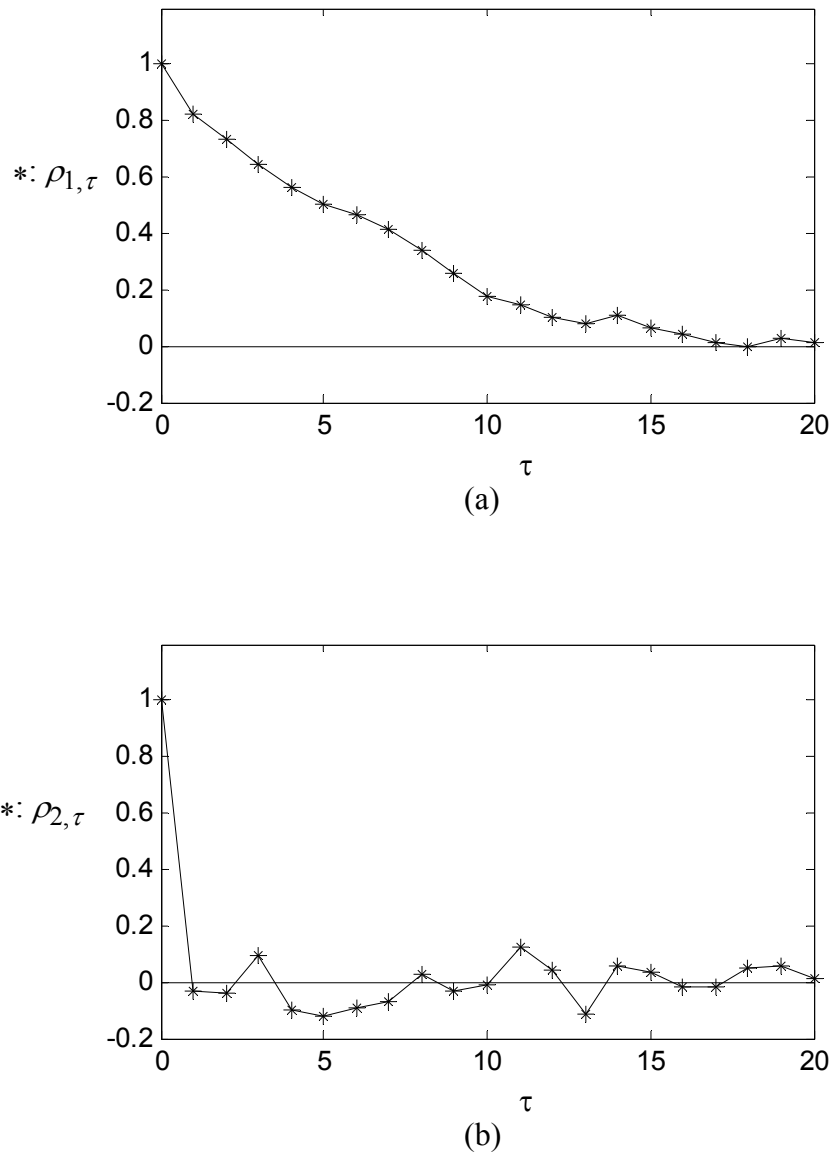


Figure 14 Sample autocorrelation functions of the estimated source signals in the simulation example; (a) sample autocorrelation function of estimates of v_1 and (b) sample autocorrelation function of estimates of v_2

In order to evaluate the performance of the second-order and fourth-order methods over the entire Monte Carlo simulation, consider the performance measure $J_i = E[\|\hat{c}_i - c_i\| \|c_i\|^{-1}]$, where \hat{c}_i denotes an estimate of c_i ($i = 1, 2$). The average value of $\|\hat{c}_i - c_i\| \|c_i\|^{-1}$ over the 10,000 replicates is used to estimate J_1 and J_2 for both methods. The results, which are shown in the first row of Table 1, indicate that both methods perform similarly for this example.

Table 1 Performance of the Second-order and Fourth-order Methods as Their Assumptions Come Closer to Being Violated.

v_1 autocorrelation	v_2 distribution	Fourth-order method		Second-order method	
		J_1	J_2	J_1	J_2
$\phi = 0.9$	Bernoulli	0.075	0.097	0.103	0.082
$\phi = 0.9$	uniform	0.103	0.116	0.104	0.083
$\phi = 0.9$	triangular	0.234	0.236	0.103	0.082
$\phi = 0.9$	Gaussian	0.362	0.360	0.104	0.082
$\phi = 0.7$	Bernoulli	0.075	0.098	0.116	0.098
$\phi = 0.5$	Bernoulli	0.075	0.098	0.144	0.132
$\phi = 0.3$	Bernoulli	0.075	0.097	0.277	0.270
$\phi = 0$	Bernoulli	0.074	0.098	0.568	0.567
$\phi = 0$	Gaussian	0.361	0.360	0.567	0.567

The remainder of this section investigates the performance of the two methods as their assumptions come closer to being violated. While the first source remained Gaussian, the distribution of the second source is modified from the Bernoulli distribution to the uniform, triangular, and Gaussian distributions shown in Figure 15, each having zero mean and unit variance. This represents the second source distribution coming successively closer to the Gaussian distribution in terms of its kurtosis. Note that the kurtosis for the Bernoulli, uniform, triangular, and Gaussian distributions are -2 , -1.2 , -0.6 , and 0 , respectively. When the second source is exactly Gaussian, the assumptions of the fourth-order method are violated. The results, using 10,000 Monte Carlo replicates to estimate J_1 and J_2 , are shown in Table 1. The performance of the fourth-order method clearly deteriorates as the distribution of the second source comes closer to the Gaussian. Its performance is still reasonable ($J_i \approx 0.1$), however, when the second source distribution is uniform. The performance of the second-order method is unaffected by the source distribution.

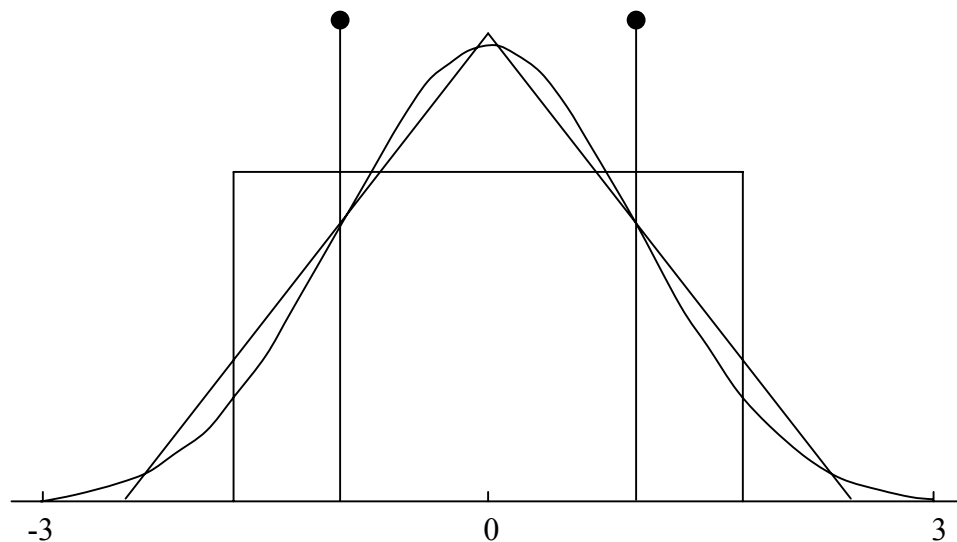


Figure 15 The Bernoulli, uniform, triangular, and Gaussian distributions (with mean zero and unit variance) used for the second source. The Bernoulli distribution is discrete, whereas the others are continuous distributions.

The situation is reversed as the assumptions regarding the source autocorrelation in the second-order method come closer to being violated. While the second source remains temporally uncorrelated, the autocorrelation of the first source is reduced by decreasing the AR parameter ϕ , as illustrated in Figure 16. For $\phi = 0$, the first source is uncorrelated, and the assumptions of the second-order method are violated. Table 1 indicates that the performance of the second-order method

deteriorates rapidly for $\phi < 0.5$, whereas the fourth-order method is unaffected by the source autocorrelation.

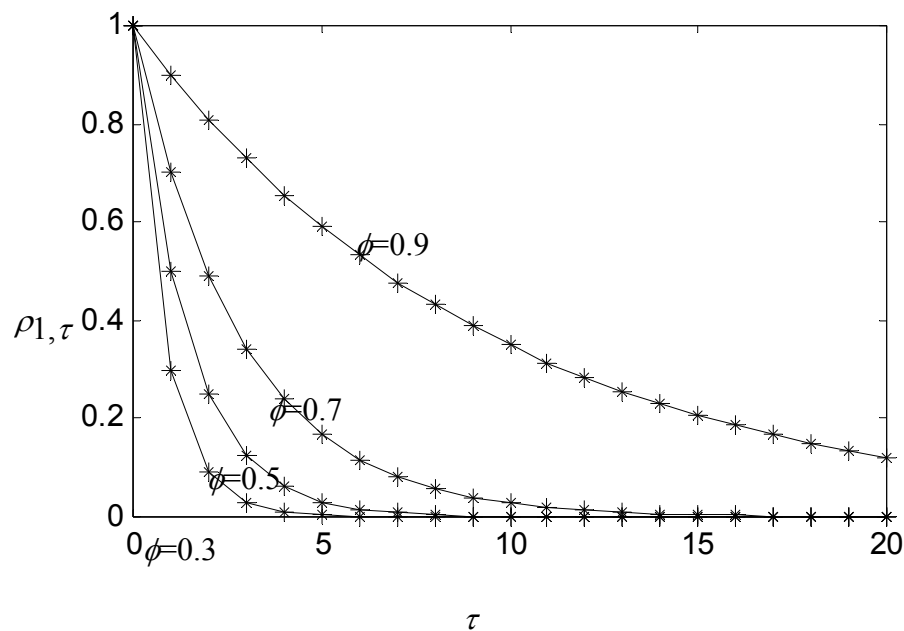


Figure 16 Autocorrelation function $\rho_{1,\tau} = \phi^\tau$ of the first-order AR source v_1 , for various ϕ .

The last row of Table 1 shows the results when the assumptions for both methods are violated, in which case neither method performs well. In comparison, the A&S method is still quite effective ($J_1 = 0.108$, $J_2 = 0.085$) in this situation when $\{x_{10}, x_{11}\}$ is selected as the first measurement subset. For the reasons discussed above,

however, it performs poorly ($J_1 = 0.574$, $J_2 = 0.573$) when $\{x_1, x_2\}$ is selected as the first measurement subset.

It has also been observed that the performance measures for both the second-order and the fourth-order methods are roughly inversely proportional to the square root of the sample size N and the square root of the signal-to-noise ratio. This agrees with the asymptotic results discussed in Cardoso (1998), for example.

II.6 Accomodating other noise covariance structures

Throughout this dissertation, it has been assumed that $\Sigma_w = \sigma^2 \mathbf{I}$. In other words, the noise variables associated with each element of \mathbf{x} are uncorrelated and have equal, but unknown, variance. In applications where the elements of \mathbf{x} are similar entities obtained via similar measurement principles, this would often be a reasonable assumption. In this situation, one may even take the view that the noise variance for each element of \mathbf{x} *should* be equal. If $\Sigma_w = \sigma^2 \mathbf{I}$ is assumed, but a particular element of \mathbf{w} has much larger variance (because of larger measurement error, for example), this would appear as an additional variation pattern. The only nonzero element of the associated pattern vector would correspond to the element of \mathbf{w} with larger variance. This may provide an indication that the apparatus used to measure that particular element of \mathbf{x} should be recalibrated or replaced.

Many factor rotation methods only assume that $\Sigma_w = \text{diag}\{\sigma_1^2, \sigma_2^2, \dots, \sigma_n^2\}$ is diagonal (Johnson and Wichern, 1998). When the elements of \mathbf{x} represent different

entities measured on different scales, this would be more appropriate than assuming $\Sigma_w = \sigma^2 \mathbf{I}$. The blind separation algorithms may still be applied in this situation, as long as the diagonal Σ_w is known (up to multiplication by a scalar constant) or a reasonable estimate is available. Before applying the algorithms, the data would first be transformed via $\Sigma_w^{-1/2} \mathbf{x} = (\Sigma_w^{-1/2} \mathbf{C}) \mathbf{v} + \Sigma_w^{-1/2} \mathbf{w}$, where $\Sigma_w^{-1/2} = \text{diag}\{\sigma_1^{-1}, \sigma_2^{-1}, \dots, \sigma_n^{-1}\}$. Since the covariance matrix of the transformed noise $\Sigma_w^{-1/2} \mathbf{w}$ is a scalar multiple of the identity matrix, blind separation algorithms can be applied directly to the transformed data to produce an estimate of $\Sigma_w^{-1/2} \mathbf{C}$. This estimate can then be transformed back to \mathbf{C} by premultiplying by $\Sigma_w^{1/2}$.

An estimate of Σ_w would often be available in the context of manufacturing statistical process control (SPC). The estimate could be obtained by estimating the noise variances $\{\sigma_1^2, \sigma_2^2, \dots, \sigma_n^2\}$ from a sample of data collected when the process is known to be in-control (i.e., when there are no variation sources present, so that $\mathbf{x} = \mathbf{w}$). Gage repeatability and reproducibility studies might also be used to estimate the noise variances.

An alternative to estimating the noise variances is to assume they are such that $\sigma_i = \alpha T_i$ ($i = 1, 2, \dots, n$), where T_i denotes the width of the tolerance interval assigned to x_i , and α is some arbitrary scale factor. In other words, the assumption would be that the standard deviation of each x_i is proportional to its tolerance width when no variation sources are present other than the noise. Borrowing SPC terminology, this

may be viewed as *common cause* variability. This assumption translates to equal process capability ratios (the tolerance width divided by six standard deviation units) for all elements of \mathbf{x} when only common cause variability is present. Although there is no statistical validity to this assumption, it has a conceptual appeal. First, tolerances are often assigned and/or manufacturing processes designed so that common cause variability is proportional to the tolerance width. Second, suppose that with only common cause variability present, the process capability ratio for a particular element of \mathbf{x} was substantially smaller than for the other elements. If the blind separation methods were applied under the assumption of equal process capability ratios, the result would be an additional variation pattern affecting only the variable with the low process capability. This would rightly call attention to the variable in most need of quality improvement efforts.

II.7 Chapter summary

In this chapter, two blind source separation methods, second-order and fourth-order methods representing different classes of algorithms, have been applied to manufacturing variation diagnosis. The second-order method uses the information of autocovariance matrices to estimate \mathbf{Q} uniquely. The second-order method jointly diagonalizes a set of autocovariance matrices. The second-order method requires that no pair of sources share the same autocorrelation function. The fourth-order method uses the fourth-order cumulants information of sources to estimate \mathbf{Q} uniquely. The fourth-order method jointly diagonalizes a set of cumulant matrices. It requires that no

more than one of the p sources follow a Gaussian distribution. Likewise, the blind separation methods use assumptions regarding source distribution while the A&S method uses assumptions regarding the structure of \mathbf{C} . The blind source separation methods have certain advantages over the A&S method because verifying the assumptions of the blind source separation methods is more straightforward than verifying the assumptions of the A&S method. If the required assumptions are violated, none of these methods can estimate the variation patterns uniquely. This limitation motivates us to combine the second-order and fourth-order criteria in order to relax the uniqueness conditions, which we will undertake in the next chapter.

CHAPTER III

COMBINING SECOND-ORDER AND FOURTH-ORDER CRITERIA

In Chapter II, two blind separation methods – fourth-order and second-order methods- were investigated to estimate variation patterns. Blind separation methods are able to produce unique estimates of variation patterns by imposing additional conditions on the statistical nature of the variation sources. As demonstrated in Chapter II, fourth-order and second-order methods are effective when their respective uniqueness conditions are satisfied. If their conditions are violated, however, they are unable, much like PCA and factor analysis, to produce unique estimates of the variation patterns. In practice, it is difficult to know a priori which set of conditions will be better satisfied and, consequently, which method will be more effective. In this part of the dissertation, a new method is developed for estimating the variation patterns by combining the second-order and fourth-order statistics. The uniqueness conditions of the new method, derived in Section III.2, are less restrictive versions of the conditions for the individual second-order and fourth-order methods. The result is a more black-box method with wider applicability, in which the end user is not burdened with verifying which set of conditions are better satisfied.

III.1 Combining second-order and fourth-order statistics with optimal weighting

Although derived from completely different perspectives, the second-order and fourth-order methods share a commonality. Both methods seek to jointly approximately diagonalize a set of matrices. A natural means of combining the second-order and fourth-order criteria is to jointly approximately diagonalize the cumulant matrices $\{\mathbf{M}(i,j): 1 \leq i,j \leq p\}$ together with the autocovariance matrices $\{\boldsymbol{\Sigma}_{y,\tau}: \tau = 1, 2, \dots, T\}$. More specifically, consider the set of $K = T + p^2$ matrices $\{\mathbf{A}_k: k = 1, 2, \dots, K\}$ defined as follows. The first T matrices $\{\mathbf{A}_k: k = 1, 2, \dots, T\}$ are the set of scaled autocovariance matrices $\{\boldsymbol{\Sigma}_{y,\tau}/s_1: \tau = 1, 2, \dots, T\}$, where $s_1 = p^{-1} \sum_{i=1}^p E[y_i^2]$ is the average second moment of the whitened data. The remaining p^2 matrices $\{\mathbf{A}_k: k = T+1, 2, \dots, K\}$ are the set of scaled cumulant matrices $\{\mathbf{M}(i,j)/s_2: 1 \leq i,j \leq p\}$, where $s_2 = p^{-1} \sum_{i=1}^p E[y_i^4]$ is the average fourth moment of the whitened data. For example, if $T = 3$ and $p = 2$, we have $K = 7$ and $\{\mathbf{A}_k: k = 1, 2, \dots, K\} = \{\boldsymbol{\Sigma}_{y,1}/s_1, \boldsymbol{\Sigma}_{y,2}/s_1, \boldsymbol{\Sigma}_{y,3}/s_1, \mathbf{M}(1,1)/s_2, \mathbf{M}(2,1)/s_2, \mathbf{M}(1,2)/s_2, \mathbf{M}(2,2)/s_2\}$.

Let $\boldsymbol{\alpha} = [\alpha_1, \alpha_2, \dots, \alpha_K]'$ be a vector of nonnegative weighting coefficients, to be determined. The estimate of \mathbf{Q} is taken to be the orthogonal matrix \mathbf{U} that minimizes

$$\sum_{k=1}^K \alpha_k \text{off}[\mathbf{U}' \mathbf{A}_k \mathbf{U}], \quad (13)$$

where $\text{off}[\bullet]$ denotes the sum of the squares of the off-diagonal elements of a matrix. This can be viewed as jointly approximately diagonalizing the weighted set of matrices $\{\alpha_k^{1/2} \mathbf{A}_k : k = 1, 2, \dots, K\}$. The algorithm in the Appendix can be used to perform the joint approximate diagonalization.

It is considered to seek a means of "optimally" selecting the weighting coefficients α . Some of the matrices in the set $\{\mathbf{A}_k : k = 1, 2, \dots, K\}$ will contain more information than others and should therefore be given higher weight. For example, suppose that after a certain time lag ($\tau \geq 3$, say) the autocorrelation functions for each source become identical, but that at time lags one and two the autocorrelation functions differ substantially. Then it is better to use larger weighting coefficients for the two matrices $\Sigma_{y,1/s_1}$ and $\Sigma_{y,2/s_1}$ and smaller coefficients for $\{\Sigma_{y,\tau/s_1} : \tau \geq 3\}$, since the latter set contains very little information that can aid in separating the sources. As an other example, consider an extreme case where the fourth-order uniqueness condition happens to be satisfied, but all sources are temporally uncorrelated so that the matrices $\{\Sigma_{y,\tau/s_1} : \tau > 0\}$ contain no useful information. In this case it would be better to assign all of the weight to the cumulant matrices and no weight to the autocovariance matrices. In the opposite extreme, if all sources are Gaussian but the second-order uniqueness conditions are satisfied, it would better to assign all of the weight to the autocovariance matrices and no weight to the cumulant matrices. Using large coefficients for matrices that contain no information only adds noise to the estimation problem. The method proposed below for assigning the

weighting coefficients results in weights that are commensurate with the information contained in each matrix.

In the following, the overscore symbol " $\hat{\cdot}$ " is used to distinguish between theoretical quantities and their estimates from the sample data. Theoretically, every matrix in $\{\mathbf{A}_k: k = 1, 2, \dots, K\}$ is exactly diagonalized by \mathbf{Q} , so that the criterion (13) is zero for any choice of $\boldsymbol{\alpha}$. The joint diagonalizer $\hat{\mathbf{Q}}$ that minimizes (13) with \mathbf{A}_k replaced by $\hat{\mathbf{A}}_k$ will depend on $\boldsymbol{\alpha}$ and will generally differ from \mathbf{Q} . An attractive strategy for selecting $\boldsymbol{\alpha}$ is to attempt to minimize some measure of the error between \mathbf{Q} and $\hat{\mathbf{Q}}$.

Represent the error between $\hat{\mathbf{Q}}$ and \mathbf{Q} via $\delta\mathbf{E}$, defined such that $\hat{\mathbf{Q}} = \mathbf{Q}(\mathbf{I} + \delta\mathbf{E})$. It is straightforward to adapt a result from Cardoso (1994) to the criterion (13), which gives the following approximate expression for $\delta\mathbf{E}$. The i^{th} row, j^{th} column element of $\delta\mathbf{E}$ is ($1 \leq i \neq j \leq p$)

$$\delta\mathbf{E}_{i,j} \approx \frac{\sum_k \alpha_k (d_k(j) - d_k(i)) \mathbf{q}'_i \hat{\mathbf{A}}_k \mathbf{q}_j}{\sum_k \alpha_k (d_k(j) - d_k(i))^2}, \quad (14)$$

where \mathbf{q}_i is the i^{th} column of \mathbf{Q} , and $d_k(i)$ is the i^{th} diagonal element of $\mathbf{Q}'\mathbf{A}_k\mathbf{Q}$. The error $\delta\mathbf{E}_{i,j}$ is affected by three types of quantities: $\boldsymbol{\alpha}$, $\{d_k(j) - d_k(i): k = 1, 2, \dots, K\}$, and $\mathbf{q}'_i \hat{\mathbf{A}}_k \mathbf{q}_j$. Although $\mathbf{q}'_i \mathbf{A}_k \mathbf{q}_j = 0$ for $1 \leq i \neq j \leq p$ ($\mathbf{Q}'\mathbf{A}_k\mathbf{Q}$ is exactly diagonal), $\mathbf{q}'_i \hat{\mathbf{A}}_k \mathbf{q}_j$ will generally differ from zero. Writing $\mathbf{q}'_i \hat{\mathbf{A}}_k \mathbf{q}_j = \mathbf{q}'_i (\hat{\mathbf{A}}_k - \mathbf{A}_k) \mathbf{q}_j$, the term

$\mathbf{q}_i' \hat{\mathbf{A}}_k \mathbf{q}_j$ in (14) stems from the error in estimating \mathbf{A}_k with a finite set of sample data. The quantities $\{d_k(j) - d_k(i): k = 1, 2, \dots, K\}$ relate closely to the second-order and fourth-order uniqueness conditions. Suppose that two Gaussian sources (the i^{th} and j^{th} sources, say) have very similar autocorrelation functions. Since $d_k(j) - d_k(i)$ will be close to zero for all k in this case, it can be expected to have large error $\delta \mathbf{E}_{i,j}$ and to have difficulty separating the i^{th} and j^{th} sources. This is consistent with the theoretical uniqueness condition derived in Section III.2 for the combined method, since two Gaussian sources with identical autocorrelation functions violate the uniqueness condition.

While (14) provides some insight into the factors that affect accuracy, selecting $\boldsymbol{\alpha}$ in an attempt to minimize it directly would not be straightforward. Rather, the suboptimal approach of selecting $\boldsymbol{\alpha}$ is proposed to maximize the denominator terms in (14), which will generally result in smaller values of the $\delta \mathbf{E}_{i,j}$ terms in (14). Specifically, it is recommended selecting $\boldsymbol{\alpha}$ to maximize

$$\sum_{i \neq j} \sum_k \alpha_k (d_k(j) - d_k(i))^2 = \sum_k \alpha_k \sum_{i \neq j} (d_k(j) - d_k(i))^2 \quad (15)$$

under some equality constraint on the norm of $\boldsymbol{\alpha}$ ($\boldsymbol{\alpha}'\boldsymbol{\alpha}$ equals some constant value). Since rescaling $\boldsymbol{\alpha}$ does not affect the solution to (13), it does not matter what value is specified for the norm of $\boldsymbol{\alpha}$. Equation (15) is maximized by selecting

$$\alpha_k \propto \sum_{j \neq i} (d_k(j) - d_k(i))^2. \quad (16)$$

In other words, the weight assigned to \mathbf{A}_k is proportional to $\sum_{j \neq i} (d_k(j) - d_k(i))^2$, which is closely related to the information contained in \mathbf{A}_k . If $\sum_{j \neq i} (d_k(j) - d_k(i))^2 = 0$ for some k , there is no information in \mathbf{A}_k that can be used to separate the sources.

(16) cannot be implemented exactly, since the $d_k(i)$ terms are the diagonal entries of $\mathbf{Q}'\mathbf{A}_k\mathbf{Q}$, and the true values of \mathbf{Q} and $\{\mathbf{A}_k: k = 1, 2, \dots, K\}$ cannot be known. In light of this, it is recommended to first obtain an initial estimate $\hat{\mathbf{Q}}_0$ of \mathbf{Q} by minimizing (13) with equal weighting ($\alpha_k = 1: k = 1, 2, \dots, K$). The i^{th} diagonal element of $\hat{\mathbf{Q}}_0'\hat{\mathbf{A}}_k\hat{\mathbf{Q}}_0$ can then be substituted for $d_k(i)$ in (16) to obtain the final weighting coefficients. The entire procedure for the combined method is summarized as follows. For notational convenience, the " $\hat{}$ " symbol on all quantities is omitted, which are meant to be estimated values from the sample data. The algorithm in the Appendix is used for Steps 5 and 8.

- 1) From the data sample $\{\mathbf{x}_i: i = 1, 2, \dots, N\}$, calculate the sample covariance matrix $\mathbf{\Sigma}_x = N^{-1}\sum_{i=1}^N (\mathbf{x}_i - \bar{\mathbf{x}})(\mathbf{x}_i - \bar{\mathbf{x}})'$ where $\bar{\mathbf{x}} = N^{-1}\sum_{i=1}^N \mathbf{x}_i$.
- 2) Based on a PCA decomposition of $\mathbf{\Sigma}_x$, calculate the whitening matrix $\mathbf{W} = [\mathbf{\Lambda}_p - \sigma^2\mathbf{I}]^{-1/2}\mathbf{Z}_p'$ and the whitened data $\{\mathbf{y}_i = \mathbf{W}\mathbf{x}_i: i = 1, 2, \dots, N\}$.

- 3) Select T and calculate the sets of cumulant and autocovariance matrices $\{\mathbf{M}(i,j): 1 \leq i, j \leq p\}$ and $\{\Sigma_{y,\tau}: \tau = 1, 2, \dots, T\}$ of the whitened data.
- 4) Calculate the average second and fourth moments s_1 and s_2 of the whitened data and form the set of matrices $\{\mathbf{A}_k: k = 1, 2, \dots, K\}$.
- 5) Find the joint approximate diagonalizer \mathbf{Q}_0 of the set $\{\mathbf{A}_k: k = 1, 2, \dots, K\}$.
- 6) Set $d_k(i)$ equal to the i^{th} diagonal element of $\mathbf{Q}'_0 \mathbf{A}_k \mathbf{Q}_0$ ($i=1,2,\dots,p; k = 1,2,\dots,K$).
- 7) Select optimal weights α according to (16).
- 8) Find the joint approximate diagonalizer \mathbf{Q} of the set $\{\alpha_k^{1/2} \mathbf{A}_k: k = 1, 2, \dots, K\}$.
- 9) Take the estimate of \mathbf{C} to be $\mathbf{Z}_p[\Lambda_p - \sigma^2 \mathbf{I}]^{1/2} \mathbf{Q}$.

In Step 3, we recommend using a relatively large value for T (e.g., $T = 10$ to 20). The reason is that if there happens to be little information contained in the autocovariance matrices at larger time lags, the weighting scheme (16) tends to automatically discount them by assigning them small weights. For example, suppose the source autocovariance decays to very small values for time lags greater than 10, but $T = 20$ has been chosen. Consider a value of k such that \mathbf{A}_k corresponds to $\Sigma_{y,\tau}$ for some time lag between 10 and 20. Since $d_k(i)$ is the autocorrelation function (scaled by s_1) for the i^{th} source at that time lag, $d_k(i)$ will be close to zero for $i = 1, 2, \dots, p$. Equation (16) would then select a small value for α_k , and the autocovariance matrices for time lags greater than 10 would be largely ignored in the joint diagonalization.

III.2 Uniqueness condition for the combined method

This section derives the uniqueness condition for the combined method, which is a less restrictive version of the uniqueness conditions for the individual second-order and fourth-order methods. The derivation parallels that presented in Belouchrani, et al. (1997) for the second-order method. The uniqueness condition is derived in the context that the second and fourth moments of the data are known, which is equivalent to having an infinitely large sample of data. For the finite sample sizes one must work with in practice, the effectiveness of the methods depends on the extent to which the conditions are satisfied, as discussed in Chapter II.

Since \mathbf{Q} diagonalizes the entire set $\{\mathbf{A}_k: k = 1, 2, \dots, K\}$, and \mathbf{Q} is orthogonal, we can write $\mathbf{A}_k = \mathbf{Q}\mathbf{D}_k\mathbf{Q}'$ with $\mathbf{D}_k = \text{diag}\{d_k(1), \dots, d_k(p)\}$. Recall that \mathbf{A}_k is either of the form $\Sigma_{y,\tau}/s_1$ for some τ or of the form $\mathbf{M}(s,m)/s_2$ for some s and m . In the former case $d_k(i) = \rho_{i,\tau}/s_1$, and in the latter case $d_k(i) = C_{i,i,i,i}(\mathbf{v})q_{s,i}q_{m,i}/s_2$.

Proposition 1: Suppose that no pair of Gaussian sources share the exact same autocorrelation function, and consider two arbitrary sources v_i and v_j ($i \neq j$). Then there exists an index k such that $d_k(i) \neq d_k(j)$.

Proof: There are three possibilities: both v_i and v_j are Gaussian (Case 1); one source is Gaussian and the other source is not Gaussian (Case 2); and neither source is Gaussian (Case 3). The proof is separated by case.

Case 1: By assumption, the two Gaussian sources must have different autocorrelation function. Thus, there exists a time lag τ such that $\rho_{i,\tau} \neq \rho_{j,\tau}$, which completes the proof for Case 1.

Case 2: Let v_i denote the Gaussian source and v_j denote the non-Gaussian source. Since v_i is Gaussian, $C_{i,i,i,i}(\mathbf{v})$ is zero, which implies that $C_{i,i,i,i}(\mathbf{v})\mathbf{q}_{s,i}\mathbf{q}_{m,i}=0$ for all $1 \leq s, m \leq p$. Since v_j is non-Gaussian, $C_{j,j,j,j}(\mathbf{v}) \neq 0$, and there exists an s and m such that $C_{j,j,j,j}(\mathbf{v})\mathbf{q}_{s,j}\mathbf{q}_{m,j} \neq 0 = C_{i,i,i,i}(\mathbf{v})\mathbf{q}_{s,i}\mathbf{q}_{m,i}$. This completes the proof for Case 2.

Case 3: Since both sources are non-Gaussian, $C_{i,i,i,i}(\mathbf{v}) \neq 0$ and $C_{j,j,j,j}(\mathbf{v}) \neq 0$. Since \mathbf{q}_i and \mathbf{q}_j are orthogonal and have unit norm, there exist an s and m (possibly equal) such that $C_{i,i,i,i}(\mathbf{v})\mathbf{q}_{s,i}\mathbf{q}_{m,i} \neq C_{j,j,j,j}(\mathbf{v})\mathbf{q}_{s,j}\mathbf{q}_{m,j}$, which completes the proof for Case 3.

Theorem 1 (uniqueness condition for the combined method): If no pair of Gaussian sources share the exact same autocorrelation function, then the orthogonal joint diagonalizer of the set $\{\alpha_k^{1/2} \mathbf{A}_k : k = 1, 2, \dots, K\}$ is unique and equal to \mathbf{Q} (up to an interchange of its columns).

Proof: Let \mathbf{U} be any orthogonal joint diagonalizer of the set $\{\alpha_k^{1/2} \mathbf{A}_k : k = 1, 2, \dots, K\}$, and let \mathbf{u} denote any column of \mathbf{U} . Since $\{\mathbf{q}_s : s = 1, 2, \dots, p\}$ are orthogonal, \mathbf{u} can be represented as some linear combination $\mathbf{u} = \sum_{s=1}^p \beta_s \mathbf{q}_s$, where at least one of the coefficients (say β_j) is nonzero. For any $1 \leq j \leq p$ with $j \neq i$ there exists an index k such that $d_k(i) \neq d_k(j)$ by Proposition 1. Equation (7) implies that $\alpha_k \neq 0$.

Since \mathbf{U} diagonalizes $\alpha_k^{1/2}\mathbf{A}_k$, \mathbf{u} is an eigenvector of \mathbf{A}_k . If γ denotes the corresponding eigenvalue, we have $\gamma\mathbf{u}=\mathbf{A}_k\mathbf{u}$. Substituting $\mathbf{u} = \sum_{s=1}^p \beta_s \mathbf{q}_s$ gives $\sum_{s=1}^p \beta_s \gamma \mathbf{q}_s = \sum_{s=1}^p \beta_s \mathbf{A}_k \mathbf{q}_s = \sum_{s=1}^p \beta_s d_k(s) \mathbf{q}_s$, where the last equality follows from the fact that $\mathbf{A}_k = \mathbf{Q}\mathbf{D}_k\mathbf{Q}'$. Equating the coefficients of each \mathbf{q}_s implies that $\beta_s[d_k(s)-\gamma]=0$ for $s=1,\dots,p$. Since $\beta_i \neq 0$, it follows that $\gamma = d_k(i) \neq d_k(j)$, which in turn implies that $\beta_j = 0$. Since j ($\neq i$) was arbitrary, $\beta_j = 0$ for any $j \neq i$, and thus $\mathbf{u}=\mathbf{q}_i$. Repeating for each column of \mathbf{U} completes the proof.

Theorem 1 states that the uniqueness condition for the combined method is that no pair of *Gaussian* sources share the same autocorrelation function. In other words, multiple Gaussian sources are allowed as long as the subset of Gaussian sources have different autocorrelation functions. The autocorrelation functions of the non-Gaussian sources are irrelevant. Suppose the sources are divided into subsets that have the same autocorrelation function (e.g., one subset of uncorrelated sources, a second subset of moderately correlated sources, and a third subset of highly correlated sources). An equivalent statement of the uniqueness condition is that within each subset having the same autocorrelation function there is at most one Gaussian source. Hence, multiple sources with the same autocorrelation function are also allowed. The uniqueness condition for the combined method is therefore less restrictive than the individual uniqueness conditions for the second-order and fourth-order methods. The following section provides an example in which the uniqueness condition for the combined method is satisfied but the conditions for the individual methods are not.

III.3 Performance analysis

This section compares the performance of the second-order method, the fourth-order method, and the combined method in a simulation example. The performance of the methods in situations where their uniqueness conditions are satisfied, and in situations where they are violated, are both considered. The following example represents the situation where the uniqueness conditions are satisfied for all three methods. In the example, a simple beam, illustrated in Section II.5, is used. There are three variation sources in the baseline example, with \mathbf{c}_1 , \mathbf{c}_2 , and \mathbf{c}_3 illustrated in Figures 10(a), 10(b), and 17, respectively. The beam can be considered a subcomponent of a larger assembly, in which case the third variation patterns can represent a bending of the beam about the midpoint. Alternatively, the beam can be considered a separate part, in which case the third variation pattern may represent variation in the thickness such that, when the ends of the beam are larger, the center is smaller. The pattern vectors were scaled so that $\mathbf{c}'_1\mathbf{c}_1 = \mathbf{c}'_2\mathbf{c}_2 = \mathbf{c}'_3\mathbf{c}_3 = n\sigma^2$. The sample size was $N = 200$ in all cases.

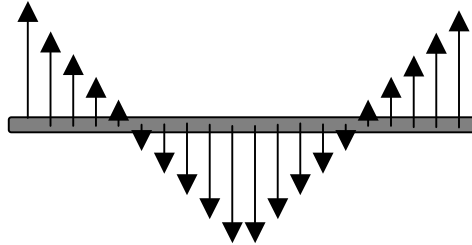


Figure 17 Illustration of the third variation pattern \mathbf{c}_3 in the example: \mathbf{c}_3 representing a beam bending.

The source distributions for the baseline example are chosen so that the uniqueness conditions of both the second-order and the fourth-order methods are satisfied. The third source $\{v_{3,t}; t = 1, 2, \dots\}$ is generated via the first-order AR model $v_{3,t} = \phi v_{3,t-1} + a_t$, with AR parameter $\phi = 0.9$. Figure 18 shows typical sets of 200 observations of three different first-order AR processes, each with a different level of autocorrelation. The top, middle, and bottom panels of Figure 18 represent high autocorrelation ($\phi = 0.9$), moderate autocorrelation ($\phi = 0.6$), and no autocorrelation ($\phi = 0$), respectively. The first source $\{v_{1,t}; t = 1, 2, \dots\}$ is generated as an independent sequence of discrete random variables taking on values of ± 1 with

equal probability 0.5, which is referred to as the (scaled and shifted) Bernoulli distribution. The second source $\{v_{2,t}; t = 1, 2, \dots\}$ is generated via

$$v_{2,t} = \begin{cases} v_{2,t-1} & \text{with probability } q \\ -v_{2,t-1} & \text{with probability } 1 - q \end{cases} \quad (17)$$

with $q = 0.05$ and starting value $v_{2,1}$ drawn from the Bernoulli distribution. It can be shown that $v_{2,t}$ is a stationary process with a marginal Bernoulli distribution and autocorrelation function $\rho_{2,\tau} = (2q-1)^\tau = (-0.9)^\tau$. The parameter q can be used to control the autocorrelation of Bernoulli sources just like ϕ can be used to control the autocorrelation of Gaussian sources. For $q < 0.5$, the lag-one autocorrelation will be negative. A typical realization of 100 observations for $q = 0.05$ is shown in Figure 19(a). This could represent the effects of multiple tooling, as discussed in Section II.5. For $q > 0.5$, the source autocorrelation will be positive. A typical realization of 100 observations for $q = 0.95$ is shown in Figure 19(b). This could represent the situation where the process mean jumps back and forth between two different values at occasional random times. For $q = 0.5$, the source will have no temporal autocorrelation, which is illustrated in Figure 19(c). The uncorrelated $v_{1,t}$ in the example can be viewed as being generated via the same model (17) with $q = 0.5$.

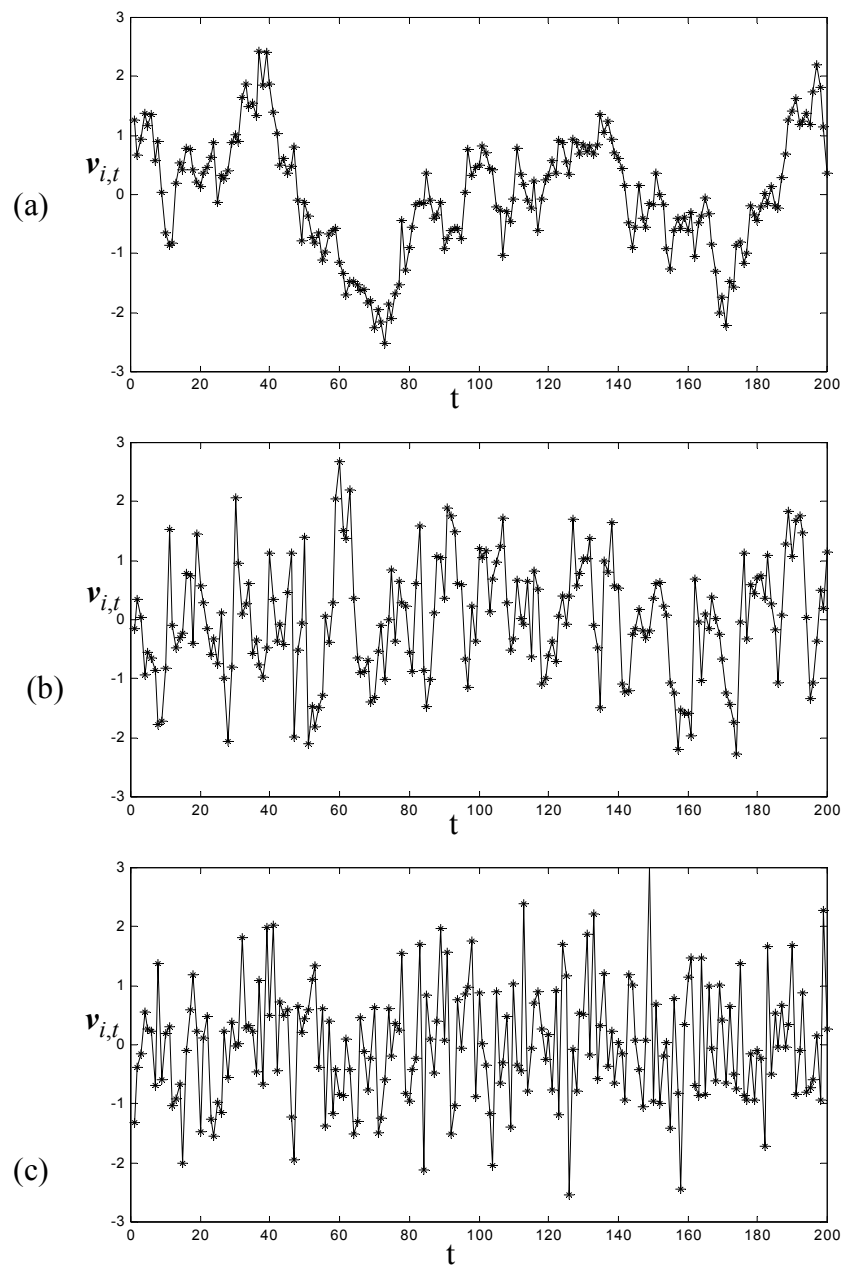
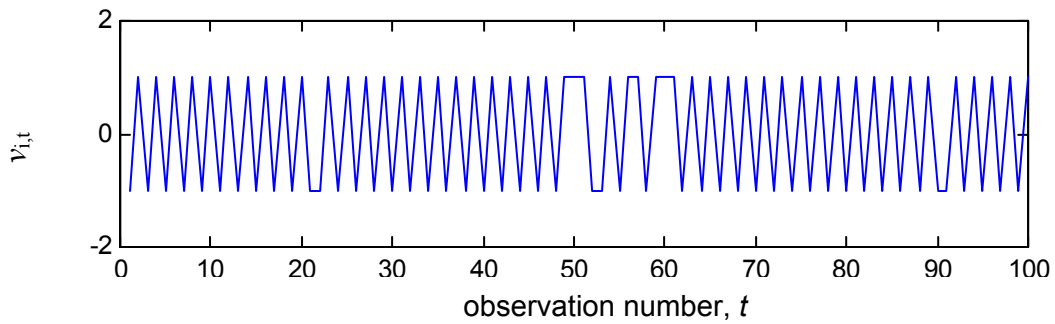
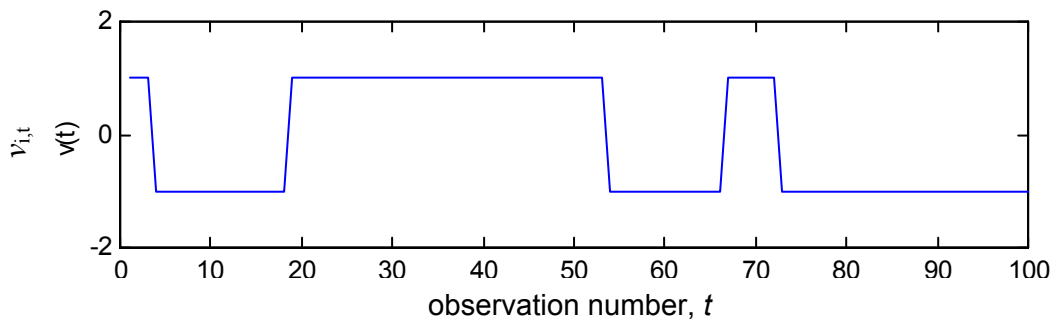


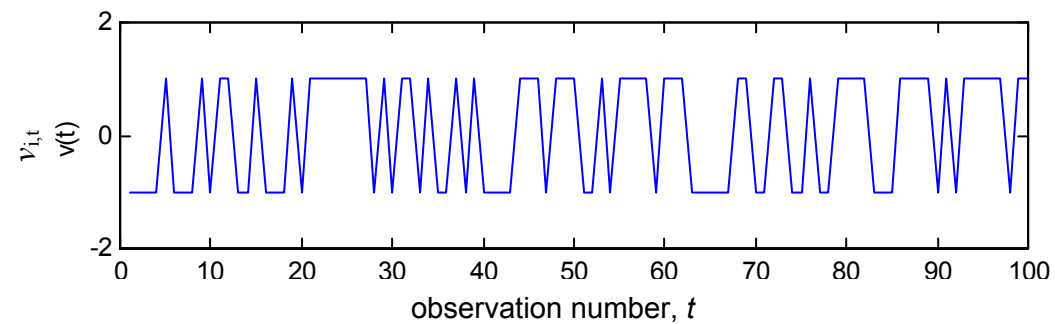
Figure 18 Illustration of first-order AR source signals with different levels of autocorrelation: (a) high autocorrelation ($\phi = 0.9$); (b) moderate autocorrelation ($\phi = 0.6$); (c) no autocorrelation ($\phi = 0$).



(a) $q = 0.05$: negative autocorrelation



(b) $q = 0.95$: positive autocorrelation



(c) $q = 0.5$: no autocorrelation

Figure 19 Illustration of autocorrelated Bernoulli sources with different levels of autocorrelation (different values of q).

The performance measure J_j , defined in Section II.5, is used to evaluate the methods. The average value of a Monte Carlo simulation with 10,000 replicates is used to approximate J_j in all cases. $T = 20$ was chosen for the second-order and combined methods.

The Monte Carlo results for the three methods in the first example are shown in the first three rows of Table 2. Since the autocorrelation functions of the three sources differ [$\rho_{1,\tau} = 0$, $\rho_{2,\tau} = (-0.9)^\tau$, $\rho_{3,\tau} = 0.9^\tau$], and only one source is Gaussian, the uniqueness conditions for both the second-order and the fourth-order methods are satisfied in the first example. As might be expected, Table 2 demonstrates that the second-order and fourth-order methods both perform quite well in this situation.

Table 2 Summary of the Monte Carlo Simulation Results Comparing the Performance of the Three Methods.

source properties	method	J ₁	J ₂	J ₃
no conditions violated	fourth-order method	0.103	0.083	0.076
	second-order method	0.102	0.109	0.108
	combined method	0.084	0.097	0.096
fourth-order conditions violated	fourth-order method	0.609	0.570	0.575
	second-order method	0.137	0.129	0.128
	combined method	0.106	0.114	0.113
second-order conditions violated	fourth-order method	0.106	0.105	0.106
	second-order method	0.640	0.611	0.610
	combined method	0.111	0.111	0.110
second-order and fourth-order conditions violated	fourth-order method	0.123	0.348	0.349
	second-order method	0.468	0.469	0.137
	combined method	0.109	0.900	0.123

To investigate the effects of violating the fourth-order uniqueness conditions, the three sources are generated as Gaussian first-order AR processes via $v_{i,t} = \phi v_{i,t-1} + a_t$. AR parameter values of 0, -0.7, and 0.7 are used for sources one, two, and three, respectively. The source autocorrelation functions are therefore $\rho_{1,\tau} = 0$, $\rho_{2,\tau} = (-0.7)^\tau$, $\rho_{3,\tau} = 0.7^\tau$, and the uniqueness condition for the second-order method is satisfied. Since all three sources were Gaussian, the uniqueness condition for the

fourth-order method is violated. Rows 4 through 6 of Table 2 show the Monte Carlo results for this situation. The performance of the fourth-order method is substantially worse than in the first example, whereas the second-order method still performed well. The combined method is slightly more effective than the second-order method, most likely because the combined method automatically assigns less weight to the autocovariance matrices at larger time lags.

To investigate the effects of violating the second-order uniqueness condition, each of the three sources are generated as independent sequences of uniformly distributed random variables with zero mean and unit variance. Since all three sources are temporally uncorrelated, the second-order uniqueness conditions are violated. The fourth-order uniqueness conditions are still satisfied, however, because all three sources are non-Gaussian. Rows 7 through 9 of Table 2 show the Monte Carlo results for this situation. The performance of the second-order method is now substantially worse than in the first example. The performances of the fourth-order method and the combined method are roughly the same, and both are reasonably good.

The final simulation represents the situation where the uniqueness conditions of both the second-order and the fourth-order methods are violated, but the conditions of the combined method are satisfied. Everything is as in the first example, except that the second source is changed from an autocorrelated Bernoulli random variable with $q = 0.05$ to a temporally uncorrelated Gaussian random variable. There are two sources (v_2 and v_3) that follow a Gaussian distribution, so the uniqueness condition of the fourth-order method is violated. There are also two sources with the same

autocorrelation function ($\rho_{1,\tau} = \rho_{2,\tau} = 0$ for all $\tau > 0$), so the uniqueness condition of the second-order method is violated. Since the two Gaussian sources have different autocorrelation functions, however, the uniqueness condition of the combined method is satisfied. The last three rows of Table 2 show that the combined method performs quite well, whereas the second-order and fourth-order methods do not. It is interesting to note that the fourth-order method is able to separate the first source reasonably well ($J_1 = 0.123$) but is unable to separate the two Gaussian sources ($J_2 = 0.348$ and $J_3 = 0.349$). In contrast, the second-order method is able to separate the third source reasonably well ($J_3 = 0.137$) but is unable to separate the two temporally uncorrelated sources ($J_1 = 0.468$ and $J_2 = 0.469$). It is essentially this "block separability" characteristic of the blind source separation methods that allows the combined method to fully separate the sources.

This section has only investigated the effects of violating the uniqueness conditions. There are a number of other factors that affect the overall accuracy of the methods, including the number of sources p , the sample size N , the dimension n of the measurement vector, the magnitude of the noise variance relative to the severity of the variation patterns, and how close the pattern vectors are to being linearly independent. Additional simulation results indicate that these factors affect all three methods by roughly the same degree. Since the focus of this section is on the relative performance of the combined method versus the individual second-order and fourth-order methods, the details of these simulations are omitted.

III.4 Chapter summary

Both the second-order and fourth-order methods seek to jointly approximately diagonalize a set of matrices (autocovariance matrices for the second-order method and fourth-order cumulant matrices for the fourth-order method). Taking advantage of this commonality, the new method presented in this chapter seeks to jointly approximately diagonalize autocovariance matrices with fourth-order cumulant matrices. Each matrix contains a different level of information, however. Accordingly, the new method assigns weight optimally (by minimizing some measure of estimation accuracy) to each matrix depending on the information contained in it.

When the second-order and the fourth-order methods are combined optimally, the required assumptions for uniquely estimating \mathbf{Q} are more relaxed. The uniqueness condition of the combined method is derived so that no pair of Gaussian sources share the exact same autocorrelation function. This assumption is less restrictive than the individual required assumptions of the second-order and fourth-order methods. Therefore, the combined method has broader applicability than either. Also, the burden of verifying which set of uniqueness conditions are better satisfied is reduced, resulting in a more black-box method that requires less statistical expertise on the part of the user.

CHAPTER IV

BLIND SOURCE SEPARATION WITH PARTIAL PRIOR KNOWLEDGE

In previous chapters, several blind separation methods are examined for estimating un-modeled spatial variation patterns without prior knowledge about the manufacturing process. All of the methods in Chapters II and III can be referred to as blind identification methods. As discussed in the introduction, there is another approach for identifying variation patterns which involves classifying pre-modeled variation patterns (hereafter referred to as classifying methods). The classifying methods require that all of the potential variation patterns be pre-modeled through intensive off-line pre-modeling based on engineering knowledge of the process. The presence of too many potential variation sources and the complexity of modern manufacturing processes often make pre-modeling of all potential patterns impossible and, therefore, prevent the wide applicability of the classifying methods. The blind identification methods have an advantage over the classifying methods in the sense that no off-line pre-modeling is required.

The blind identification methods do have certain disadvantages when compared to the classifying methods, however. The blind identification methods estimate variation patterns from on-line measurement data, which means that the accuracy of the methods is affected by a number of factors, such as the number of variation sources p , the sample size N , the dimension n of the measurement vector, the

signal-to-noise ratio, and how close the required assumptions are to being violated. For example, if the sample size N is very small ($N < 50$) and the signal-to-noise ratio is small ($\mathbf{c}'_i \mathbf{c}_i (n\sigma^2)^{-1} < 0.25$ for $i = 1, 2, \dots, p$), the estimates of the variation patterns will not be accurate ($J_i > 0.3$) in the examples used in Chapters II and III (the performance measures are roughly proportional to the square root of N and the signal-to-noise ratio). While the accuracy of the estimated variation patterns depends on a number of factors, the pre-modeled variation patterns are not affected by these factors. Pre-modeling variation patterns totally depend on engineering knowledge of the process. If the manufacturing process is understood adequately and pre-modeling of all potential variation patterns is possible, the pre-modeled variation patterns are the most accurate. Also, the blind identification methods require additional assumptions to estimate the variation patterns uniquely. If the required assumptions are violated, no method can estimate the variation patterns uniquely. These advantages and disadvantages of the blind identification methods and classifying methods are summarized in Table 3.

Table 3 Advantages and Disadvantages of the Method of Blindly Identifying Un-modeled Variation Patterns and the Method of Classifying Pre-modeled Variation Patterns.

	the method of classifying pre-modeled variation patterns	the method of blindly identifying un-modeled variation patterns
advantages	<ul style="list-style-type: none"> produce the most accurate estimate of variation patterns 	<ul style="list-style-type: none"> can be applied in broader situations than off-line based approach (off-line analysis is not required)
disadvantages	<ul style="list-style-type: none"> cannot be applied if all potential variation patterns are not pre-modeled 	<ul style="list-style-type: none"> produce less accurate estimate variation patterns due to a number of factors cannot estimate variation patterns if the assumptions are violated

Although pre-modeling of all potential variation patterns is impossible in many manufacturing processes, *partial* variation patterns often can be pre-modeled. This partial prior knowledge is illustrated as follows with an autobody example. In the autobody assembly process, the autobody is measured at measurement stations that follow major subassembly stations. Before the autobody is measured, it is fixed firmly by pins mating with a square hole and slot located on the bottom of the autobody as Figure 20(a). Since the same hole/pin is used to locate the underbody at many previous assembly stations, the square hole often becomes rounded as in Figure 20(b). Once the hole becomes rounded, it no longer constrains the autobody fully in the y-plane anymore. For example, some autobodies may be translated to the negative y-direction as in Figure 20(c). In the figure, the dashed line represents the nominal autobody position, and the solid line represents the actual translated autobody position. For some other autobody, the position may be translated to the positive y-direction. In a sample of all the measured autobodies, the rounded hole causes a distinct variation pattern. The root cause of this measurement variation pattern is rarely fixed or is fixed very slowly, however, because the overall quality of the autobody is not affected.

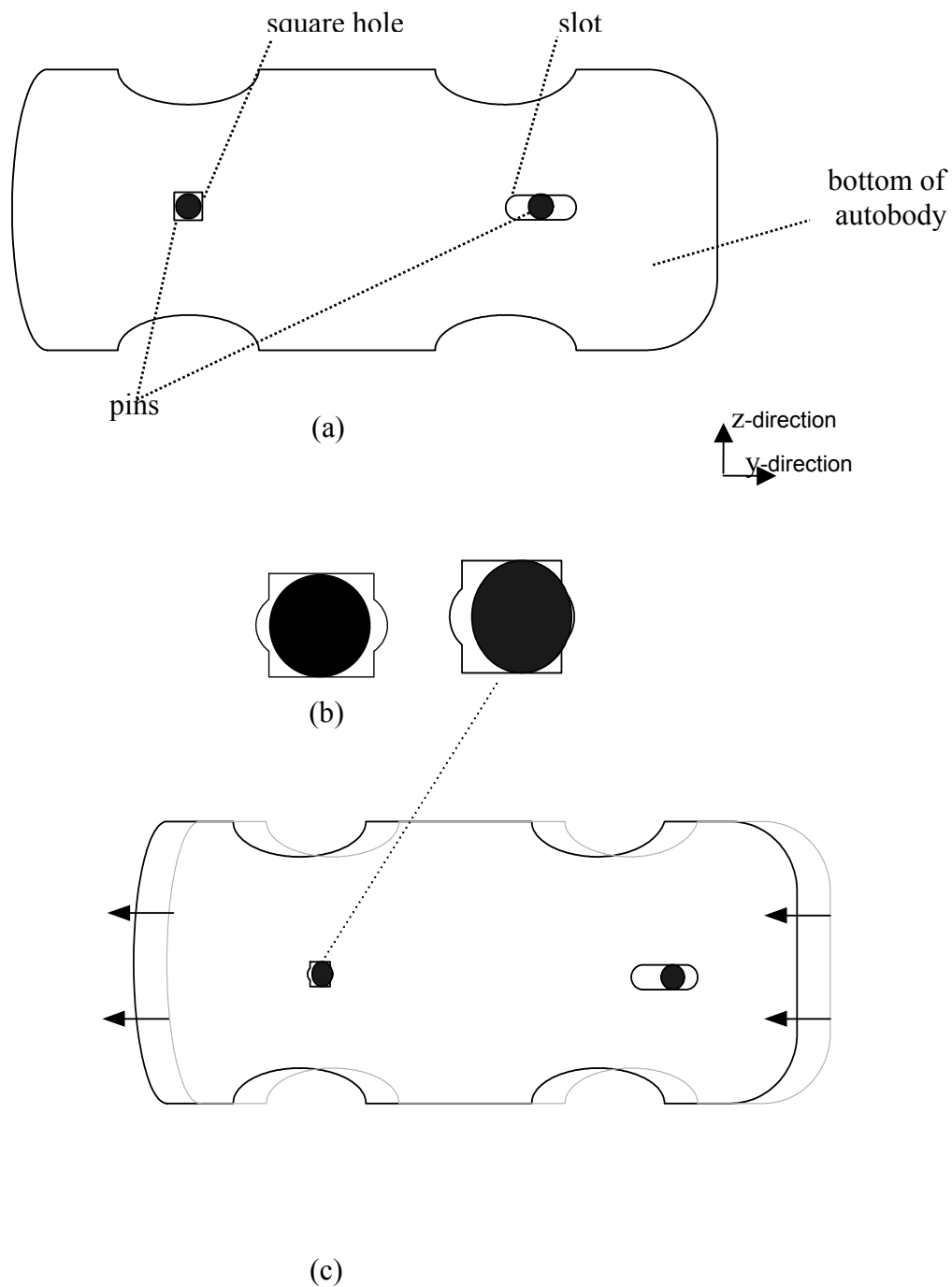


Figure 20 Illustration of the bottom of an autobody in the y-z plane: (a) bottom of the autobody, (b) a rounded hole, and (c) a translation of the entire autobody

This measurement variation pattern can be pre-modeled from the information above. Let u_1 denote the random variable representing the amount the whole autobody translates in the y-direction, and \mathbf{b}_1 denote the corresponding variation pattern scaled to unit norm ($\mathbf{b}_1^T \mathbf{b}_1 = 1$). Since all of the measurement features are affected equally in the y-direction due to this variation source, the elements of \mathbf{b}_1 corresponding to the y-direction coordinates have the same sign and magnitudes, and the elements of \mathbf{b}_1 corresponding to the z-direction coordinates are all zeros. The pre-modeled pattern vector \mathbf{b}_1 in the whole autobody is shown in Figure 21. Twenty-six measurement points are selected from the entire autobody for the analysis.

The pre-modeled variation pattern \mathbf{b}_1 provides partial prior knowledge. Since all potential variation patterns are not pre-modeled (only one variation pattern \mathbf{b}_1 is pre-modeled), the methods for classifying pre-modeled variation patterns cannot be applied (see Section IV.2). The methods for estimating un-modeled variation patterns cannot utilize this partial information (note that these methods are trying to estimate \mathbf{b}_1 and un-modeled variation patterns together from the on-line measurement data). However, a new method is presented in this chapter that is referred to as blind source separation with partial prior knowledge. This method can be used for only estimating the un-modeled variation patterns by utilizing information from pre-modeled variation

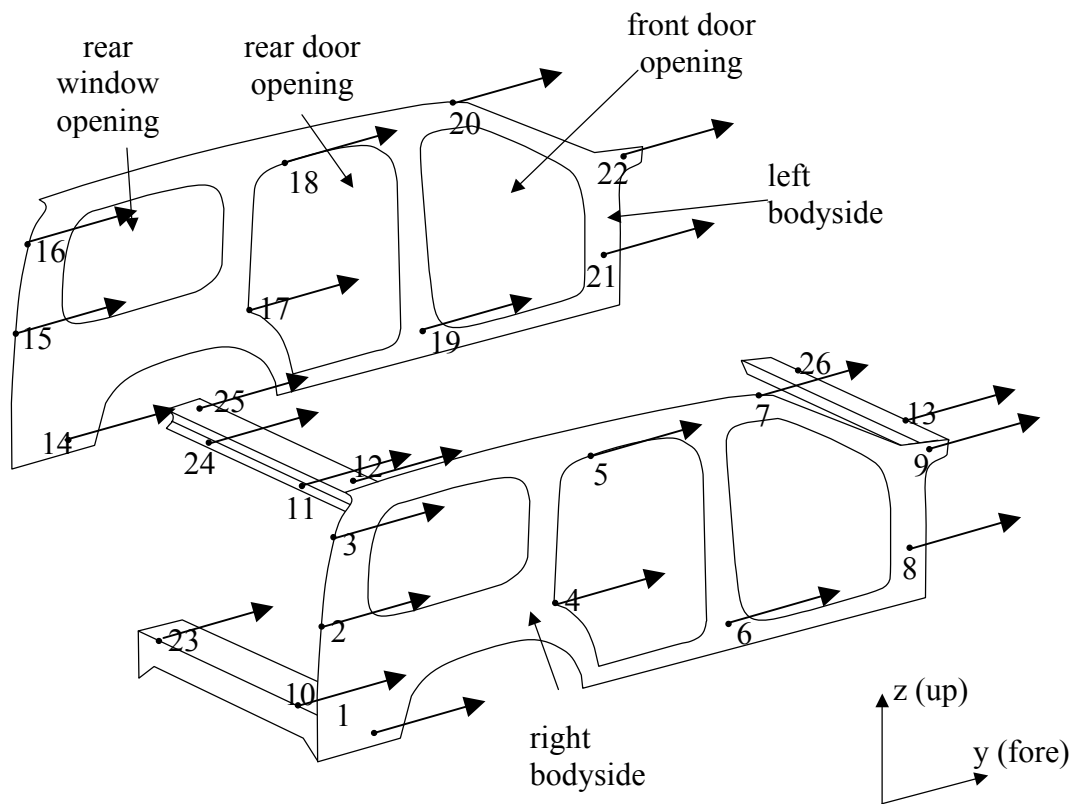


Figure 21. Illustration of the pre-modeled measurement variation pattern in autobody assembly (a translation of the entire autobody).

patterns. The new method has broader applicability than the methods of classifying pre-modeled variation patterns, since pre-modeling of all of the potential variation patterns is not required. With the new method, only partial variation patterns need to be pre-modeled. When the new method utilizes partial prior knowledge, the accuracy of the estimates of un-modeled variation patterns are superior to those of the blind separation method that does not utilize partial prior knowledge (see Section IV.4). Therefore, the new method has advantages over both the blind identification methods and the classifying methods.

In addition, the new method can be used in situations where it is necessary to determine the presence or absence of important pre-modeled variation patterns, and it can also accommodate some un-modeled variation patterns. In other words, the new method can determine the presence of pre-modeled variation patterns without depending on un-modeled variation patterns (see Section IV.3.2).

IV.1 Pre-modeling spatial variation patterns from engineering knowledge

This section discusses how to pre-model variation pattern vectors from engineering knowledge in manufacturing processes. Let u_1, u_2, \dots, u_r denote the random variable representing potential variation sources, and $\mathbf{b}_1, \mathbf{b}_2, \dots, \mathbf{b}_r$ denote corresponding pattern vectors. Then, $\mathbf{b}_i u_i$ describes the effect of the i^{th} potential source on the measurement data. In practice, most variation patterns involve some degree of nonlinearity, however. A more generic representation of the effect of the i^{th} potential source would be $\mathbf{f}_i(u_i)$, where \mathbf{f}_i is some nonlinear mapping from 1-dimensional space to n-dimensional space. Then, $\mathbf{b}_i u_i$ may be viewed as a linearization of a more exact nonlinear mapping, where \mathbf{b}_i is the partial derivative vector $\partial \mathbf{f}_i / \partial u_i$. The suitability of a linear representation depends on the accuracy of the linear approximation to $\mathbf{f}_i(u_i)$. Apley and Shi (1998) argued that the linear approximation provides a good representation of a variety of commonly encountered variation patterns in autobody manufacturing, including those due to stamping, welding, and material handling faults. Refer to Apley and Shi (1998) for more detailed discussion on how to model $\mathbf{b}_1, \mathbf{b}_2, \dots, \mathbf{b}_r$ from off-line analysis.

Apley and Shi (1998) discussed modeling spatial variation patterns in a single stage manufacturing process. In the overall process, there are several stages in which the operation performed at previous stages affects those that follow. This multistage manufacturing process is common in modern manufacturing. In a single stage process, the measurement data are affected by variation sources present in that stage only. In a

multistage process, the measurement data in a stage are affected not only by the variation sources present in that stage but also the variation sources present in previous stages. Jin and Shi (1999) proposed a “state space” model to describe accumulative variation patterns for multistage manufacturing processes. Refer to Jin and Shi (1999) for a definition of the state space model and further discussion on analytical modeling in multistage processes. The state space model has also been applied to manufacturing variation diagnosis (Ding, Ceglarek and Shi, 2002), but because this dissertation is focused on a single stage manufacturing process, we have not used the state space model here. The analytical modeling for a single stage process, as discussed in Apley and Shi (1998), is sufficient for the method presented in this section.

IV.2 Limitation of classifying pre-modeled variation patterns

This section examines the reasons that classifying methods can lead to erroneous results when all of the potential variation patterns are not pre-modeled. The classifying method of Apley and Shi (1998) is used to represent the approach of classifying pre-modeled patterns (in the rest of this section, the classifying method will be represented by this particular method). Suppose that r variation patterns are pre-modeled from the off-line analysis and there exist p un-modeled variation patterns present in a set of sample data. Let $\mathbf{x} = [x_1, x_2, \dots, x_n]'$ be an $n \times 1$ random vector that represents a set of n measured characteristics from the product or process. It is assumed that \mathbf{x} obeys the model

$$\mathbf{x} = \mathbf{B}\mathbf{u} + \mathbf{C}\mathbf{v} + \mathbf{w}, \quad (18)$$

where $\mathbf{B} = [\mathbf{b}_1, \mathbf{b}_2, \dots, \mathbf{b}_r]$ is an $n \times r$ constant matrix with linearly independent columns. Each column of \mathbf{B} represents pre-modeled potential variation patterns, and is scaled (without loss of generality) to have an unit norm ($\mathbf{b}_i' \mathbf{b}_i = 1$). It is assumed that $[\mathbf{B} \ \mathbf{C}]$ has full rank $r+p$. The vector $\mathbf{u} = [u_1, u_2, \dots, u_r]'$ is a $r \times 1$ zero-mean random vector with independent components, and \mathbf{u} is independent of \mathbf{v} and \mathbf{w} . It is assumed that $\text{var}(u_i) = \sigma_i^2$ for $i = 1, 2, \dots, r$. The notation and assumptions of \mathbf{C} , \mathbf{v} , and \mathbf{w} are the same as for model (1) used in Chapters I, II and III. Note that model (18) is the same as model (1) if there are no pre-modeled variation patterns.

The rest of this section uses an example to show why the classifying method cannot be applied in a situation where there are un-modeled variation patterns. The classifying method has two steps; 1) find the least square estimates of \mathbf{u} , and 2) determine which pre-modeled variation sources are present by using some test statistics based on the least square estimates of \mathbf{u} . The following discussion shows that the test statistics are no longer valid when there are un-modeled variation patterns.

The classifying methods find the least square estimates of \mathbf{u} as

$$\hat{\mathbf{u}}_j = (\mathbf{B}'\mathbf{B})^{-1}\mathbf{B}'\mathbf{x}_j, \quad \text{for } j = 1, 2, \dots, N. \quad (19)$$

Let $\hat{\sigma}_i^2$ define $N^{-1} \sum_{j=1}^N \hat{u}_{i,j}^2$ where $u_{i,j}$ denotes the j^{th} observation of u_i . If there are no un-modeled variation patterns, $\hat{\sigma}_i^2$ has the following statistics

$$\hat{\sigma}_i^2 \sim [\sigma_i^2 + \sigma_w^2 [\mathbf{B}'\mathbf{B}]_{i,i}^{-1}] \frac{\chi^2(N)}{N}, \quad (20)$$

where $(\bullet)_{i,i}^{-1}$ denotes the i^{th} diagonal element of $(\bullet)^{-1}$ and $\chi^2(N)$ is a chi-squared random variable with N degrees-of-freedom. Based on (20), the classifying method determines whether the pre-modeled variation pattern is present or not by using a test statistic F_i , defined as

$$F_i \equiv \frac{\hat{\sigma}_i^2}{\left(\mathbf{B}'\mathbf{B} \right)_{i,i}^{-1} \hat{\sigma}_w^2}, \quad (21)$$

where $\hat{\sigma}_w^2 = (N(n-r))^{-1} \sum_{j=1}^N (\mathbf{x}_j - \mathbf{B}\mathbf{u}_j)' (\mathbf{x}_j - \mathbf{B}\mathbf{u}_j)$. The classifying method compares F_i to a threshold γ where γ denotes the $1-\alpha$ percentile of $F(N, N(n-r))$, which is a F -distribution random variable with $N, N(n-r-p)$ degrees of freedom. If F_i is greater than γ , it would be concluded that the i^{th} pre-modeled variation source is present. Otherwise, it would be concluded that the i^{th} pre-modeled variation source is not present. If there are un-modeled variation patterns, the statistical property of (20) is no longer valid. $\hat{\sigma}_i^2$ would approximately follow $[\sigma_i^2 + [(\mathbf{B}'\mathbf{B})^{-1}\mathbf{B}'\mathbf{C}\mathbf{C}'\mathbf{B}((\mathbf{B}'\mathbf{B})^{-1})]_{i,i} + \sigma_w^2 [\mathbf{B}'\mathbf{B}]_{i,i}^{-1}] \chi^2(N)/N$, so the statistical property of $\hat{\sigma}_i^2$ will generally differ from (20) if \mathbf{C} and \mathbf{B} are not orthogonal. Since the test statistic is based on the statistical property of $\hat{\sigma}_i^2$, $F_i > \gamma$ does not guarantee the presence of the i^{th} pre-modeled variation source.

For example, suppose that one variation pattern \mathbf{b}_1 is pre-modeled as illustrated in Figure 21, and there is one un-modeled variation pattern \mathbf{c}_1 as illustrated in Figure 22. \mathbf{c}_1 represents a translation of the right bodyside. Suppose that the pre-modeled variation pattern \mathbf{b}_1 is not present ($\sigma_1^2 = 0$) while \mathbf{c}_1 is present. Note that the magnitude or severity of the un-modeled variation pattern is expressed by $\mathbf{c}_1' \mathbf{c}_1$, and suppose that $\mathbf{c}_1' \mathbf{c}_1 = 26$ and $\sigma_w^2 = 1$ (the signal-to-noise ratio $\mathbf{c}_1' \mathbf{c}_1 (n \sigma^2)^{-1} = 1$ in this case). Then, theoretically, F_1 becomes $3.33 > 1.24$ (1.24 is 99 percentile of $F(N, N(n-r))$ when $N=200$). Therefore, it might be concluded that \mathbf{b}_1 is present, while actually \mathbf{b}_1 is not present. In other words, the classifying method may conclude that some pre-modeled variation patterns are present even when they are not, and vice versa.

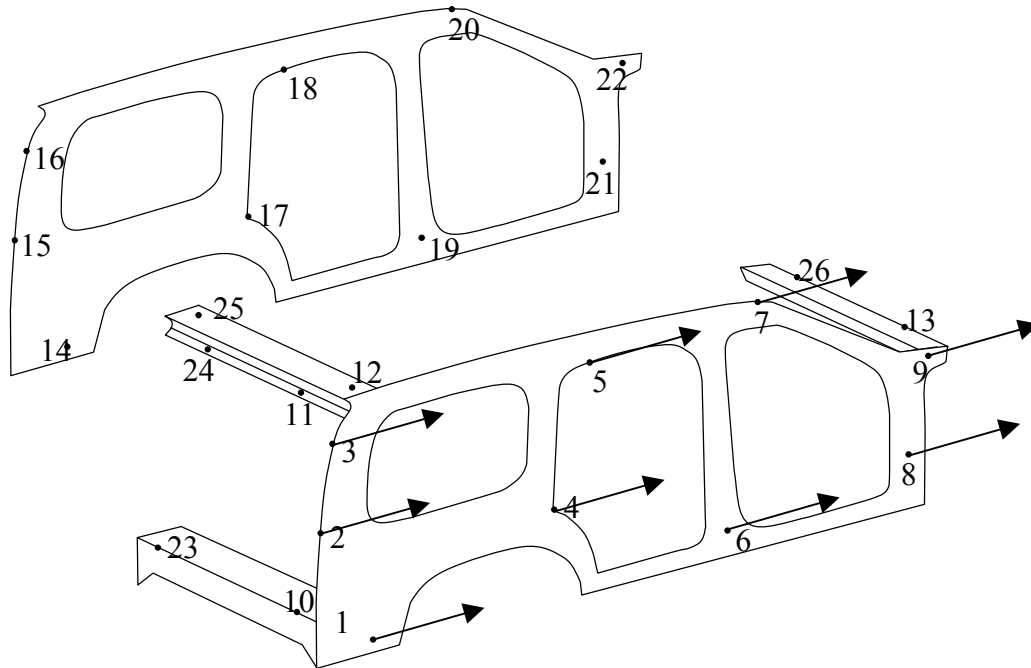


Figure 22. Illustration of c_1 in autobody assembly (a translation of the right bodyside).

IV.3 Blind separation approach with partial prior knowledge

This section presents a new method, referred to as the blind source separation approach with partial a priori knowledge, which is a blind source separation approach that utilizes pre-modeled variation patterns. This method has two steps: 1) estimate the un-modeled variation patterns from the measurement data (Section IV.3.1), and 2) classify the pre-modeled variation patterns by using some test statistic (Section IV.3.2).

IV.3.1 Estimating the un-modeled variation patterns

To estimate the un-modeled variation patterns, a version of measurement data projected orthogonally onto the subspace V_1 is first analyzed where V_1 denotes $\text{span}\{\mathbf{b}_i\}_{i=1}^r$. Let \mathbf{P} denote the projection matrix that projects orthogonally onto V_1 , then $\mathbf{P} = \mathbf{B}(\mathbf{B}'\mathbf{B})^{-1}\mathbf{B}'$. Let \mathbf{P}^\perp denote the projection matrix onto V_1^\perp , which denotes the orthogonal complement of V_1 , then $\mathbf{P}^\perp = \mathbf{I} - \mathbf{B}(\mathbf{B}'\mathbf{B})^{-1}\mathbf{B}'$. For $j = 1, \dots, p$, each un-modeled pattern vector \mathbf{c}_j , can be decomposed into two parts as $\mathbf{c}_j = \mathbf{P}\mathbf{c}_j + \mathbf{P}^\perp\mathbf{c}_j$, since $\mathbf{P} + \mathbf{P}^\perp = \mathbf{I}$ the identity matrix. $\mathbf{P}\mathbf{c}_j$ lies in V_1 ; hence $\mathbf{P}\mathbf{c}_j$ can be represented as the linear combination of \mathbf{b}_i , $i = 1, \dots, r$, with relative coefficients $\alpha_{i,j}$'s as

$\mathbf{P}\mathbf{c}_j = \sum_{i=1}^r \alpha_{i,j} \mathbf{b}_i$. Combining for $j = r+1, \dots, p$,

$$\mathbf{P}\mathbf{C} = \mathbf{B} \begin{bmatrix} \alpha_{1,1} & \alpha_{1,2} & \cdots & \alpha_{1,p} \\ \alpha_{2,1} & \alpha_{2,2} & \cdots & \alpha_{2,p} \\ \vdots & \vdots & \ddots & \vdots \\ \alpha_{r,1} & \alpha_{r,2} & \cdots & \alpha_{r,p} \end{bmatrix} = \mathbf{B}\mathbf{A} \quad (22)$$

where the i^{th} row, the j^{th} column element of \mathbf{A} is $\alpha_{i,j}$ ($1 \leq i \leq r$, $1 \leq j \leq p$). To simplify, let $\tilde{\mathbf{C}} = [\tilde{\mathbf{c}}_1, \tilde{\mathbf{c}}_2, \dots, \tilde{\mathbf{c}}_p] = \mathbf{P}^\perp[\mathbf{c}_1, \mathbf{c}_2, \dots, \mathbf{c}_p]$, then (18) becomes

$$\begin{aligned} \mathbf{x} &= \mathbf{B}\mathbf{u} + \mathbf{C}\mathbf{v} + \mathbf{w} \\ &= \mathbf{B}\mathbf{u} + (\mathbf{B}\mathbf{A} + \tilde{\mathbf{C}})\mathbf{v} + \mathbf{w}. \end{aligned} \quad (23)$$

Define $\tilde{\mathbf{x}} = \mathbf{P}^\perp \mathbf{x}$. Then, premultiplying (23) by \mathbf{P}^\perp , the new model becomes

$$\tilde{\mathbf{x}} = \tilde{\mathbf{C}} \mathbf{v} + \tilde{\mathbf{w}} \quad (24)$$

where $\tilde{\mathbf{w}} = \mathbf{P}^\perp \mathbf{w}$ since $\mathbf{P}^\perp \mathbf{B} = (\mathbf{I} - \mathbf{B}(\mathbf{B}'\mathbf{B})^{-1}\mathbf{B}')\mathbf{B} = \mathbf{B} - \mathbf{B}(\mathbf{B}'\mathbf{B})^{-1}\mathbf{B}'\mathbf{B} = \mathbf{0}_{n \times p}$ where $\mathbf{0}_{n \times p}$ denotes a $n \times p$ zero matrix.

Though the new model (24) is similar to model (1), there is a difference between them. Note that $\tilde{\mathbf{C}}$ is a $n \times p$ constant matrix with linearly independent columns; $\mathbf{v} = [v_1, v_2, \dots, v_p]'$ is a $p \times 1$ zero-mean random vector with independent components, each scaled (without loss of generality) to have unit variance. However, $\Sigma_{\tilde{\mathbf{w}}} \neq \sigma^2 \mathbf{I}$ (model (1) assumed that $\Sigma_{\mathbf{w}} = \sigma^2 \mathbf{I}$). The covariance matrix of $\tilde{\mathbf{w}}$ becomes $\Sigma_{\tilde{\mathbf{w}}} = \sigma^2 \mathbf{P}^\perp$, since $\Sigma_{\tilde{\mathbf{w}}} = \mathbf{P}^\perp \Sigma_{\mathbf{w}} \mathbf{P}^\perp = \sigma^2 \mathbf{P}^\perp \mathbf{P}^\perp = \sigma^2 \mathbf{P}^\perp$ where the last equality comes from the property of the projection matrix. In this case, the discussion in Section II.6 (dealing with noise covariance structures other than $\sigma^2 \mathbf{I}$) cannot be applied, because $\Sigma_{\tilde{\mathbf{w}}}^{-1/2}$ should be obtained in order to apply the discussion in Section II.6. However, $\Sigma_{\tilde{\mathbf{w}}}^{-1/2}$ does not exist since $\Sigma_{\tilde{\mathbf{w}}}$ is not of full rank by the property of the projection matrix.

Due to the difference in assumptions between the models (24) and (1) regarding the noise covariance structure, the blind separation methods discussed in Chapters II and III are not directly applicable. The concepts of the blind separation

methods can be extended to estimate $\tilde{\mathbf{C}}$ from the projected data $\tilde{\mathbf{x}}$, however. The following discussion shows how to accomplish this.

Like the other blind separation methods in Chapters II and III, the covariance matrix of $\tilde{\mathbf{x}}$ is analyzed. From the model (24) and the assumptions, the covariance matrix of $\tilde{\mathbf{x}}$ is

$$\Sigma_{\tilde{\mathbf{x}}} = \tilde{\mathbf{C}}\tilde{\mathbf{C}}' + \sigma^2\mathbf{P}^\perp. \quad (25)$$

Theorem 2: Let $\{\mathbf{z}_i: i = 1, 2, \dots, n\}$ denote an orthonormal set of eigenvectors of $\Sigma_{\tilde{\mathbf{x}}}$, and let $\{\lambda_i: i = 1, 2, \dots, n\}$ denote the corresponding eigenvalues in descending order. Let $\{\delta_i: i = 1, 2, \dots, p\}$ denote the p nonzero eigenvalues of $\tilde{\mathbf{C}}\tilde{\mathbf{C}}'$, arranged in descending order. Then $\lambda_i = \delta_i + \sigma^2$ ($1 \leq i \leq p$), $\lambda_i = \sigma^2$ ($p+1 \leq i \leq n-r$) and $\lambda_i = 0$ ($n-r+1 \leq i \leq n$).

Proof: Let V_2 denote $\text{span}\{\tilde{\mathbf{c}}_i\}_{i=1}^p$. Then there are three possibilities for the eigenvectors of $\Sigma_{\tilde{\mathbf{x}}}$: that the eigenvectors lie in V_2 (Case 1), that the eigenvectors lie in $(V_1 \oplus V_2)^\perp$ (Case 2), and that the eigenvectors lie in V_1 (Case 3). The proof is separated by case.

Case 1: Let $\mathbf{z}_i, i = 1, 2, \dots, p$, denote the eigenvectors of $\Sigma_{\tilde{\mathbf{x}}}$ that lie in V_2 . Since $\mathbf{z}_i \in$

$V_2 \subset V_1^\perp$ for $1 \leq i \leq p$, the projection of \mathbf{z}_i onto V_1^\perp does not make the change to $\mathbf{P}^\perp\mathbf{z}_i = \mathbf{z}_i$. Premultiplying (25) by $\mathbf{z}_i, i = 1, 2, \dots, p$, it becomes

$$\Sigma_{\tilde{\mathbf{x}}}\mathbf{z}_i = \tilde{\mathbf{C}}\tilde{\mathbf{C}}'\mathbf{z}_i + \sigma^2\mathbf{P}^\perp\mathbf{z}_i. \text{ Then } \tilde{\mathbf{C}}\tilde{\mathbf{C}}'\mathbf{z}_i = \Sigma_{\tilde{\mathbf{x}}}\mathbf{z}_i - \sigma^2\mathbf{P}^\perp\mathbf{z}_i = \lambda_i\mathbf{z}_i - \sigma^2\mathbf{P}^\perp\mathbf{z}_i.$$

Therefore \mathbf{z}_i , $i = 1, 2, \dots, p$, is also the eigenvectors of $\tilde{\mathbf{C}}\tilde{\mathbf{C}}'$. Note that $\text{span}\{\tilde{\mathbf{c}}_i\}_{i=1}^p = \text{span}\{\mathbf{z}_i\}_{i=1}^p$; hence, the eigenvalue of $\tilde{\mathbf{C}}\tilde{\mathbf{C}}'$ corresponding to \mathbf{z}_i , $i = 1, 2, \dots, p$, should be nonzero. Since $\lambda_1 \geq \lambda_2 \geq \dots \geq \lambda_p > \sigma^2$, $\delta_i = \lambda_i - \sigma^2$ ($1 \leq i \leq p$), which completes the proof for Case 1.

Case 2: Let \mathbf{z}_i , $i = p+1, 2, \dots, n-r$, denote the eigenvectors of $\Sigma_{\tilde{\mathbf{x}}}$ that lie in

$(V_1 \oplus V_2)^\perp$. Since $\mathbf{z}_i \in (V_1 \oplus V_2)^\perp \subset V_1^\perp$ for $p+1 \leq i \leq n-r$, the projection of \mathbf{z}_i onto V_1^\perp does not make the change to $\mathbf{P}^\perp \mathbf{z}_i = \mathbf{z}_i$. Since $\mathbf{z}_i \in (V_1 \oplus V_2)^\perp \subset V_2^\perp$ for $p+1 \leq i \leq n-r$, these eigenvectors are orthogonal to any column of $\tilde{\mathbf{C}}$, which implies $\tilde{\mathbf{C}}\tilde{\mathbf{C}}' \mathbf{z}_i$ is a zero vector with a proper dimension.

Premultiplying (25) by \mathbf{z}_i , $i = p+1, 2, \dots, n-r$, it becomes $\Sigma_{\tilde{\mathbf{x}}} \mathbf{z}_i = \tilde{\mathbf{C}}\tilde{\mathbf{C}}' \mathbf{z}_i + \sigma^2 \mathbf{P}^\perp \mathbf{z}_i = \sigma^2 \mathbf{P}^\perp \mathbf{z}_i = \sigma^2 \mathbf{z}_i$. Therefore $\lambda_i = \sigma^2$ ($p+1 \leq i \leq n-r$), which completes the proof for Case 2.

Case 3: Let \mathbf{z}_i , $i = n+r-1, n+r-2, \dots, n$, denote the eigenvectors of $\Sigma_{\tilde{\mathbf{x}}}$ that lie in V_1 .

Since $\mathbf{z}_i \in V_1$ for $n+r-1 \leq i \leq n$, the projection of \mathbf{z}_i onto V_1^\perp is a zero vector with proper dimension $\mathbf{P}^\perp \mathbf{z}_i = \mathbf{0}$. Since V_1 and V_2 are orthogonal spaces, \mathbf{z}_i , $i = n+r-1, n+r-2, \dots, n$, are orthogonal to any column of $\tilde{\mathbf{C}}$, which implies $\tilde{\mathbf{C}}\tilde{\mathbf{C}}' \mathbf{z}_i$ is a zero vector with a proper dimension. Premultiplying (25) by \mathbf{z}_i , i

$= p+1, 2, \dots, n-r$, it becomes $\Sigma_{\tilde{\mathbf{x}}} \mathbf{z}_i = \tilde{\mathbf{C}}\tilde{\mathbf{C}}' \mathbf{z}_i + \sigma^2 \mathbf{P}^\perp \mathbf{z}_i = \mathbf{0}$. Therefore $\lambda_i = \sigma^2$ ($n+r-1 \leq i \leq n$), which completes the proof for Case 3.

By using Theorem 2, $\Sigma_{\tilde{\mathbf{x}}}$ can be decomposed in terms of its eigenvectors and eigenvalues as

$$\begin{aligned} \Sigma_{\tilde{\mathbf{x}}} &= \sum_{i=1}^n \lambda_i \mathbf{z}_i \mathbf{z}_i' = \sum_{i=1}^p (\lambda_i - \sigma^2) \mathbf{z}_i \mathbf{z}_i' + \sum_{i=1}^{n-r} \sigma^2 \mathbf{z}_i \mathbf{z}_i' \\ &= \mathbf{Z}_p [\Lambda_p - \sigma^2 \mathbf{I}] \mathbf{Z}_p' + \sigma^2 \mathbf{P}^\perp \end{aligned} \quad (26)$$

where $\mathbf{Z}_p = [\mathbf{z}_1, \mathbf{z}_2, \dots, \mathbf{z}_p]$ and $\Lambda_p = \text{diag}\{\lambda_1, \lambda_2, \dots, \lambda_p\}$. Comparing (25) and (26), just as in Chapters I and II, $\tilde{\mathbf{C}}$ must be in the form $\tilde{\mathbf{C}} = \mathbf{Z}_p [\Lambda_p - \sigma^2 \mathbf{I}]^{1/2} \mathbf{Q}$ and the rest of problem reduces to find \mathbf{Q} . The estimate of σ^2 can be obtained from the mean of $\lambda_{p+1}, \lambda_{p+2}, \dots, \lambda_{n-r}$, which are the eigenvalues of $\Sigma_{\tilde{\mathbf{x}}}$ from $p+1$ largest to $n-r$ largest.

Like in the other blind separation methods, a transformed version of whitened data is used to estimate \mathbf{Q} .

Theorem 3: Suppose that $\tilde{\mathbf{x}}$ follows the model (24). Define $\tilde{\mathbf{y}} = \mathbf{W} \tilde{\mathbf{x}}$ where $\mathbf{W} = [\Lambda_p - \sigma^2 \mathbf{I}]^{-1/2} \mathbf{Z}_p'$ is the $p \times n$ whitening matrix. Then,

$$\tilde{\mathbf{y}} = \mathbf{W} \tilde{\mathbf{x}} = \mathbf{Q} \mathbf{v} + \mathbf{W} \mathbf{w}. \quad (27)$$

Proof: By the property of the projection matrix and Theorem 2, $\mathbf{P}^\perp \mathbf{z}_i = \mathbf{z}_i$ ($1 \leq i \leq n-r$) and $\mathbf{P}^\perp \mathbf{z}_i = \mathbf{0}$, ($n-r+1 \leq i \leq n$). Then, \mathbf{z}_i ($1 \leq i \leq n$) are the eigenvectors of \mathbf{P}^\perp with corresponding eigenvalues 1 or 0. \mathbf{P}^\perp can be decomposed in terms of its eigenvectors and eigenvalues as $\mathbf{P}^\perp = \sum_{i=1}^{n-r} \mathbf{z}_i \mathbf{z}_i'$. Premultiplying \mathbf{W} by \mathbf{P}^\perp , it becomes $\mathbf{W}\mathbf{P}^\perp = \sum_{i=1}^{n-r} \mathbf{W}\mathbf{z}_i \mathbf{z}_i' = \mathbf{W}$, where the last equality follows from the property of the eigenvectors. Using the relationship $\tilde{\mathbf{C}} = \mathbf{Z}_p[\Lambda_p - \sigma^2 \mathbf{I}]^{1/2} \mathbf{Q}$, the transformed data becomes $\tilde{\mathbf{y}} = \mathbf{W} \tilde{\mathbf{x}} = \mathbf{W}[\tilde{\mathbf{C}} \mathbf{v} + \mathbf{P}^\perp \mathbf{w}] = \mathbf{Q}\mathbf{v} + \mathbf{W}\mathbf{P}^\perp \mathbf{w} = \mathbf{Q}\mathbf{v} + \mathbf{W}\mathbf{w}$.

Since (27) is identical to (5) in Section II.2, either the second-order method, the fourth-order method or the combined method can be used to estimate \mathbf{Q} . Here, we recommend using the combined method to estimate \mathbf{Q} uniquely. \mathbf{Q} can be estimated uniquely when no pair of Gaussian sources among \mathbf{v} share the exact same autocorrelation function. When \mathbf{Q} is estimated uniquely, the estimate of $\tilde{\mathbf{C}}$ is taken to be $\mathbf{Z}_p[\Lambda_p - \sigma^2 \mathbf{I}]^{1/2} \mathbf{Q}$.

Up to this point, we have been discussing how to estimate $\tilde{\mathbf{C}}$. However, what we really want is to estimate \mathbf{C} . Noting that $\mathbf{C} = \mathbf{B}\mathbf{A} + \tilde{\mathbf{C}}$, it follows that we need to find \mathbf{A} in order to estimate \mathbf{C} , which the following theorem describes how to do.

Theorem 4: Suppose \mathbf{x} follows the model (18) and $\mathbf{C} = \mathbf{B}\mathbf{A} + \tilde{\mathbf{C}}$. Then, $\mathbf{A} = (\mathbf{B}'\mathbf{B})^{-1} \mathbf{B}' \Sigma_{\mathbf{x}} \tilde{\mathbf{C}} ((\tilde{\mathbf{C}}' \tilde{\mathbf{C}})^{-1})'$.

Proof: From (23), $(\mathbf{B}'\mathbf{B})^{-1}\mathbf{B}'\mathbf{x} = (\mathbf{B}'\mathbf{B})^{-1}(\mathbf{B}'\mathbf{B}\mathbf{u} + \mathbf{B}'\mathbf{B}\mathbf{A}\mathbf{v} + \mathbf{B}'\tilde{\mathbf{C}}\mathbf{v} + \mathbf{B}'\mathbf{w}) = \mathbf{u} + \mathbf{A}\mathbf{v} + (\mathbf{B}'\mathbf{B})^{-1}\mathbf{B}'\tilde{\mathbf{C}}\mathbf{v} + (\mathbf{B}'\mathbf{B})^{-1}\mathbf{B}'\mathbf{w} = \mathbf{u} + \mathbf{A}\mathbf{v} + (\mathbf{B}'\mathbf{B})^{-1}\mathbf{B}'\mathbf{w}$, where the last equality comes from the fact that $\tilde{\mathbf{C}}$ is contained in the orthogonal complement of \mathbf{B} ($\mathbf{B}'\tilde{\mathbf{C}} = \mathbf{0}$). Similarly, $(\tilde{\mathbf{C}}'\tilde{\mathbf{C}})^{-1}\tilde{\mathbf{C}}'\mathbf{x} = (\tilde{\mathbf{C}}'\tilde{\mathbf{C}})^{-1}(\tilde{\mathbf{C}}'\mathbf{B}\mathbf{u} + \tilde{\mathbf{C}}'\mathbf{B}\mathbf{A}\mathbf{v} + \tilde{\mathbf{C}}'\tilde{\mathbf{C}}\mathbf{v} + \tilde{\mathbf{C}}'\mathbf{w}) = \mathbf{v} + (\tilde{\mathbf{C}}'\tilde{\mathbf{C}})^{-1}\tilde{\mathbf{C}}'\mathbf{w}$. Since $E[\mathbf{v}\mathbf{v}'] = \mathbf{I}$, $E[\mathbf{u}\mathbf{v}'] = \mathbf{0}$, $E[\mathbf{u}\mathbf{w}'] = \mathbf{0}$, $E[\mathbf{v}\mathbf{w}'] = \mathbf{0}$ and $E[\mathbf{w}\mathbf{w}'] = \mathbf{I}$ with proper dimensions, $(\mathbf{B}'\mathbf{B})^{-1}\mathbf{B}'\Sigma_{\mathbf{x}}\tilde{\mathbf{C}}((\tilde{\mathbf{C}}'\tilde{\mathbf{C}})^{-1})' = (\mathbf{B}'\mathbf{B})^{-1}\mathbf{B}'E[\mathbf{x}\mathbf{x}']\Sigma_{\mathbf{x}}\tilde{\mathbf{C}}((\tilde{\mathbf{C}}'\tilde{\mathbf{C}})^{-1})' = E[(\mathbf{B}'\mathbf{B})^{-1}\mathbf{B}'\mathbf{x}((\tilde{\mathbf{C}}'\tilde{\mathbf{C}})^{-1}\tilde{\mathbf{C}}'\mathbf{x})'] = E[(\mathbf{u} + \mathbf{A}\mathbf{v} + (\mathbf{B}'\mathbf{B})^{-1}\mathbf{B}'\mathbf{w})(\mathbf{v} + (\tilde{\mathbf{C}}'\tilde{\mathbf{C}})^{-1}\tilde{\mathbf{C}}'\mathbf{w})'] = \mathbf{A} + (\mathbf{B}'\mathbf{B})^{-1}\mathbf{B}'\tilde{\mathbf{C}}((\tilde{\mathbf{C}}'\tilde{\mathbf{C}})^{-1})' = \mathbf{A}$.

In this section, we present a method for estimating un-modeled variation patterns $\mathbf{c}_1, \mathbf{c}_2, \dots, \mathbf{c}_p$ from on-line measurement data \mathbf{x} when there are pre-modeled variation patterns $\mathbf{b}_1, \mathbf{b}_2, \dots, \mathbf{b}_r$. This is the first step in the blind source separation approach with partial prior knowledge, and the procedure is summarized as follows. For notational convenience, the " \wedge " symbol is omitted on all quantities, which are meant to be estimated values from the sample data.

Step 1 : Estimate un-modeled variation patterns

- 1) Construct $\mathbf{B} = [\mathbf{b}_1, \mathbf{b}_2, \dots, \mathbf{b}_r]$ from the pre-modeled variation patterns.
- 2) Obtain projected data vector $\tilde{\mathbf{x}} = \mathbf{P}^\perp \mathbf{x}$ where $\mathbf{P}^\perp = \mathbf{I} - \mathbf{B}(\mathbf{B}'\mathbf{B})^{-1}\mathbf{B}'$.
- 3) From the projected data sample $\{\tilde{\mathbf{x}}_j : j = 1, 2, \dots, N\}$, calculate the sample

covariance matrix $\Sigma_{\tilde{\mathbf{x}}} = N^{-1}\sum_{j=1}^N (\tilde{\mathbf{x}}_j - \bar{\tilde{\mathbf{x}}})(\tilde{\mathbf{x}}_j - \bar{\tilde{\mathbf{x}}})'$ where $\bar{\tilde{\mathbf{x}}} = N^{-1}\sum_{j=1}^N \tilde{\mathbf{x}}_j$.

- 4) Based on a PCA decomposition of $\Sigma_{\tilde{\mathbf{x}}}$, calculate the whitening matrix $\mathbf{W} = [\Lambda_{p-r} - \sigma^2 \mathbf{I}]^{-1/2} \mathbf{Z}_{p-r}'$ and the whitened data $\{\tilde{\mathbf{y}}_j = \mathbf{W} \tilde{\mathbf{x}}_j : j = 1, 2, \dots, N\}$.
- 5) Find the orthogonal matrix \mathbf{Q} by using the combined method.
- 6) Take the estimate of $\tilde{\mathbf{C}}$ to be $\mathbf{Z}_p [\Lambda_p - \sigma^2 \mathbf{I}]^{1/2} \mathbf{Q}$.
- 7) From the data sample $\{\mathbf{x}_j : j = 1, 2, \dots, N\}$, calculate the sample covariance matrix $\Sigma_{\mathbf{x}} = N^{-1} \sum_{j=1}^N (\mathbf{x}_j - \bar{\mathbf{x}})(\mathbf{x}_j - \bar{\mathbf{x}})'$ where $\bar{\mathbf{x}} = N^{-1} \sum_{j=1}^N \mathbf{x}_j$.
- 8) Take the estimate of \mathbf{A} to be $(\mathbf{B}'\mathbf{B})^{-1} \mathbf{B}' \Sigma_{\mathbf{x}} \tilde{\mathbf{C}} ((\tilde{\mathbf{C}}' \tilde{\mathbf{C}})^{-1})'$.
- 9) Take the estimate of \mathbf{C} to be $\mathbf{B}\mathbf{A} + \tilde{\mathbf{C}}$.

IV.3.2 Classifying the pre-modeled variation patterns

The second step of the method is to determine which *potential* (pre-modeled) variation patterns are present in the data. The author recommends using the method of classifying pre-modeled variation patterns presented by Apley and Shi (1998). The test statistic, proposed by Apley and Shi (1998), to determine which potential patterns are present is very simple and also easy to calculate. The following discussion shows why the method of Apley and Shi (1998) can be directly applicable after un-modeled variation patterns are estimated. For simplicity, it is assumed that span of the estimates of $\tilde{\mathbf{C}}$ is equal to the span of $\tilde{\mathbf{C}}$, which means that the whitening matrix $\mathbf{W} = [\Lambda_p - \sigma^2 \mathbf{I}]^{-1/2} \mathbf{Z}_p'$ is known.

Suppose that the uniqueness conditions of estimating un-modeled variation patterns are satisfied. Then, the un-modeled variation patterns are to be estimated accurately. Once the un-modeled variation patterns are identified, we can use the estimates as pre-modeled variation patterns. Since all of the variation patterns are pre-modeled (including the estimates of the un-modeled variation patterns), the classifying method becomes directly applicable. Now, suppose that the uniqueness conditions of estimating un-modeled variation patterns the method are violated. Then, the blind separation method produces the estimates of $\tilde{\mathbf{C}}$ as $\tilde{\mathbf{C}}\mathbf{U}$ by some $p \times p$ orthogonal matrix \mathbf{U} . The following lemma shows the estimate of \mathbf{C} is $\mathbf{C}\mathbf{U}$.

Lemma 1: Let the estimate of $\tilde{\mathbf{C}}$ is $\tilde{\mathbf{C}}\mathbf{U}$, the estimate of \mathbf{C} is $\mathbf{C}\mathbf{U}$.

Proof : From theorem 4, the estimate of \mathbf{A} becomes $\hat{\mathbf{A}} = (\mathbf{B}'\mathbf{B})^{-1}\mathbf{B}'\Sigma_x\tilde{\mathbf{C}}\mathbf{U}$
 $((\mathbf{U}'\tilde{\mathbf{C}}'\tilde{\mathbf{C}}\mathbf{U})^{-1})' = (\mathbf{B}'\mathbf{B})^{-1}\mathbf{B}'\Sigma_x\tilde{\mathbf{C}}((\tilde{\mathbf{C}}'\tilde{\mathbf{C}})^{-1})'\mathbf{U} = \mathbf{A}\mathbf{U}$. Since $\mathbf{C} = \mathbf{B}\mathbf{A} + \tilde{\mathbf{C}}$, $\hat{\mathbf{C}} = \mathbf{B}\hat{\mathbf{A}} + \hat{\tilde{\mathbf{C}}} = \mathbf{B}\mathbf{A}\mathbf{U} + \tilde{\mathbf{C}}\mathbf{U} = \mathbf{C}\mathbf{U}$.

Then, the following theorem shows that the test statistic F_i , defined in Theorem 5, does not depend on \mathbf{U} , which means that determining the presence of the i^{th} source does not depend on whether the uniqueness conditions of uniquely identifying \mathbf{C} are satisfied or not where $\hat{\mathbf{C}} = \mathbf{C}\mathbf{U}$.

Theorem 5: Let F_i denote the test statistic of determining the presence of the i^{th} pre-modeled variation source, defined as

$$F_i \equiv \frac{\hat{\sigma}_i^2}{\left([\mathbf{B} \ \hat{\mathbf{C}}]' [\mathbf{B} \ \hat{\mathbf{C}}] \right)_{i,i}^{-1} \hat{\sigma}_w^2} \quad (28)$$

where $\hat{\sigma}_i^2 = N^{-1} \sum_{j=1}^N \hat{u}_{i,j}^2$,

$\hat{\sigma}_w^2 = (N(n-r-p))^{-1} \sum_{j=1}^N (\mathbf{x}_j - \mathbf{B} \hat{\mathbf{u}}_j - \hat{\mathbf{C}} \hat{\mathbf{v}}_j)' (\mathbf{x}_j - \mathbf{B} \hat{\mathbf{u}}_j - \hat{\mathbf{C}} \hat{\mathbf{v}}_j)$, $[\hat{\mathbf{u}}_j' \ \hat{\mathbf{v}}_j']' = ([\mathbf{B} \ \hat{\mathbf{C}}]' [\mathbf{B} \ \hat{\mathbf{C}}])^{-1} [\mathbf{B} \ \hat{\mathbf{C}}]' \mathbf{x}_j$, and $\hat{\mathbf{C}} = \mathbf{C}\mathbf{U}$. Then, F_i does not depend on \mathbf{U} .

Proof :

$$\begin{aligned} \begin{bmatrix} \hat{\mathbf{u}}_j \\ \hat{\mathbf{v}}_j \end{bmatrix} &= \left([\mathbf{B} \ \mathbf{C}\mathbf{U}]' [\mathbf{B} \ \mathbf{C}\mathbf{U}] \right)^{-1} [\mathbf{B} \ \mathbf{C}\mathbf{U}]' \mathbf{x}_j \\ &= \left(\mathbf{U}_0' [\mathbf{B} \ \mathbf{C}]' [\mathbf{B} \ \mathbf{C}] \mathbf{U}_0 \right)^{-1} \mathbf{U}_0' [\mathbf{B} \ \mathbf{C}]' \mathbf{x}_j \quad \left(\text{where } \mathbf{U}_0 = \begin{bmatrix} \mathbf{I} & \mathbf{0} \\ \mathbf{0} & \mathbf{U} \end{bmatrix} \right) \\ &= \mathbf{U}_0' \left([\mathbf{B} \ \mathbf{C}]' [\mathbf{B} \ \mathbf{C}] \right)^{-1} \mathbf{U}_0 \mathbf{U}_0' [\mathbf{B} \ \mathbf{C}]' \mathbf{x}_j \\ &= \mathbf{U}_0' \left([\mathbf{B} \ \mathbf{C}]' [\mathbf{B} \ \mathbf{C}] \right)^{-1} [\mathbf{B} \ \mathbf{C}]' \mathbf{x}_j \\ &= \mathbf{U}_0' \begin{bmatrix} \hat{\mathbf{u}}_{0,j} \\ \hat{\mathbf{v}}_{0,j} \end{bmatrix} \quad \left(\text{where } \begin{bmatrix} \hat{\mathbf{u}}_{0,j} \\ \hat{\mathbf{v}}_{0,j} \end{bmatrix} = \left([\mathbf{B} \ \mathbf{C}]' [\mathbf{B} \ \mathbf{C}] \right)^{-1} [\mathbf{B} \ \mathbf{C}]' \mathbf{x}_j \right) \end{aligned}$$

Therefore, $\hat{\mathbf{u}}_j = \hat{\mathbf{u}}_{0,j}$ and $\hat{\mathbf{v}}_j = \mathbf{U} \hat{\mathbf{v}}_{0,j}$. Since $\hat{\mathbf{u}}_j = \hat{\mathbf{u}}_{0,j}$, $\hat{\sigma}_i^2$ does not depend on \mathbf{U} .

Also, $\hat{\sigma}_w^2 = (N(n-r-p))^{-1} \sum_{j=1}^N (\mathbf{x}_j - \mathbf{B} \hat{\mathbf{u}}_j - \hat{\mathbf{C}} \hat{\mathbf{v}}_j)' (\mathbf{x}_j - \mathbf{B} \hat{\mathbf{u}}_j - \hat{\mathbf{C}} \hat{\mathbf{v}}_j)$

$$= (N(n-r-p))^{-1} \sum_{j=1}^N (\mathbf{x}_j - \mathbf{B} \hat{\mathbf{u}}_{0,j} - \mathbf{C} \hat{\mathbf{v}}_{0,j})' (\mathbf{x}_j - \mathbf{B} \hat{\mathbf{u}}_j - \mathbf{C} \hat{\mathbf{v}}_{0,j}).$$

Therefore, $\hat{\sigma}_w^2$ does not depend on \mathbf{U} . Similarly,

$$\left(\begin{bmatrix} \mathbf{B} & \hat{\mathbf{C}} \end{bmatrix} \begin{bmatrix} \mathbf{B} & \hat{\mathbf{C}} \end{bmatrix}' \right)_{i,i}^{-1} = \left(\begin{bmatrix} \mathbf{B} & \mathbf{C} \end{bmatrix} \begin{bmatrix} \mathbf{B} & \mathbf{C} \end{bmatrix}' \right)_{i,i}^{-1}.$$

Therefore, F_i does not depend on \mathbf{U} .

Using Theorem 5, the test statistic proposed by Apley and Shi (1998) is directly applicable whether the uniqueness conditions of the blind separation method with partial prior knowledge are satisfied or not. The remainder of this section summarizes the classifying procedure of Apley and Shi (1998) with modifications for fitting the model (18). For notational convenience, “ $\hat{\cdot}$ ” has been omitted as before.

Step 2: Classify pre-modeled variation patterns

- 10) Estimate \mathbf{u}_j and \mathbf{v}_j as $[\mathbf{u}'_j \ \mathbf{v}'_j]' = ([\mathbf{B} \ \mathbf{C}]' [\mathbf{B} \ \mathbf{C}])^{-1} [\mathbf{B} \ \mathbf{C}]' \mathbf{x}_j$ for $j = 1, 2, \dots, N$.
- 11) Calculate $\sigma_i^2 = N^{-1} \sum_{j=1}^N u_{i,j}^2$ where $u_{i,j}$ denotes the j^{th} observation of u_i for $i = 1, 2, \dots, n$.
- 12) Calculate $\sigma_w^2 = (N(n-r-p))^{-1} \sum_{j=1}^N (\mathbf{x}_j - \mathbf{B} \mathbf{u}_j - \mathbf{C} \mathbf{v}_j)' (\mathbf{x}_j - \mathbf{B} \mathbf{u}_j - \mathbf{C} \mathbf{v}_j)$.
- 13) Calculate test statistics $F_i \equiv \sigma_i^2 / \left(\begin{bmatrix} \mathbf{B} & \mathbf{C} \end{bmatrix}' \begin{bmatrix} \mathbf{B} & \mathbf{C} \end{bmatrix} \right)_{i,i}^{-1} \sigma_w^2$, for $i = 1, 2, \dots, r$.
- 14) Determine whether the i^{th} pre-modeled variation source is present or not by comparing F_i and γ where γ denotes the $1-\alpha$ percentile of $F(N, N(n-r-p))$.

IV.4 Performance Comparison

The purpose of this section is to compare in a simulation example the performance of the blind separation method with partial prior knowledge and the combined method. A simple beam example is used, and $n = 20$ measurement points are distributed uniformly across the beam. There is one pre-modeled variation source (u_1) with \mathbf{b}_1 and two un-modeled variation sources (v_1 and v_2) with \mathbf{c}_1 and \mathbf{c}_2 illustrated in Figure 23(a), 23(b) and 23(c), respectively. The pre-modeled variation sources and the un-modeled variation pattern vectors are scaled so that $\sigma_1^2 = \mathbf{c}_1' \mathbf{c}_1 = \mathbf{c}_2' \mathbf{c}_2 = n\sigma_w^2$.

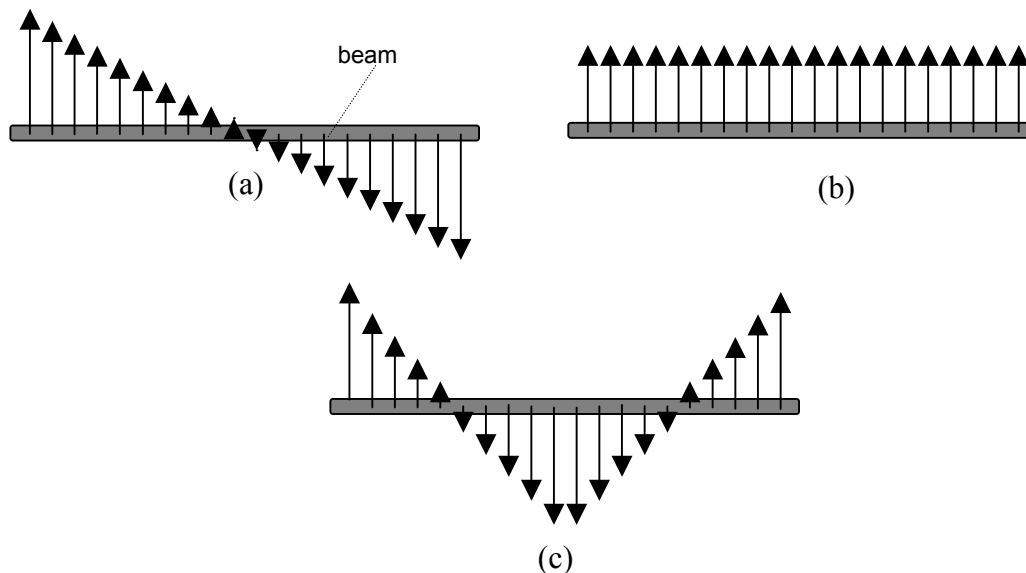


Figure 23 Illustration of the three variation patterns used in Section IV.4: (a) \mathbf{b}_1 , representing a beam rotation, (b) \mathbf{c}_1 , representing a beam translation, and (c) \mathbf{c}_2 , representing a beam bending.

As a baseline example, the situation is considered where the uniqueness conditions of both the blind separation method with partial prior knowledge and the combined method are satisfied. Note that the combined method does not distinguish between the pre-modeled variation sources and the un-modeled variation sources, while the blind separation method with partial prior knowledge does. Therefore, the uniqueness condition of the combined method in this example is that no pair of Gaussian sources among u_1 , v_1 and v_2 share the exact same autocorrelation function. The uniqueness condition of the blind separation method with partial prior knowledge in this example is that no pair of Gaussian sources among v_1 and v_2 share the exact same autocorrelation function. The first un-modeled source $v_{1,t}$ follows a first-order Gaussian AR process with AR parameter $\phi = 0.9$. The second un-modeled source $v_{2,t}$ has two values ± 1 with equal probability 0.5; hence it follows a Bernoulli distribution. The first pre-modeled source $u_{1,t}$ is uncorrelated Gaussian random variables with a zero mean and unit variance.

A sample of $N = 200$ simulated observations are used, and the autocovariance matrices for lags $\tau = 1, 2, \dots, 20$ are used for both methods. Let $J_{\mathbf{b}_1} = E[\|\hat{\mathbf{b}}_1 - \mathbf{b}_1\|]$ (\mathbf{b}_1 has unit norm), $J_{\mathbf{c}_i} = E[\|\hat{\mathbf{c}}_i - \mathbf{c}_i\|] \mathbf{c}_i^{-1}$. The performance measure $J_{\mathbf{b}_1}$, $J_{\mathbf{c}_1}$, $J_{\mathbf{c}_2}$ and the test statistic F_1 are averaged from a Monte Carlo simulation with 10,000 replicates. The results are shown in the first row in Table 4. The blind source separation with partial prior knowledge performed slightly better in estimating \mathbf{c}_1 and \mathbf{c}_2 than the

combined method for the baseline example. Note that the combined method estimates \mathbf{b}_1 from the measurement data, and the blind separation method with partial prior knowledge tests the presence of \mathbf{b}_1 . The blind separation method with partial prior knowledge concludes that \mathbf{b}_1 is present in the baseline example since $F_1 = 20.35 > 1.47$ where 1.47 is the 99 percentile of $F(N, N(n-r-p))$, $N=200$, $n=20$, $r=1$, and $p=2$.

Table 4 Summary of the Monte Carlo Simulation Results Comparing the Performance of the Two Methods.

v_1 autocorrelation	v_2 distribution	Blind source separation with partial prior knowledge			Combined method		
		F_1	$J_{\mathbf{c}_1}$	$J_{\mathbf{c}_2}$	$J_{\mathbf{b}_1}$	$J_{\mathbf{c}_1}$	$J_{\mathbf{c}_2}$
$\phi = 0.9$	Bernoulli	20.35	0.1163	0.1034	0.0899	0.1223	0.1088
$\phi = 0.7$	Bernoulli	20.48	0.1082	0.1079	0.0973	0.1248	0.1093
$\phi = 0.5$	Bernoulli	20.50	0.1008	0.1139	0.1384	0.1536	0.1144
$\phi = 0.3$	Bernoulli	20.42	0.0987	0.1180	0.2776	0.2832	0.1191
$\phi = 0$	Bernoulli	20.49	0.0981	0.1188	0.4411	0.4417	0.1200
$\phi = 0$	Gaussian	20.54	0.4331	0.4329	0.4509	0.4670	0.4673

The next examples represent situations where the uniqueness condition of the combined method is violated or comes close to being violated, while the uniqueness condition of the blind separation method with partial prior knowledge is satisfied.

Everything is the same as in the baseline example, except that the autocorrelation of the second source has been reduced by decreasing the AR parameter ϕ . As the autocorrelation of v_2 is decreased, the autocorrelation functions of the two Gaussian sources (u_1 and v_1) become closer; hence the accuracy of the estimates of the combined method decreases rapidly in identifying the first and second variation patterns as in Table 4. The combined method separates the third source reasonably well in these situations. Since there is only one Gaussian source (v_1) among the unmodeled variation sources (v_1 and v_2), the uniqueness condition of the blind separation method with partial prior knowledge is not affected by changing ϕ . Table 4 also shows that the blind separation method with partial prior knowledge performs quite well since it does not depend on ϕ . The last row of Table 4 shows the results when the assumptions for both methods are violated, in which case neither method separates the second and third sources well.

As the number of sources increases, the likelihood of the combined method assumptions being violated also increases because it becomes more likely that two or more Gaussian sources will have approximately the same autocorrelation function. As the number of pre-modeled sources increases, it becomes increasingly likely that the uniqueness condition of the blind separation method with partial prior knowledge will be satisfied since the pre-modeled variation sources do not require any additional assumptions regarding distributions.

In practice, there is no a priori knowledge as to whether the uniqueness conditions of the methods are satisfied or not. To verify the assumptions from the measurement data, histograms of estimated signals and sample autocorrelation functions can be plotted. For illustration, a Monte Carlo simulation with one replicate is used in a situation where v_1 is changed to be uncorrelated ($\rho_{1,\tau} = 0$ for all $\tau > 0$), and the rest is as in the baseline example. When the blind separation method with partial prior knowledge is applied, Figure 24 shows histograms and sample autocorrelation functions for the three source signals. Among the un-modeled sources (v_1 and v_2), the second un-modeled source appears to be non-Gaussian, which satisfies the uniqueness condition of the blind separation method with partial prior knowledge. Estimates of the three pattern vectors and corresponding estimated source signals are plotted in Figure 25. As expected, the estimates are reasonably good. The combined method results in a misleading interpretation, however. Figure 26 shows that u_1 and v_1 appear to follow Gaussian distribution with quite similar autocorrelation functions. Figure 27 shows that the estimates of \mathbf{b}_1 seem to be the rotation about the right two-third point, and the estimates of \mathbf{c}_1 seem to be the rotation of the beam about the left end point, which are incorrect conclusions. These results appear in Table 4.

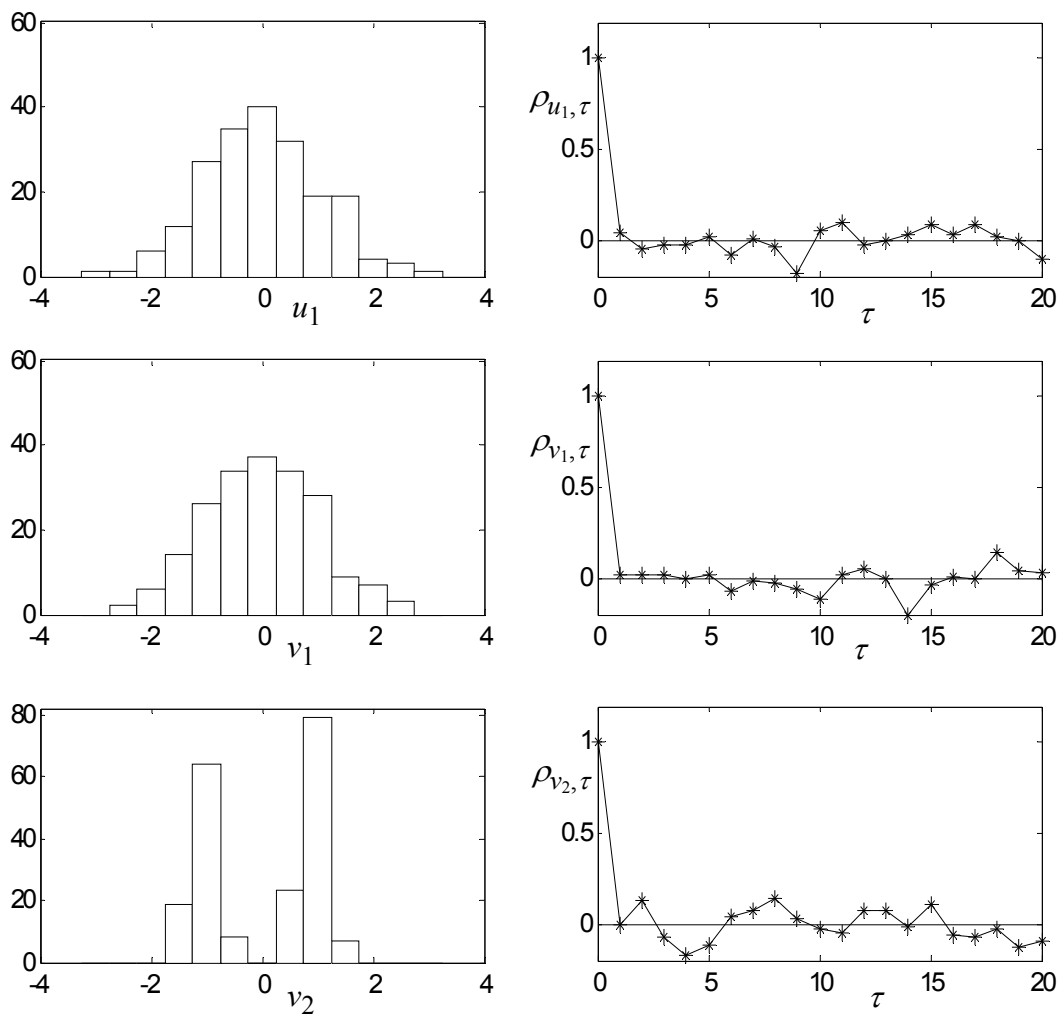


Figure 24 Histograms (left panels) and sample autocorrelation functions (right panels) for three source signals, by using the blind separation method with partial prior knowledge.

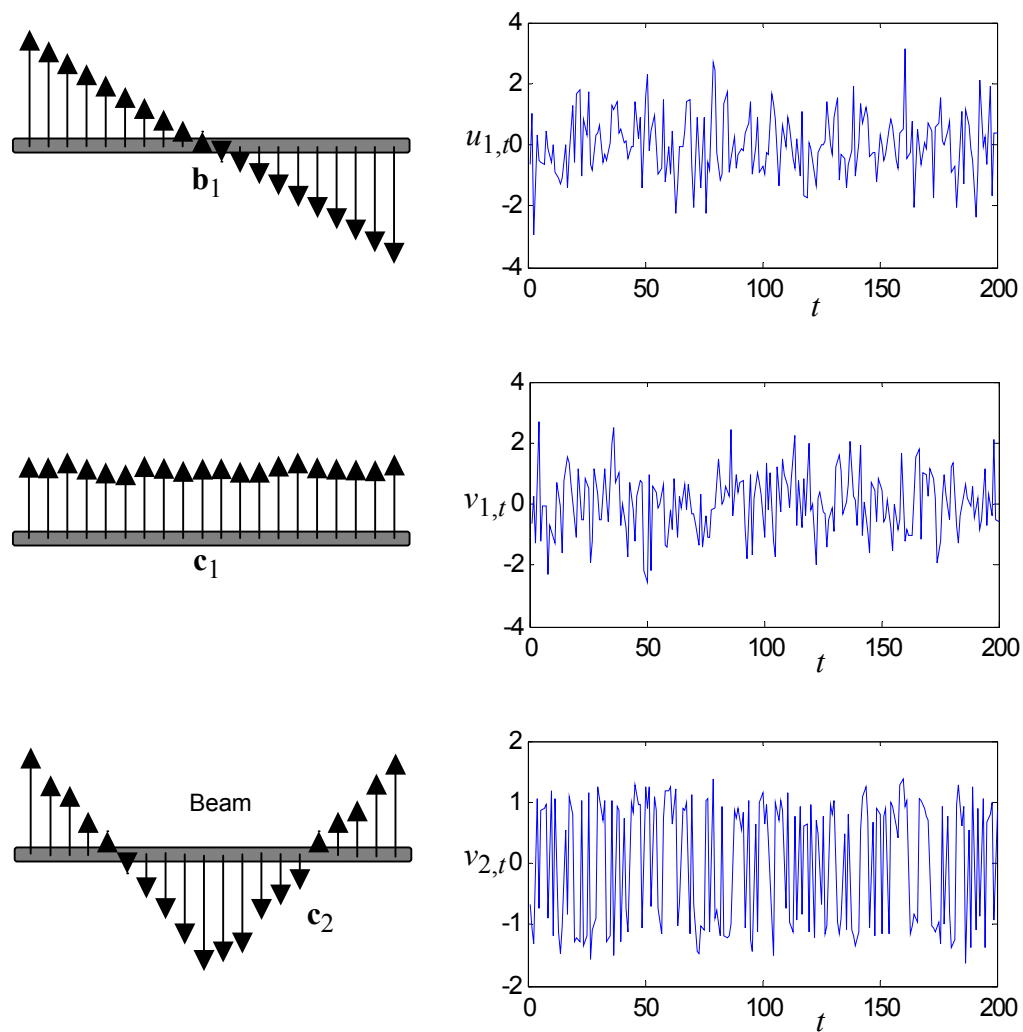


Figure 25 Estimates of the three pattern vectors \mathbf{b}_1 , \mathbf{c}_1 and \mathbf{c}_2 (left panels) and source signal $u_{1,t}$, $v_{1,t}$ and $v_{2,t}$ (right panels), using the knowledge involved blind separation method.

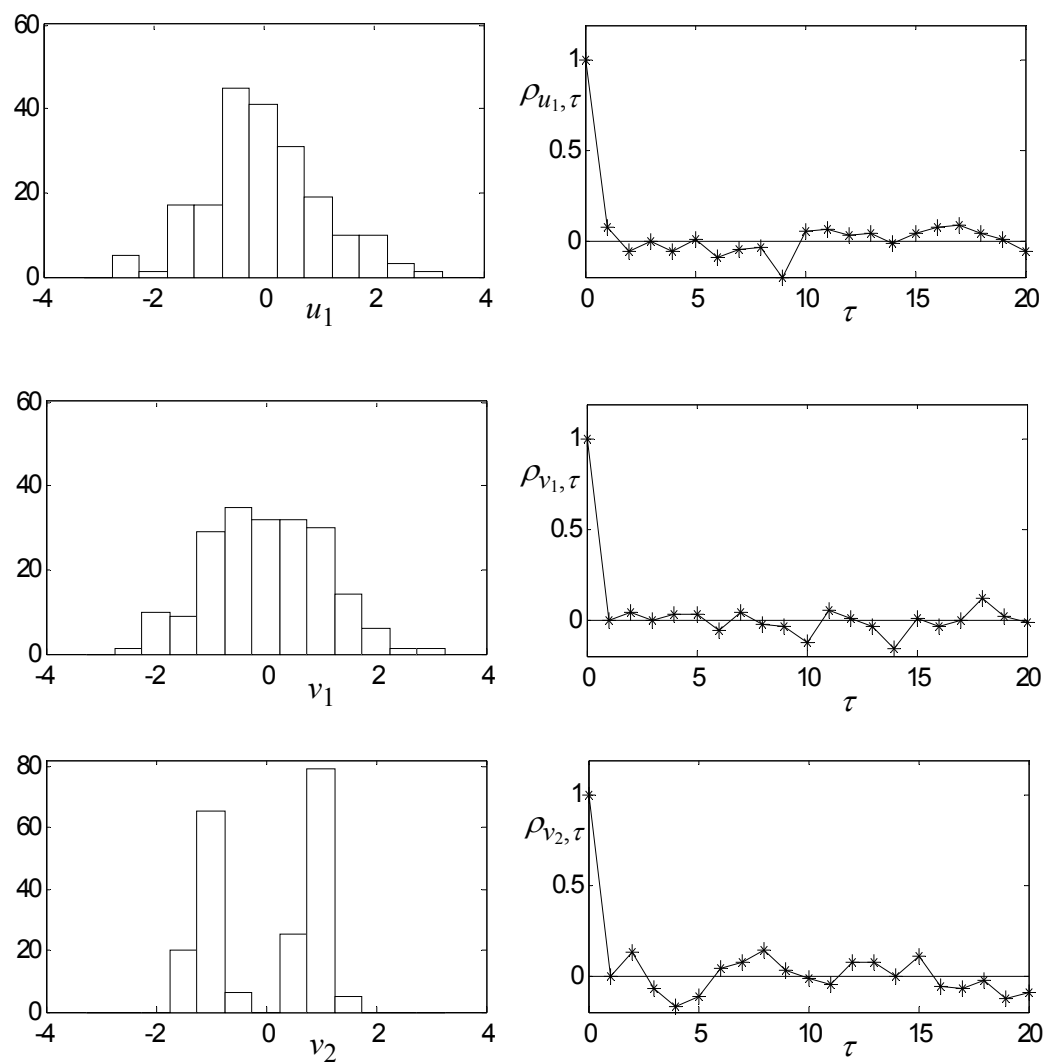


Figure 26 Histograms (left panels) and sample autocorrelation functions (right panels) for three source signals, using the combined method.

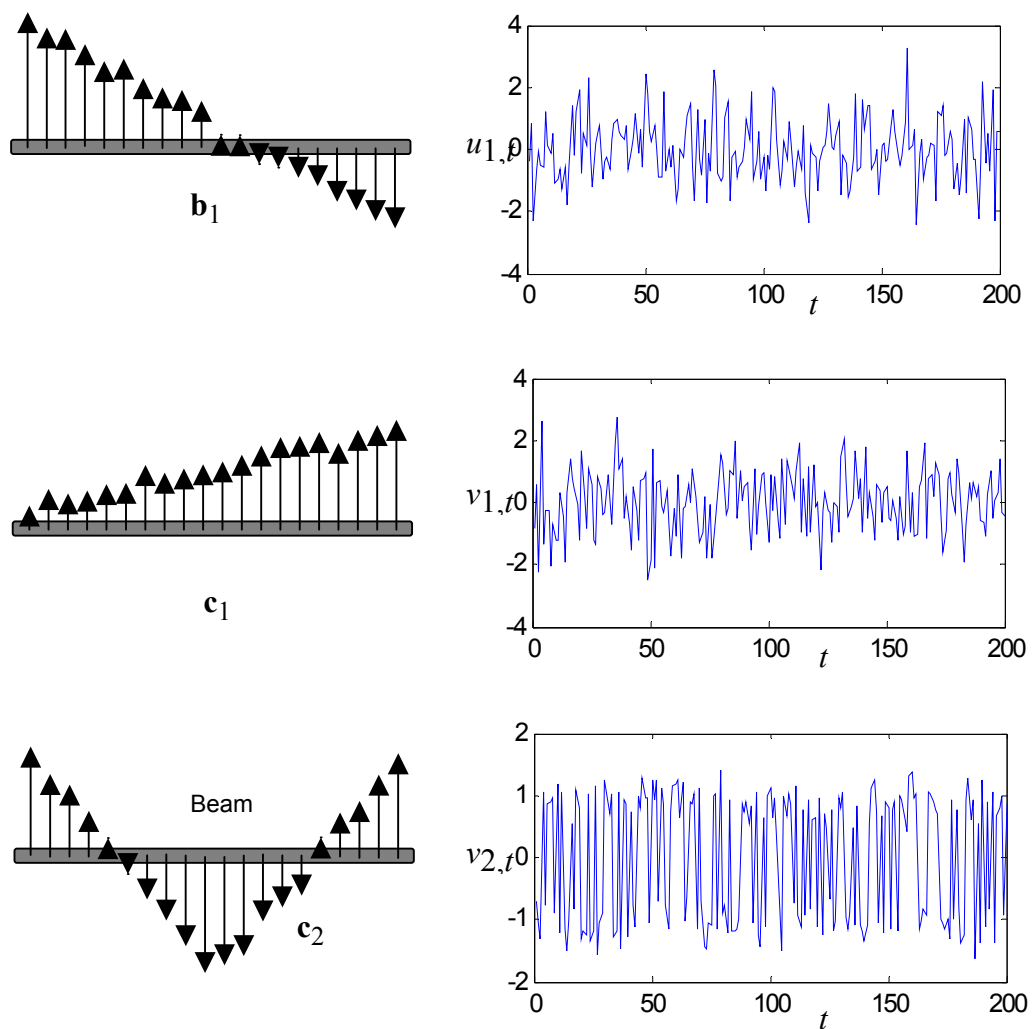


Figure 27 Estimates of the three pattern vectors \mathbf{b}_1 , \mathbf{c}_1 and \mathbf{c}_2 (left panels) and source signals $u_{1,t}$, $v_{1,t}$ and $v_{2,t}$ (right panels), using the combined method.

IV.5 Chapter summary

This chapter has presented a new method, a blind source separation approach utilizing partial prior knowledge. The new method can be applied when partial pre-modeled variation patterns are available. The new method requires two steps for identifying variation patterns present in manufacturing processes. The first step is to estimate un-modeled variation patterns by using information from pre-modeled variation patterns. A method similar to the combined method is used to estimate un-modeled variation patterns. The second step is to classify pre-modeled variation patterns to determine whether they are present or not. This procedure is the same as the method proposed by Apley and Shi (1998).

Our new method combines the advantages of the estimating un-modeled variation pattern approach and the classifying pre-modeled variation pattern approach. Our new method does not need to pre-model all of the potential variation patterns, plus it has wider applicability than the classifying pre-modeled pattern approach because it is applicable when only partial variation patterns are pre-modeled. In addition, the performance accuracy is improved by utilizing the partial prior information. Note that the new method is the same as the combined method if no partial prior variation patterns are available. Also, the new method is the same as the method proposed by Apley and Shi (1998) if all of the potential variation patterns are pre-modeled.

CHAPTER V

OVERALL STRATEGY

Several blind separation methods (including the blind separation method with partial prior knowledge) for identifying variation patterns have been presented in previous chapters. These blind separation methods require assumptions regarding the distribution of sources whereas the A&S method requires assumptions regarding the structure of \mathbf{C} . Since they employ different assumptions to estimate variation patterns uniquely, they can be used in different situations. This difference also enables us to use the blind separation methods and the A&S method together. This chapter presents an overall strategy for using all of these methods in combination. The strategy makes it possible to identify variation patterns which cannot be identified by using any individual method. The ultimate objective of the strategy is to identify as many variation patterns as possible.

V.1 Block separability of the blind separation methods

Recall that the blind separation method with partial prior knowledge and the combined method can identify variation patterns uniquely if no pair of Gaussian sources (among un-modeled sources with partial a priori knowledge) share the exact same autocorrelation function. Some sources can be separated from other sources, however, even though the uniqueness conditions are not fully satisfied. A variation

source can be separated from others if it follows a non-Gaussian distribution or it has a different autocorrelation function than the other Gaussian sources. Let “block” define a set of two or more variation sources that follow a Gaussian distribution with the same autocorrelation function. The blind separation methods can separate sources from others if they do not belong to the same block. For example, suppose that there exist five un-modeled variation sources, referred to as v_1 , v_2 , v_3 , v_4 and v_5 . Suppose that v_1 follows a Bernoulli distribution with no temporal autocorrelation, and the second and third source follows the first-order Gaussian AR model with AR parameter $\phi = 0.9$. Also suppose that the fourth and fifth sources are assumed to follow uncorrelated Gaussian distributions. Since two pairs of Gaussian sources, $\{v_2, v_3\}$ and $\{v_4, v_5\}$, have the exact same autocorrelation function, the uniqueness condition of the blind separation method is violated. The first source can be separated from the other sources, however, because v_1 follows a non-Gaussian distribution. The second source can be separated from the fourth and fifth sources since they have different autocorrelation functions, but cannot be separated from the third source. Hence, the second and third sources are within the same block. Likewise, the first block contains the second and third sources $\{v_2, v_3\}$ and the second block contains the fourth and fifth sources $\{v_4, v_5\}$.

As discussed in Section II.5, the performance of the blind separation method depends on the extent to which its assumptions are satisfied with a finite sample size. Likewise, the block separability of the blind separation method also depends on

whether two Gaussian-like sources have similar autocorrelation functions. As discussed in previous chapters, histograms of the estimated source signals and plots of the sample autocorrelation functions can be used to determine blocks. The author recommends that the sources that seem to follow Gaussian distributions be found first. Consider crankshaft example in Section II.3. Figure 8 shows examples of histograms of estimated source signals. Figure 8(a) shows a typical histogram of estimated Gaussian sources. In Figure 8(b), it appears that the estimated source does not follow a symmetric distribution, but is an example of a non-Gaussian source. In Figure 8(c), the estimated source has a long tail; hence it also provides an example of a non-Gaussian source. The existence of a long tail and symmetry of distribution are attributes to consider in determining whether the sources follow a Gaussian distribution or not.

Once the Gaussian sources are identified, the sources that have similar autocorrelation functions should be identified. This can be accomplished by plotting the sample autocorrelation functions together. Figure 9 shows three sample autocorrelation functions ($\rho_{1,\tau}$, $\rho_{2,\tau}$, and $\rho_{3,\tau}$). Figure 9 demonstrates that $\rho_{1,\tau}$ and $\rho_{3,\tau}$ are similar. If the corresponding sources follow a Gaussian distribution, they cannot be separated from each other, and they belong to the same block. However, some ambiguity is involved in selecting inseparable sources since choosing *similar* autocorrelation functions is very subjective. This is also true of a number of factors that affect the accuracy of blind separation methods, such as sample size N and signal-to-noise ratio. Section II.5 discusses this issue in more detail.

By using the guidelines discussed above, it can be determined whether two sources are separable or not. If a source does not belong to a particular block, that source can be considered a separable source and the corresponding estimates of its variation patterns can be considered as reasonable estimates. If sources are not separable from each other, these sources can be considered within the same block and the corresponding estimates of their variation patterns cannot be considered as reasonable estimates. Section V.2 discusses how we can try to separate sources within the same block by using the A&S method.

V.2 Overall strategy for identifying spatial variation patterns

This section presents an overall strategy for identifying spatial variation patterns by using the blind separation methods and the A&S method in combination. The first step of the strategy is to check the availability of pre-modeled variation patterns. If pre-modeled variation patterns are available, the blind separation method with partial prior knowledge, introduced in Chapter IV, should be used. Otherwise, the combined method, introduced in Chapter III, is to be used. Regardless of which methods are used, the variation sources should be checked to determine whether they are separable or within the same block (see discussion in Section V.1). Also, which pre-modeled (potential) variation patterns are present should be determined.

After selecting the blocks, the A&S method is recommended for separating sources within the same block. Suppose the i^{th} block has sources $v_{i_1} v_{i_2} \dots v_{i_k}$ and that $\mathbf{d}_{i_1}, \mathbf{d}_{i_2}, \dots, \mathbf{d}_{i_k}$ denote the estimated corresponding pattern vectors by using blind

separation methods. Let \mathbf{C}_i denote $[\mathbf{c}_{i_1}, \mathbf{c}_{i_2}, \dots, \mathbf{c}_{i_k}]$ and \mathbf{D}_i denote $[\mathbf{d}_{i_1}, \mathbf{d}_{i_2}, \dots, \mathbf{d}_{i_k}]$. Although $\mathbf{C}_i \neq \mathbf{D}_i$, it can be shown that $\mathbf{C}_i \mathbf{C}_i' = \mathbf{D}_i \mathbf{D}_i'$. Let $\mathbf{\Sigma}_i$ denote $\mathbf{C}_i \mathbf{C}_i'$. Since $\mathbf{\Sigma}_i$ (this is the information needed to use the A&S method) can be calculated from $\mathbf{d}_{i_1}, \mathbf{d}_{i_2}, \dots, \mathbf{d}_{i_k}$, the A&S method can estimate \mathbf{C}_i if \mathbf{C}_i possesses the structure of (12) in Section II.4.1. Refer to Apley and Shi (2001) for a more detailed algorithm.

The overall strategy which is illustrated in Figure 28 is summarized as follows:

- 1) check the availability of pre-modeled variation patterns, 2) apply the blind separation method with partial prior knowledge if pre-modeled variation patterns are available; otherwise apply the combined method, 3) based on the discussion in Section V.1, identify the un-modeled sources that can be separated and the blocks that cannot and also determine which pre-modeled variation sources are present, and 4) for each block, calculate $\mathbf{\Sigma}_i$, and apply the A&S method.

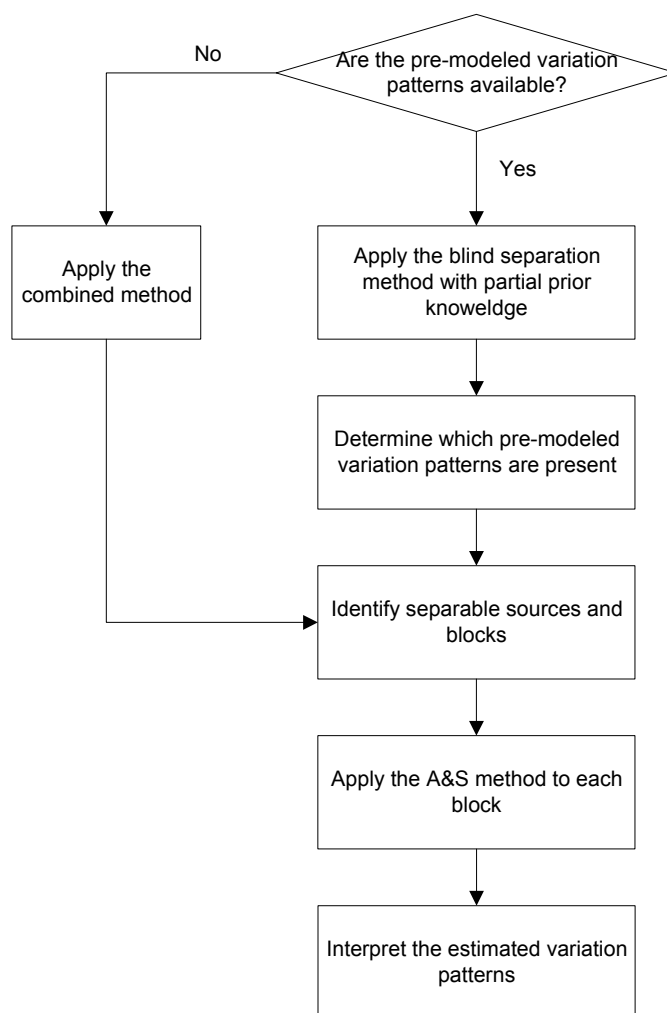


Figure 28 Flowchart of the overall strategy.

The overall strategy enables us to identify variation patterns, which cannot be identified by using any single method. For example, consider the situation where $n=6$, $p=5$, $\mathbf{c}_1=[1 \ 1 \ 1 \ 1 \ 1 \ 1]'$, $\mathbf{c}_2=[1.5 \ 1 \ 0.5 \ -0.5 \ -1 \ -1.5]'$, $\mathbf{c}_3=[0 \ 0 \ 1 \ 1 \ 1 \ -1]'$, $\mathbf{c}_4=[-1.5 \ 0 \ 1.5 \ 1.5 \ 0 \ -1.5]'$, and $\mathbf{c}_5=[-1 \ 1 \ 0 \ 0 \ -1 \ 1]'$. Suppose that the first source follows a Bernoulli distribution, the second and the third sources follow the first-order Gaussian AR process with an AR parameter 0.9, and the fourth and fifth sources follow an uncorrelated Gaussian distribution. It is assumed that there are no pre-modeled variation patterns available; hence the combined method is applied first. From the block separability of the blind separation methods, the first variation pattern \mathbf{c}_1 can be identified since the corresponding source follows a non-Gaussian distribution. Since the second and third sources have the same autocorrelation function, they are within the same block, referred to as the first block. Similarly, the fourth and fifth sources are within the same block, referred to as the second block. The A&S method can be applied to each block. In examining the first block matrix $\mathbf{C}_1=[\mathbf{c}_2, \mathbf{c}_3]$, we notice that the measurement subset $\{x_1, x_2\}$ is affected by the second source only (among second and third sources). Since \mathbf{C}_1 possesses the structure of (12), the A&S method can estimate \mathbf{c}_2 and \mathbf{c}_3 . Similarly, $\mathbf{C}_2=[\mathbf{c}_4, \mathbf{c}_5]$ possesses the structure of (12); hence the A&S method can estimate \mathbf{c}_4 and \mathbf{c}_5 . Likewise, the overall strategy enables us to identify all of the variation patterns whereas the combined method can only estimate \mathbf{c}_1 and the A&S method cannot estimate any variation patterns.

V.3 Illustration of applying the overall strategy

To illustrate the overall strategy, a simulation example is used in which a beam represents the manufacturing part as in Section II.5. There is one pre-modeled variation pattern vector \mathbf{b}_1 and three un-modeled variation patterns \mathbf{c}_1 , \mathbf{c}_2 , and \mathbf{c}_3 as illustrated in Figures 29(a), (b), (c) and (d), respectively. The first pattern represents a large measurement error at the left-most measurement point. $N=200$, $n=20$, and $\sigma_1^2 = \mathbf{c}_1' \mathbf{c}_1 = \mathbf{c}_2' \mathbf{c}_2 = \mathbf{c}_3' \mathbf{c}_3 = n\sigma_w^2$ is chosen for the simulation.

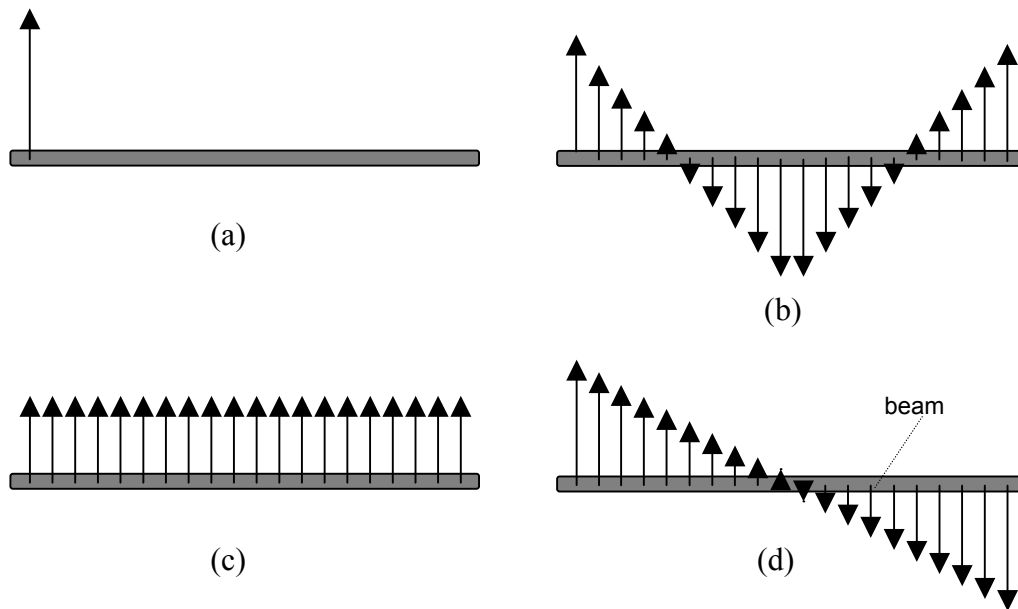


Figure 29 Illustration of the four variation patterns used in Chapter V: (a) \mathbf{b}_1 , represents a large measurement error at the left-most point, (b) \mathbf{c}_1 , (c) \mathbf{c}_2 and (d) \mathbf{c}_3 .

The source distributions of the example are chosen so that the uniqueness conditions of the blind separation method with partial prior knowledge are partially satisfied. u_1 , v_2 and v_3 were generated via an uncorrelated Gaussian distribution. v_1 was generated via (17) with $q=0.05$ and the starting value drawn with a marginal Bernoulli distribution. For an illustration of the strategy, a Monte Carlo simulation with one replicate is used.

Step 1 : Check the availability of the pre-modeled variation pattern

A pre-modeled variation pattern is available, so the blind separation method with partial prior knowledge is used.

Step 2 : Apply the blind separation method

The estimates of the variation patterns are illustrated in Figure 30.

Step 3 : Identify separable sources and blocks (by plotting histograms of estimated source signals and sample autocorrelation functions), and determine which pre-modeled variation patterns are present.

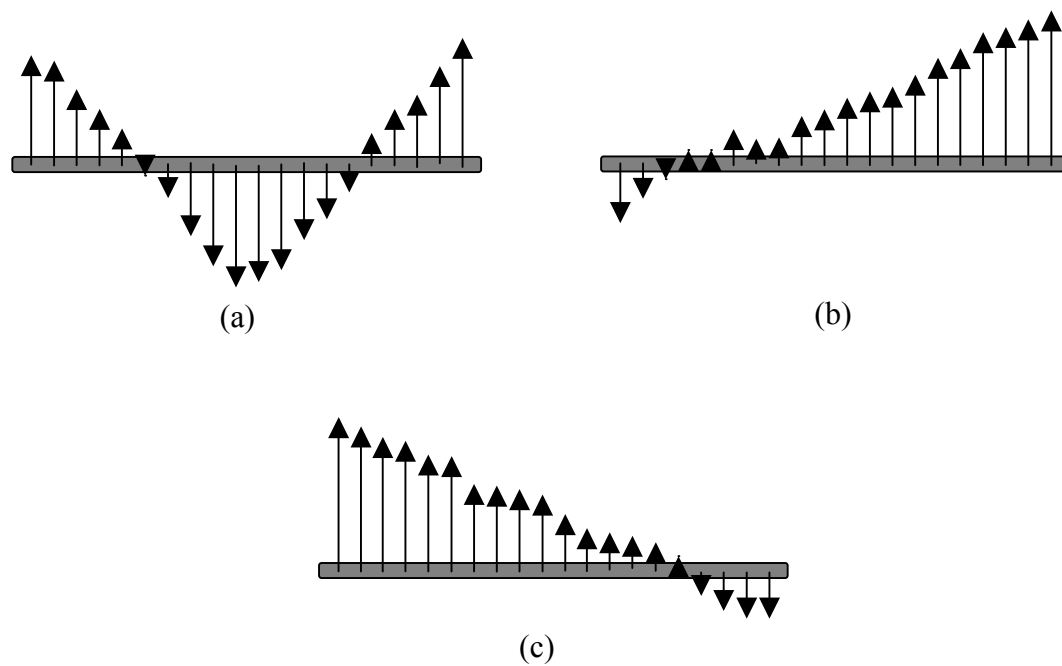


Figure 30 Illustration of estimates of the un-modeled variation patterns used in Section V.3: (a) the estimates of \mathbf{c}_1 , (b) the estimates of \mathbf{c}_2 and (c) the estimates of \mathbf{c}_3 .

After examining the histograms of the estimated source signals (Figure 31), we conclude that v_2 and v_3 follow Gaussian distributions. By plotting the sample autocorrelation functions of v_2 and v_3 (Figure 32), we also conclude that they have similar autocorrelation functions. Therefore, v_1 does not belong to any block, and v_2 and v_3 belong to the same block. In the next step, the A&S method is applied to separate v_2 and v_3 from each other. The result agrees with the result in Step 2, since \mathbf{c}_1 is reasonably estimated while \mathbf{c}_2 and \mathbf{c}_3 are not. Also, the test statistic, defined at (28) in Section IV.3.2, is $F_1 = 14.2270$. The 99 percentile of $F(N, N(n-r-p))$ is about 1.47, where $N=200$, $n=20$, $r=1$ and $p=3$. Since $F_1 > 1.32$, we conclude that u_1 is present.

Step 4 : Identify \mathbf{c}_2 and \mathbf{c}_3 using the A&S method.

When $\{x_{10}, x_{11}\}$ was selected as the measurement subset affected by only one of v_2 or v_3 , the estimates of \mathbf{c}_2 and \mathbf{c}_3 are illustrated in Figure 33, and these estimates are reasonable. As discussed in Sections II.4 and II.5, there is user subjectivity in choosing the measurement subset and selecting the wrong measurement subset may result in a misleading interpretation.

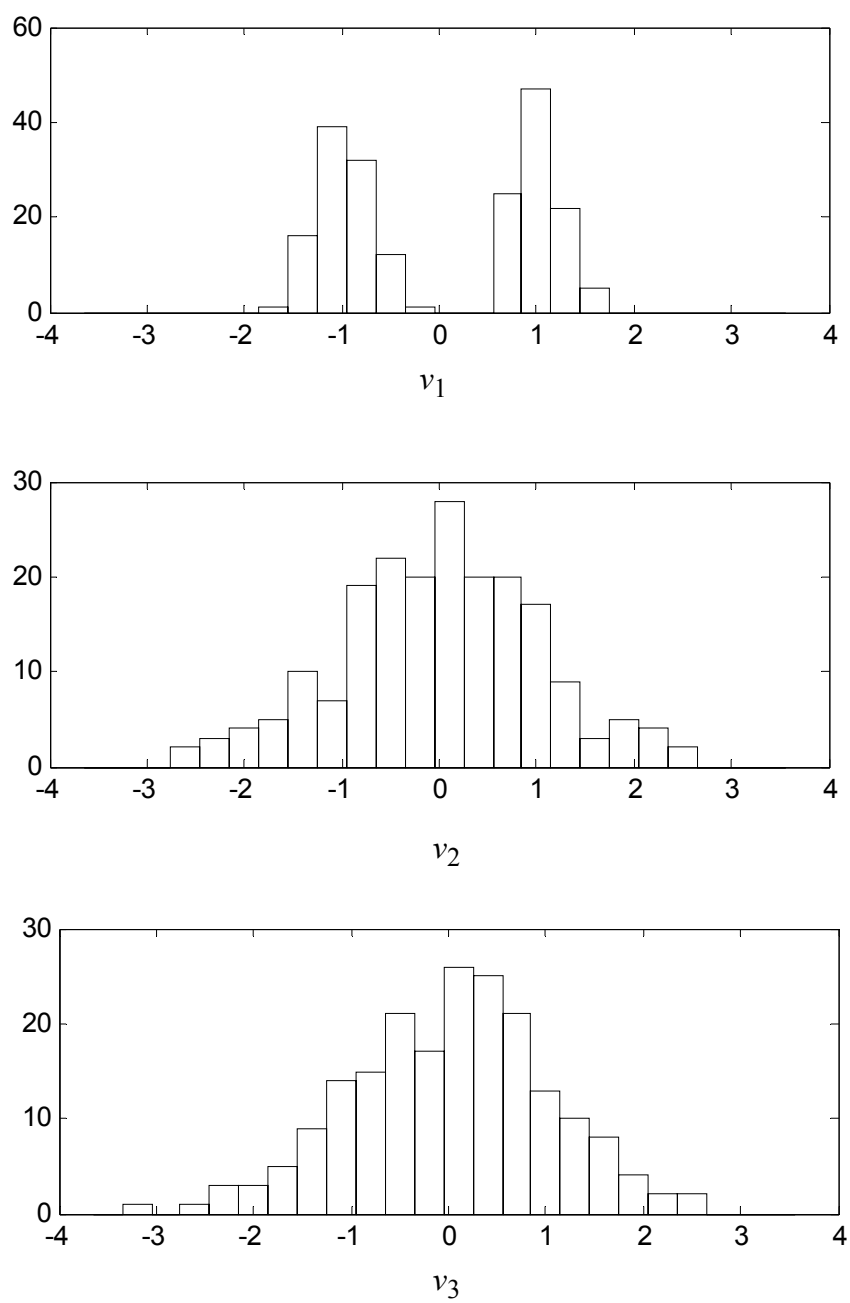


Figure 31 Illustration of histograms of the estimated source signals.

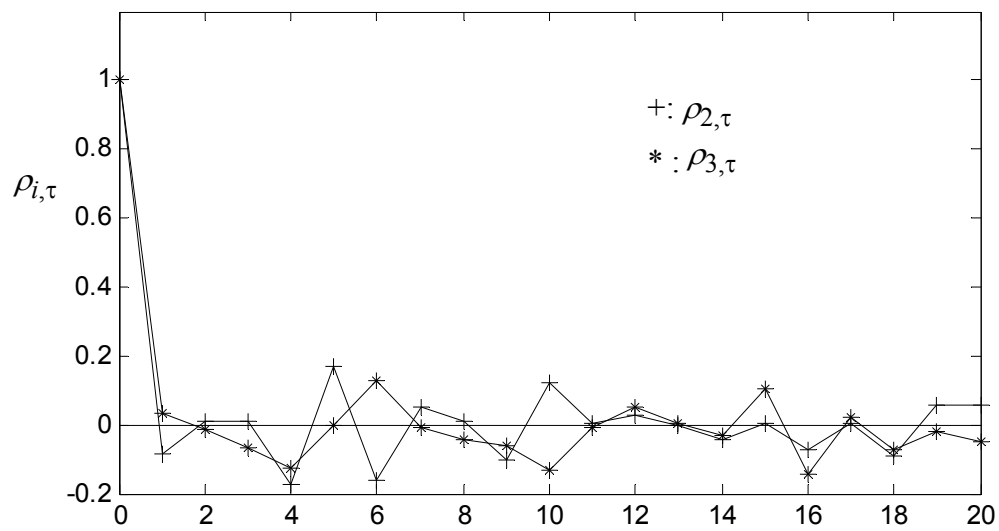


Figure 32 Illustration of sample autocorrelation functions of v_2 and v_3 .

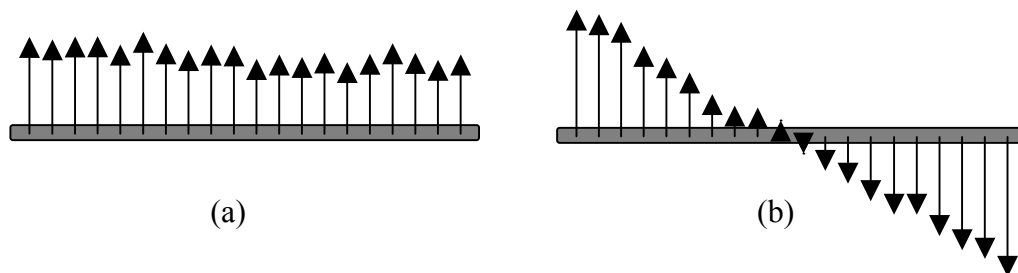


Figure 33 Estimates of \mathbf{c}_2 and \mathbf{c}_3 using the A&S method: (a) estimates of \mathbf{c}_2 , and (b) estimates of \mathbf{c}_3 .

V.4 Chapter summary

This chapter has presented an overall strategy for how to use the blind separation methods and the A&S method in combination. The first step of the strategy is to determine which blind separation methods are to be applied based on the availability of pre-modeled variation patterns. After applying the blind separation methods, one must verify which variation sources are separable and which are within a same block. Histograms of the estimated source signals and sample autocorrelation functions are used to identify separable sources and blocks. If the blind separation method with partial prior knowledge is used, the pre-modeled variation patterns that are present must also be determined. After identifying blocks, the A&S method is applied to each block. For the A&S method, Σ_i should be calculated from the estimates of the variation patterns by using blind separation methods so that the A&S method can be applied without any modification.

The overall strategy enables us to separate variation sources, which cannot be separated by using any other methods (blind separation methods or the A&S method), which is illustrated with the examples in Section V.2 and Section V.3. There is, however, a high level of user subjectivity involved in selecting the separable sources and blocks. This overall strategy could be further enhanced by developing a measure of separability for any two sources.

CHAPTER VI

CONCLUSION AND FUTURE WORKS

This dissertation has focused on identifying spatial variation patterns to identify and eliminate the underlying root causes of process variation. In general, there are two different approaches used for identifying variation patterns – classifying pre-modeled variation patterns and estimating un-modeled variation patterns. The classifying approach requires modeling all of the potential variation patterns from off-line, a condition which precludes the wide applicability of the approach. As a consequence, estimating variation patterns from on-line measurement data has more practical significance. However, the existing methods for estimating un-modeled patterns also have several limitations, such as a high level of user subjectivity. To find a more generic and black-box type (i.e., requiring less user input) method, several blind source separation methods have been proposed and investigated in this dissertation.

Since the existing blind source separation methods employ a model whose structure is nearly identical to the model used for manufacturing variation diagnosis, it can be directly applied. The existing blind separation methods (the second-order and fourth-order methods) require additional assumptions for uniquely estimating variation patterns. When these methods are compared to an existing method for estimating un-modeled patterns (the A&S method), they have advantages in the sense

that verification of the required assumptions is more straightforward. If required assumptions are violated, no method can estimate variation patterns reasonably.

In this dissertation, the existing blind separation methods have been further enhanced to be more effective and more black-box like. The second-order and fourth-order criteria have been combined and optimally weighted. The optimal weights have been chosen by minimizing some measure of estimation accuracy. The optimal weights are generally relative to the information contained in each second-order and fourth-order criteria. Combining second-order and fourth-order criteria further relaxes the required assumptions of the second-order and fourth-order methods. The blind separation methods have been further enhanced by utilizing partial prior knowledge. There are two steps in the new method, which are estimating the un-modeled variation patterns and classifying the pre-modeled variation patterns. By incorporating partial information from off-line analysis, the new method can estimate un-modeled variation patterns more accurately.

The rest of this section discusses issues for the future study.

- This dissertation has presented an overall strategy for using the blind separation methods with the A&S method. By using this overall strategy, variation patterns, which cannot be identified by any single method, can be identified. However, the overall strategy involves a high level of user subjectivity in selecting separable sources and blocks. Criteria for measuring the separability of any two sources should be further studied in order to reduce the user subjectivity. These criteria may be usable for interpreting

estimates of variation patterns using any of the blind source separation methods.

- It should be noted that all of the methods discussed in this dissertation are based on the linear model (1). If this model (1) does not adequately represent reality, all of the blind source separation methods in this dissertation may be inapplicable. The extension of the blind separation methods to nonlinear variation patterns should be studied further. For example, estimating linear un-modeled variation patterns with partially pre-modeled nonlinear variation patterns is one likely area for further study. Another is the estimation of nonlinear un-modeled variation patterns using blind source separation concepts.
- As discussed in Section IV.1, this dissertation has focused on a single stage manufacturing process. In multistage manufacturing processes, the state space model can be used to describe the overall assembly process (Jin and Shi, 1999; Ding, et al, 2002). The extension of blind source separation concepts to the state space model in multistage manufacturing processes should be an area for future study.
- All of the blind separation methods in this dissertation are based on second-order and fourth-order statistics. The third-order statistic can also be used for blind source separation (Comon, 1994). The third-order statistic is not widely used in signal processing applications, however, since they usually deal with symmetric sources. Therefore, the third-order statistic contains

little information in signal processing applications. In the manufacturing process, skewed source signals are often examined as in crankshaft example in Section II.3. Therefore, the third-order statistic may contain useful information for manufacturing variation diagnosis. By including the third-order statistic (more information), the blind separation methods would become more effective in estimating un-modeled variation patterns.

- Every estimate of variation patterns involves estimation error. Plotting the variation patterns as arrows as in Figures 1 and 2 may not be sufficient for interpreting the estimates of the variation patterns. Considering the confidence interval of the estimates of the variation patterns, more interpretable visualization methods should be developed.

REFERENCES

- Apley, D. W. and Shi, J. (2001), "A Factor-Analysis Method for Diagnosing Variability in Multivariate Manufacturing Processes," *Technometrics*, 43, 84-95.
- Apley, D. W., and Shi, J. (1998), "Diagnosis of Multiple Fixture Faults in Panel Assembly," *ASME Journal of Manufacturing Science and Engineering*, 120, 793-801.
- Barton, R.R, and Gonzalez-Barreto, D.R (1996), "Process-oriented Basis Representation for Multivariate Process Diagnostics," *Quality Engineering*, 9, 107-118.
- Belouchrani, A., Abed-Meraim, K., Cardoso, J.F. and Moulines, E. (1997), "A Blind Source Separation Technique Using Second-Order Statistics", *IEEE Transactions on Signal Processing*, 45, 434-444.
- Box, G.E.P., Jenkins, G.M. and Reinsel, G.C. (1994). *Time Series Analysis: Forecasting and Control, (3rd ed.)*, Prentice Hall, Englewood Cliffs, NJ.
- Cardoso, J.F. (1994), "Perturbation of Joint Diagonalizers," Technical Report Ref.#94d027, Telecom Paris.
- Cardoso, J.F. (1998), "Blind Signal Separation: Statistical Principles," *Proceedings of the IEEE*, 86, 2009 –2025.

- Cardoso, J.F. and Souloumiac, A. (1993), "Blind Beamforming for Non-Gaussian Signals," *IEEE Proceedings*, 140, 362-370.
- Ceglarek, D., and Shi, J. (1996), "Fixture Failure Diagnosis for Autobody Assembly Using Pattern Recognition," *ASME Journal of Engineering for Industry*, 118, 55–66.
- Ceglarek, D., Shi, J., and Shou, Z. (1993), "Variation Reduction for Body Assembly: Methodologies and Case Studies Analysis," Technical Report of the "2 mm" Program, University of Michigan, Ann Arbor.
- Ceglarek, D., and Shi, J. (1995), "Dimensional Variation Reduction for Automotive Body Assembly," *Manufacturing Review*, 8, 139-154.
- Comon, P. (1994), "Independent Component Analysis, a New Concept?" *Signal Processing*, 36, 287-314.
- Ding, Y., Ceglarek, D. and Shi, J. (2002), "Fault Diagnosis of Multistage Manufacturing Processes by Using State Space Approach," *Journal of Manufacturing Science and Engineering*, 124, 313-322.
- Glass, S. and Thomsen, J. (1993), "How SMT Boards are Assembled", *Printed Circuit Fabrication*, 16, 42-47.
- Golub, G.H. and Loan, C.F.V. (1989), *Matrix Computations*, Johns Hopkins Univ. Press. Baltimore, MD.
- Haykin, S., ed. (2000), *Unsupervised Adaptive Filtering, Vol. 1*, Wiley, NY.
- Hyvarinen, A. (1999), "Survey on Independent Component Analysis", *Neural Computing Surveys*, 2, 94-128.

- Hyvarinen, A. and Oja, E. (2000), "Independent Component Analysis: Algorithms and Applications", *Neural Networks*, 13, 411-430.
- Jackson, J. E. (1980), "Principal Components and Factor Analysis: Part I – Principal Components," *Journal of Quality Technology*, 12, 201–213.
- Jackson, J. E. (1981), "Principal Components and Factor Analysis: Part II – Additional Topics Related to Principal Components," *Journal of Quality Technology*, 13, 46–58.
- Jin, J. and Shi, J. (1999), "State Space Modeling of Sheet Metal Assembly for Dimensional Control," *ASME Journal of Manufacturing Science and Engineering*, 121, 756-762.
- Johnson, R. A., and Wichern, D. W. (1998), *Applied Multivariate Statistical Analysis*, (4th ed.), Prentice Hall, Upper Saddle River, NJ.
- Monzingo, R. A. and Miller, T.W. (1980), *Introduction to Adaptive Arrays*, Wiley, NY.
- Reed, C.W. and Yao, K. (1998), "Performance of Blind Beamforming Algorithms," *Ninth IEEE Signal Processing Workshop*, Portland, OR, 256 –259.
- Rosenblatt, M. (1985), *Stationary Sequences and Random Fields*, Birkhauser, Boston, MA.
- Stuart, A. and Ord, J. K. (1987), *Kendall's Advanced Theory of Statistics, Vol. 1, Distribution*, (5th ed.), Wiley, NY.

Tong, L., Soon, V.C., Huang, Y.F. and Liu, R. (1990), "AMUSE: A New Blind Identification Algorithm", *IEEE International Symposium on Circuits and Systems*, 3, 1784-1787.

Wax, M. and Sheinvald, J. (1997), "A Least-squares Approach to Joint Diagonalization," *IEEE Signal Processing Letters*, 4, 52-53.

APPENDIX A

JOINT APPROXIMATE DIAGONALIZATION

This appendix summarizes the algorithm of Cardoso and Souloumiac (1994), to be used for jointly approximately diagonalizing a set of matrices $\{\mathbf{A}_k: k = 1, 2, \dots, K\}$. The algorithm involves representing the orthogonal matrix \mathbf{U} as the product of a series of Givens rotation matrices (Golub and Van Loan, 1989). For a specified rotation angle θ and a pair of indices i and j with $1 \leq i \neq j \leq p$, the Givens rotation matrix $\mathbf{U}(i,j,\theta)$ is defined as a slightly modified version of the identity matrix. All elements of $\mathbf{U}(i,j,\theta)$ are the same as the identity matrix, except that $u_{ii}(i,j,\theta) = \cos(\theta)$, $u_{jj}(i,j,\theta) = -\sin(\theta)$, $u_{ji}(i,j,\theta) = \sin(\theta)$, $u_{ij}(i,j,\theta) = \cos(\theta)$, where $u_{kl}(i,j,\theta)$ denotes the k^{th} -row, l^{th} -column element of $\mathbf{U}(i,j,\theta)$. As the algorithm iterates over i and j , the θ that determines each $\mathbf{U}(i,j,\theta)$ is chosen to minimize

$$\sum_{k=1}^K \text{off}[\mathbf{U}'(i,j,\theta)\mathbf{A}_k\mathbf{U}(i,j,\theta)], \quad (30)$$

which is a function of only a single parameter θ . The matrices $\{\mathbf{A}_k: k = 1, 2, \dots, K\}$ are updated via $\mathbf{A}_k \rightarrow \mathbf{U}'(i,j,\theta)\mathbf{A}_k\mathbf{U}(i,j,\theta)$ after each new $\mathbf{U}(i,j,\theta)$ is found.

For a fixed i and j , the θ that minimizes (30) is easily determined as follows.

Define the 2×2 symmetric matrix

$$\mathbf{H} = \sum_{k=1}^K \mathbf{h}'(\mathbf{A}_k) \mathbf{h}(\mathbf{A}_k), \quad (31)$$

where $\mathbf{h}(\mathbf{A})$ is defined as $[a_{ii}-a_{jj} \ a_{ij}+a_{ji}]$ with a_{ij} denoting the i^{th} -row j^{th} -column element of a matrix \mathbf{A} . The θ that minimizes (31) is given by (Cardoso and Souloumiac, 1994)

$$\cos \theta = \sqrt{\frac{\mathbf{z}_1 + 1}{2}} \quad \text{and} \quad \sin \theta = \frac{\mathbf{z}_2}{\sqrt{2(\mathbf{z}_1 + 1)}}, \quad (32)$$

where $[\mathbf{z}_1 \ \mathbf{z}_2]'$ denotes the eigenvector of \mathbf{H} that corresponds to its largest eigenvalue.

The algorithm is iterated over i and j values with $1 \leq i \neq j \leq p$ until (31) converges.

The final \mathbf{Q} matrix is then taken to be the product (from left to right) of the individual $\mathbf{U}(i, j, \theta)$ matrices at each iteration.

VITA

Name: Ho Young Lee

Permanent Address: Samik-bila #202, 151 Dogok-dong, Kangnam-Gu
Seoul, Korea, 135-270

Educational Background: B.S. 1998. Department of Industrial Engineering

Seoul National University

M.S. 2000. Department of Industrial Engineering

Texas A&M University